Immune defense mechanisms against *Legionella longbeachae*

Victoria Madeleine Scheiding

ORCID ID:

0000-0002-0973-6909

from Lübbecke, Germany

Submitted in total fulfilment of the requirements of the joint degree of

Doctor of Philosophy (PhD)

of the Medical Faculty

The Rheinische Friedrich-Wilhelms-Universität Bonn

and

The Department of Microbiology and Immunology

The University Melbourne

Bonn/Melbourne, 2020

Performed and approved by The Medical Faculty of The Rheinische Friedrich-Wilhelms-Universität Bonn and The University of Melbourne

1. Supervisor: Prof. Dr. Natalio Garbi
2. Supervisor: Prof. Dr. Ian van Driel

Date of submission: 15. September 2019
Date of oral examination: 17. January 2020

Institute in Bonn: Institute of Experimental Immunology

Director: Prof. Dr. med. Christian Kurts

Table of content

Abbreviations

%	Percentage
°C	Degree Celsius
µg	Microgram
µl	Microliter
µm	Micrometer
ADP	Adenosine diphosphate
AMs	Alveolar macrophage
AP-1	Activator protein-1
APC	Antigen-presenting cell
Arf	ADP-ribosylation factor
ASC	Apoptosis-associated speck-like protein containing a CARD
BCR	B cell receptor
BCYE	Buffered charcoal yeast extract
CCL	Chemokine (C-C motif) ligand
CCR	C-C chemokine receptor
CD	Cluster of differentiation
CFU	Colony forming unit
cm	Centimeter
CO^2	Carbon dioxide
CR	Complement receptor
CWFG	Gelatin from cold water fish skin
CXCL	chemokine (C-X-C motif) ligand
DAPI	4',6-Diamidin-2phenylindol
DC	Dendritic cell
DNA	Deoxyribonucleic acid
EDTA	Ethylenediaminetetraacetic acid
EEA-1	Early endosome antigen-1
ER	Endoplasmic reticulum
FCS	Fetal calf serum
GEF	Guanine nucleotide exchange factor

GM-CSF	Granulocyte-macrophage colony-stimulating factor
h	hours
HEPES	4-(2-hydroxyethyl)-1-piperazineethanesulfonic acid
i.n.	intranasal
i.p.	intraperitoneal
i.t.	intratracheal
IFN	Interferon
Ig	Immunoglobulin
IL	Interleukin
ILC	Innate lymphoid cell
IRAK	interleukin-1 receptor (IL-1R) associated kinase
L	ligand
LAMP-2	Lysosome Associated membrane protein 2
LCV	Legionella-containing vacuole
m^2	Square meter
M6PR	Mannose 6-phosphate receptor
mAb	Monoclonal antibody
MAP kinase	mitogen-activated protein kinase
MC	Monocyte-derived cell
mg	Milligram
MHC	major histocompatibility complex
min	Minute
mL	Milliliter
mM	Millimolar
mm	Millimeter
MPC-1	Mitochondrial pyruvate carrier-1
MyD88	Myeloid differentiation primary response 88
NADPH	Nicotinamide adenine dinucleotide phosphate
NFκB	nuclear factor kappa-light-chain-enhancer of activated B cells
ng	Nanogram
NK cell	Natural killer cell
NLR	nucleotide-binding oligomerization domain-like receptors

O^2	Oxygen
OD	Optical density
PAMP	Pathogen-associated molecular pattern
PBS	Phosphate buffered saline
PFA	Paraformaldehyde
PI	Propidium iodide
PRR	Pattern recognition receptor
R	receptor
RCB	Red blood cells
RLR	retinoic acid-inducible gene-I-like receptors
RNA	Ribonucleic acid
RNS	Reactive nitrogen species
ROS	Reactive oxygen species
rpm	Revolutions per minute
RPMI	Roswell park memorial institute medium
RT	Room temperature
s	Second
SIRPα	Signal regulatory protein alpha
SP	Surfactant protein
SPF	specific pathogen-free
STAT3	Signal transducer and activator of transcription 3
T4P	Type IV pili
TCR	T cell receptor
TGF-β	Transforming growth factor beta
Th cell	T helper cell
TLR	Toll-like receptor
TNF-α	Tumor necrosis factor alpha
Treg	Regulatory T cell
T_{RM}	Tissue-resident memory T cells
USA	United States of America
WHO	World Health Organization
WT	wild-type

List of tables

List of figures

Abstract

The pulmonary epithelial barrier is the first line of defense against pathogens invading the lungs. If those are able to overcome this first barrier, myeloid cells of the innate immune system are instrumental for the antimicrobial defense and can directly eliminate invading microorganisms. This work aimed to identify novel mechanisms by which pulmonary epithelial cells and myeloid cells eliminate invading bacteria from the lungs. For this, infections with *Legionella longbeachae* were used to investigate a severe and often fatal form of pneumonia in humans known as Legionnaires' disease in a mouse model.

Following infection, infiltration of immune cells was dominated by neutrophils and, to a lesser extent, by monocytes. In addition to this, a significantly higher fraction of neutrophils contained *L. longbeachae* bacteria compared with other myeloid immune cells. Within host cells, bacteria translocated effector proteins mostly into neutrophils, and were residing in a vacuole resembling the Legionella-containing vacuole, as known from infections with *L. pneumophila*. However, neutrophils played an important role in the *in vivo* clearance of *L. longbeachae*, as mice depleted of this cell type exhibited significantly higher bacterial burden in the lungs. Besides neutrophils, monocytes also contributed to the control of pulmonary *L. longbeachae* infections, while lymphoid immune cells had no effect on the clearance of the bacteria.

Molecularly, it is well known that IL18 is important in anti-bacterial defense by inducing lymphocytes to release IFNγ. However, IL18 receptor (IL18R) expression on lymphoid cells did apparently not promote *L. longbeachae* clearance. Instead, expression by pulmonary stromal cells was required and sufficient for elimination of the bacteria. Stromal expression of the IL18 receptor was almost confined to the ciliated epithelial cell compartment in the bronchioles. IL18R signaling in those cells did not promote mucus production but it rather enhanced the anti-bactericidal activity of neutrophils. Therefore, these results indicate a non-canonical role of IL18 in the defense against pulmonary *L. longbeachae* infection, linking non-immune pulmonary epithelial cells with inflammatory neutrophils.

Declaration

The work that is presented in this thesis was conducted at the Rheinische Friedrich-Wilhelms University of Bonn and the University of Melbourne, in the laboratories of Prof. Natalio Garbi and Prof. Ian van Driel between April 2016 and September 2019. The research work was funded by the Bonn & Melbourne Research and Graduate Program GRK 2168 of the Deutsche Forschungsgemeinschaft (DFG) and a Melbourne Research Scholarship.

This is to certify that,

(i) the thesis comprises only original work towards the PhD except where indicated in the preface,

(ii) due acknowledgement has been made in the text to all other material used,

(iii) the thesis is less than 100 000 words in length, exclusive of tables, maps, bibliographies and appendices.

Bonn, 15 September 2019

Victoria Scheiding

Preface

My contribution to the experiments within each chapter was as follows:

Chapter 3: 99 %
Chapter 4: 98 %

I acknowledge the important contributions of others to experiments presented herein:
Chapter 3: Dr. Andrew S. Brown
Chapter 4: Gishnu Harikumar Parvathy, Jing-Wun Li, Lara Oberkirchner

Chapter 1: Introduction

1.1. Structure and function of the lung

The lungs are the primary organs of the respiratory system and their main function is the exchange of CO_2 for O_2 in erythrocytes, as they circulate through pulmonary capillaries (Porra, 2006; Carroll, 2007). This is a fundamental process for cellular respiration, where the provided O_2 fuels the aerobic metabolism while its waste product CO_2 is removed via expiration (Porra, 2006; Carroll, 2007). Functionally, the respiratory system can be separated into a conducting zone and a respiratory zone (Betts *et al.*, 2013). The components of the conducting zone include the nose, pharynx, larynx, trachea, bronchi and conducting bronchioles (Murray, 2010; Betts *et al.*, 2013). Their function is to filter out microorganisms and other particles from inhaled air, to warm it, humidify it, and direct it into the respiratory zone, where gas exchange takes place (Murray, 2010; Betts *et al.*, 2013). The respiratory zone comprises multiple terminal bronchioles and alveoli (Rhoades and Bell, 2009; Betts *et al.*, 2013). An adult human has about 300-500 million alveoli covering a total inner surface area of about 75 m^2, where inhaled microbes may attach and enter the body (Bals and Hiemstra, 2004; Rhoades and Bell, 2009). The alveoli are surrounded by an extensive network of fine capillaries and, together, they form respiratory units that are separated from each other through extremely thin membranes, called septa. These septa are formed by the capillary endothelium that is lined by squamous epithelial cells with their corresponding basement membranes and constitutes a thin air-blood barrier of less than 0.5 µm on average, allowing gas exchange by diffusion (Rhoades and Bell, 2009; Betts *et al.*, 2013).

To preserve an efficient gas exchange while avoiding invasion of harmful pathogens, the lungs are equipped with different defense mechanisms (Boyton and Openshaw, 2002). Those include physical and chemical barriers as first line of defense, as well as innate and specific immune responses (Boyton and Openshaw, 2002). Pulmonary diseases develop when pathogens overcome those initial defense mechanisms and colonize the lung tissue, thereby promoting lung injury and inflammatory responses (Eisele and Anderson, 2011).

1.2. Pneumonia

Pneumonia is the fourth cause of mortality worldwide and is caused by diverse etiological agents (WHO, 2018). It is characterized by accumulation of fluid in the pulmonary alveoli, thereby compromising gas exchange in the lungs and leading to respiratory failure in severe cases (Torres and Cillóniz, 2015). Most commonly, pneumonia results from acute pulmonary infection, when inhaled pathogens breakdown host defense mechanisms and colonize the lower respiratory tract (Amalia Alcón, Fabregas, Torres and Fabregas, 2005). Other less common causes of pneumonia include sepsis, mechanical ventilation, and trauma (Lively, 2012; Abdelrazik Othman and Salah Abdelazim, 2017).

1.2.1. Risk factors and epidemiology

High risk factors for the development of pneumonia include underlying medical conditions, such as cardiovascular diseases, congenital lung diseases and lung cancer, as well as immunosuppression, smoking, alcoholism and air pollution (Torres *et al.*, 2013). In addition, the incidence of pneumonia differs considerably between different age groups and the income level within individual countries (Gereige and Laufer, 2013). According to the World Health Organization, pneumonia is the leading infectious cause of mortality in children worldwide, killing over 800 thousand children under 5 years of age in 2017 alone (WHO, 2019). Most of those cases have been reported in low- and middle-income countries, which occur partly due to limited access to treatment (Tong, 2004; Puligandla and Laberge, 2008; Zar *et al.*, 2013). Another population at risk for developing pneumonia are people older than 65 years, where the disease accounts for a mortality rate of 23-57 % depending on the etiological agent (Tong, 2004; Schmidt-Ioanas and Lode, 2006).

1.2.2. Etiology, transmission and pathophysiology

Although respiratory viruses and fungi can cause pneumonia, most cases result from bacterial infections (Gereige and Laufer, 2013; Torres and Cillóniz, 2015; Mandell, 2015). *Streptococcus pneumoniae* is the most common causative agent for pneumonia across different age groups and accounts for two-thirds of overall

pneumonia-associated deaths (Lynch and Zhanel, 2010; Cilloniz *et al.*, 2011; Torres and Cillóniz, 2015). The second most common bacterial causative agent is *Haemophilus influenzae type b*, although a successful vaccine against those bacteria is available (WHO, 2019). Besides this, other well-known bacteria that can cause pneumonia include *Pseudomonas aeruginosa*, *Chlamydophila pneumoniae*, *Mycoplasma pneumoniae*, *Klebsiella pneumoniae* and *Legionella* spp. (Cilloniz *et al.*, 2011). Amongst viruses, the respiratory syncytial virus and influenza virus are the most common causes for pneumonia (Cilloniz *et al.*, 2011; WHO, 2019). Infections with those viruses are often followed by secondary bacterial infections that may lead to a severe form of pneumonia (Cilloniz *et al.*, 2011; WHO, 2019).

For pathogens to cause pneumonia, they need to reach and infect the lower respiratory tract. This is often achieved via inhalation of infectious aerosols released by patients during normal breathing, coughing and sneezing (Lynch and Zhanel, 2010; Singh, 2012; Torres and Cillóniz, 2015). In addition, the upper respiratory tract becomes colonized with microorganisms from an early age, including by *S. pneumoniae*, *H. influenzae* and *Staphylococcus aureus* (Schenck *et al.*, 2016). These organisms may reach the alveoli during normal breathing and can cause pneumonia if local host defenses fail (Torres and Cillóniz, 2015). In rare cases, pathogens may be able to reach the lung parenchyma and cause pneumonia by spreading from other sites of infection, as often occurs for *K. pneumoniae* or during sepsis (Torres and Cillóniz, 2015).

Independently of its etiology, pneumonia is characterized by inflammation of the pulmonary alveoli, vascular leakage and loss of epithelial impermeability, resulting in accumulation of fluid, or edema, in the alveolar space (Mandell, 2015; Sattar and Sharma, 2019). Different mechanisms are responsible for the formation of edema. Those include disruption of tight junctions between alveolar epithelial cells, leading to increased permeability and loss of Na^+ channel function on those cells (Yanagi *et al.*, 2015; Peteranderl *et al.*, 2017). This causes leakage of fluid from capillaries, resulting in pulmonary consolidation (Joannides, 1931; Brown *et al.*, 2017). Together with an increased mucus production those

mechanisms ultimately compromise the gas exchange, and in severe cases may lead to respiratory failure (Joannides, 1931; Torres and Cillóniz, 2015).

1.2.3. Diagnosis, treatment and prevention

Pneumonia is diagnosed by evaluation of the clinical symptoms through physical examination and, in suspected severe cases, by chest radiology. To identify the causative microorganism, standard microbiological tests are commonly used, as well as PCR methods (Tong, 2004). Bacterial pneumonia can be successfully treated with antibiotics. However, over the past years, there has been a rapid increase in antibiotic-resistant bacteria, such as *S. pneumoniae*, *S. aureus*, *P. aeruginosa*, *K. pneumoniae* and *M. pneumoniae* (Tong, 2004; Torres and Cillóniz, 2015; Ventola, 2015). With the exception of *H. influenzae type b and S. pneumoniae,* vaccination against bacterial pneumonia is usually ineffective (Madhi, 2008). Although influenza virus itself rarely causes pneumonia, vaccination against this virus is recommended for high-risk patients in order to prevent severe pneumonia caused by secondary bacterial infections (Tessmer *et al.*, 2011).

1.3. Legionella and Legionnaires' disease

The genus Legionella belongs to the family *Legionellaceae* and comprises over 50 different species of gram-negative bacteria, with about 70 distinct serogroups (Percival and Williams, 2014; Cunha *et al.*, 2016). More than 20 of those species are pathogenic to humans, with *L. pneumophila* and *L. longbeachae* being the most common causative agents (Percival and Williams, 2014). In response to pulmonary infection with *Legionella* spp., otherwise healthy individuals often develop a mild self-limiting disease called Pontiac fever (Appelt and Heuner, 2017). However, in susceptible individuals the infection may progress to a serious form of pneumonia, called Legionnaires' disease, constituting a high risk for morbidity and mortality in infected patients (Beauté *et al.*, 2013; Brown *et al.*, 2017).

It is estimated that Legionnaires' disease accounts for about 2-9 % of reported cases of pneumonia worldwide (Asare, 2006; Brown *et al.*, 2017).

However, due to variances in awareness, diagnostics and reporting the precise incidence of Legionnaires' disease is unknown (Cunha *et al.*, 2016). One reason for this is that the most commonly used diagnostic tool, the urinary antigen test, only detects *L. pneumophila* serogroup 1, but not other serogroups or other *Legionella* spp. (Chen et al. 2015; Brown et al. 2017). In contrast to the urinary antigen test, nucleic-acid amplification methods or sample culture methods allow the detection of various *Legionella* spp. and serogroups, but exhibit a varying sensitivity (Cunha *et al.*, 2016). Since vaccines against *Legionella* spp. are not available yet, infected patients are often treated with high doses of antibiotics, such as macrolides, ketolides, tetracyclines, and quinolones (Cunha, Burillo, and Bouza 2016). However, Legionnaires' disease still accounts for a mortality rate of about 10 % in infected patients (Soda *et al.*, 2017).

1.3.1. *Legionella pneumophila*

L. pneumophila was first identified in 1976 after an outbreak of severe pneumonia affecting 182 attendees of a Legion Convention in Philadelphia, USA (Fraser *et al.*, 1977). The newly isolated strain of *L. pneumophila* was then termed Philadelphia 1 (Asare, 2006). Today, at least 15 different serogroups of *L. pneumophila* have been described, with serogroup 1 being responsible for about 84 % of the known cases of Legionnaires' disease worldwide (Newton et al. 2010). *L. pneumophila* can be found ubiquitously within natural freshwater environments, parasitizing free-living amoeba that serve as a replicative niche (Buchrieser, 2011; Brown *et al.*, 2017). In addition, *L. pneumophila* may form complex biofilms in human-made water systems, including air-conditioners, cooling towers, fountains and spa baths, from which infectious aerosols may be formed (Newton et al. 2010).

Infection of the lungs with *L. pneumophila* occurs through inhalation of contaminated water droplets and may lead to Legionnaires' disease if pulmonary defense mechanisms fail to clear the bacteria (Percival and Williams, 2014; Brown *et al.*, 2017). Generally, *L. pneumophila* is responsible for about 95 % of the cases of Legionnaires' disease in Europe and the United States, and for

approximately 50 % of the cases in Australia and Asia (Montanaro-Punzengruber et al. 1999; Newton et al. 2010).

1.3.2. *Legionella longbeachae*

L. longbeachae was first isolated and characterized in 1980 from a patient with pneumonia in Long Beach, California (Mckinney, R. M. et al., 1981). Most cases of pulmonary disease in humans are associated with *L. longbeachae* serogroup 1 (Cazalet *et al.*, 2010). Worldwide it is responsible for about 4 % of the known cases of legionellosis, with a high impact in the southern hemisphere (Currie and Beattie 2015). In Australia, New Zealand and parts of Asia *L. longbeachae* accounts for over 50 % of the cases of Legionnaires' disease (Bacigalupe *et al.*, 2017). In contrast, the incidence of pneumonia caused by those bacteria is significantly lower in Europe (5 %). Interestingly, the number of reports of pneumonia caused by *L. longbeachae* have increased worldwide over the past decade, although the exact reason for this is not presently known (Bacigalupe et al. 2017; Whiley and Bentham 2011).

Most infections with *L. Lo*ngbeachae are associated with contact with potting soil or compost, e.g. during gardening (Casati, Gioria-Martinoni, and Gaia 2009; Gobin et al. 2009). This could be partly due to the fact that, in contrast to *L. pneumophila*, *L. longbeachae* is highly adapted to soil environment, where the bacteria are able to infect soil protozoa (Whiley and Bentham, 2011; Dolinsky *et al.*, 2014). After inhalation of contaminated soil particles, *L. longbeachae* may induce the development of severe pneumonia similar to that caused by *L. pneumophila* (Whiley and Bentham, 2011).

1.4. Pathogenesis of *Legionella* in mammalian cells

Legionella spp. are facultative intracellular, gram-negative bacteria, which replicate inside of host cells in a specialized vacuole, termed Legionella-containing vacuole (LCV). The bacteria establish this LCV through complex mechanisms, which ultimately promote their survival.

1.4.1. Attachment and entry

Tissue-resident alveolar macrophages (AMs) are believed to be the first cell type infected by *L. pneumophila*, serving as a primary replicative niche for the bacteria (Brieland *et al.*, 1994; Copenhaver *et al.*, 2014). Additionally, replication of *L. pneumophila* has been described in alveolar epithelial cells and infiltrating neutrophils (Baskerville *et al.*, 1983; Mody *et al.*, 1993; Copenhaver *et al.*, 2014). Bacterial uptake is mediated by phagocytosis, which is enhanced through opsonization with complement components and specific antibodies (Payne, 1987; Cabello and Pruzzo, 1988; Asare, 2006). Blocking of either CR1 or CR3 with monoclonal antibodies results in a significantly decreased attachment of the bacteria to host cells (Payne et al. 1987). Besides this, *L. pneumophila*-encoded factors are involved in the attachment and entry processes. For instance, type IV pili (T4P) expressed by the bacteria promote the entry into host cells, since mutations in the corresponding genes prevent attachment to macrophages and epithelial cells (Stone and Kwaik, 1998; Zhan *et al.*, 2015).

In contrast to *L. pneumophila*, although human alveolar epithelial- and monocytic cell lines can be infected with *L. longbeachae in vitro*, it is currently unknown which physiological cellular hosts can serve as a replicative niche for those bacteria (Wood *et al.*, 2015).

1.4.2. Virulence factors and intracellular life cycle

Most of the current knowledge on the intracellular life cycle of *Legionella* spp. is based on studies with *L. pneumophila,* whereas there have been only few studies with *L. longbeachae* or other *Legionella* spp. (Oliva *et al.*, 2018).

Generally, immune cells are able to engulf invading pathogens via phagocytosis into intracellular compartments called phagosomes. Phagosomes mature along the endocytic pathway and fuse with lysosomes, creating highly microbicidal phagolysosomes (Vieira *et al.*, 2002). However, *L. pneumophila* inhibits phagolysosome fusion and generates a specialized vacuole called Legionella-containing vacuole (LCV) that provides a safe environment for bacterial replication inside of host cells (Newton et al. 2010; Cazalet et al. 2010). Highlighting its importance, about 10 % of the bacterial genome encodes for

components involved in generating the LCV (Burstein *et al.*, 2016). Those comprise specific secretion systems and different virulence effector molecules that are translocated into the host cell cytosol to modify cellular mechanisms. (Zhan *et al.*, 2015). The most prominent secretion system of *L. pneumophila* and *L. longbeachae* is the Dot/Icm type IV secretion system (T4SS) (Segal *et al.*, 2005; Cazalet *et al.*, 2010; Zhan *et al.*, 2015). It is fundamental for virulence of the bacteria, as mutations in key T4SS components result in an inhibition of bacterial replication and elimination of the bacteria (Cazalet et al. 2010; Segal, Feldman, and Zusman 2005; Newton et al. 2010). The *L. pneumophila* effector molecules LidA and LegA8/AnkX/AnkN are translocated through the T4SS and inhibit fusion of the Legionella-containing phagosome with lysosomes (Ensminger and Isberg, 2009). In addition, the bacteria induce recruitment of components from the secretory pathways of the host cell, in order to complete the establishment of the LCV (Newton et al. 2010). Although the components of the T4SS are highly conserved between *L. pneumophila* and *L. longbeachae*, only 34 % of the substrates translocated by *L. pneumophila* are expressed by *L. longbeachae* (Cazalet *et al.*, 2010). Among those are mainly proteins that are involved in manipulation of the host cell secretory pathways (Cazalet *et al.*, 2010). For instance, the Legionella effector molecule RalF acts as a guanine nucleotide exchange factor (GEF) that recruits and activates the small host cell GTPase ADP-ribosylation factor (Arf) (Nagai, 2002). Arf proteins can then direct fusion of endoplasmic reticulum (ER) with the developing LCV, thereby limiting recognition by the cellular autonomous defense system (Roy, 2002; Robinson and Roy, 2006; Hubber and Roy, 2010).

Once the LCV has been established, *L. pneumophila* undergoes a biphasic life cycle. About 4 to 10 hours after phagocytosis, bacteria downregulate virulence factors and initiate replication, taking advantage of the LCV nutrient-rich environment (Cazalet *et al.*, 2010; Newton *et al.*, 2010a). As nutrients become scarce, bacteria slow down replication and increase expression of virulence factors, allowing them to exit host cells, survive in the extracellular environment and invade new cells (Oliva *et al.*, 2018). Similar to *L. pneumophila*, *L. longbeachae* has been shown to reside in phagosomes that contain rough ER-

derived membranes (Cazalet *et al.*, 2010; Wood *et al.*, 2015). However, in contrast to *L. pneumophila*, *L. longbeachae* only partially inhibits phagosomal maturation, as indicated by acquisition of the endosomal makers EEA-1, LAMP-2 and M6PR (Asare and Abu Kwaik, 2007). Nevertheless, *L. longbeachae* impairs the full maturation of phagolysosomes as demonstrated by exclusion of the lysosomal marker Cathepsin D and of the vATPase proton pump from its vacuole (Asare and Abu Kwaik, 2007). This ensures a neutral pH within the LCV that prevents bacterial degradation (Newton et al. 2010). Another difference to *L. pneumophila* is that intracellular replication of *L. longbeachae* is independent of the bacterial growth phase at the time of infection (Asare and Abu Kwaik 2007).

1.4.3. Egress from host cells

When nutrients become scarce, *L. pneumophila* first spreads into the cytosol of host cells by disrupting the LCV membrane (Molmeret and Abu Kwaik, 2002). Once in the cytosol, bacteria induce lysis of the plasma membrane and are thus released into the extracellular space, where they can start a new infectious cycle (Asare and Abu Kwaik, 2007). This two-stage egress of *L. pneumophila* is mediated trough a pore-forming activity, which is believed to be accomplished via the bacterial cytolytic toxin Rib (Molmeret and Abu Kwaik, 2002) (Alli *et al.*, 2000). Similarly, *L. longbeachae* also exits from host cells in order to start a new infectious cycle (Asare and Abu Kwaik, 2007). However, the mechanisms behind this process are still unclear for this bacterial strain.

1.5. Immune responses in the lungs

1.5.1. Immune homeostasis of the lungs

The lungs are constantly exposed to a large variety of inhaled particles and microorganisms (Brown *et al.*, 2017). Pulmonary epithelial cells and AMs are the first cells interacting with inhaled particles or pathogens (Garbi and Lambrecht, 2017; Lloyd and Marsland, 2017). In steady state, they ensure that there is no overt immune response to innocuous substances. This is facilitated through a physico-chemical barrier formed by the continuous layer of epithelial cells, as well as the production of the key immunosuppressive molecules TGFβ and CD200

(further details discussed in sections 1.5.1.1 and 1.5.1.2). However, during pulmonary invasion of harmful pathogens, the cells become activated and initiate an immediate immune response through the release of pro-inflammatory mediators, such as type-I IFNs, TNFα, IL1 and IFNγ (Garbi and Lambrecht, 2017).

1.5.1.1. The pulmonary epithelial barrier

As a first line of defense, the pulmonary epithelium forms a physico-chemical barrier, which separates the airway lumen from the lung tissue (Hallstrand *et al.*, 2014). The cellular composition of this epithelium varies along the proximal- to distal axis of the airways (Rackley and Stripp, 2012).

The trachea and bronchi of the upper respiratory tract are lined by a highly specialized pseudostratified epithelium, consisting of columnar ciliated cells, mucus-producing goblet cells and epithelial precursors, called basal cells. The bronchi branch further into several pulmonary bronchioles. Those are lined by a simple cuboidal epithelium that, in humans, is formed by ciliated cells, goblet cells, basal cells, and secretory club cells. In mice, however, the bronchiolar epithelium is devoid of goblet and basal cells (Rackley and Stripp, 2012). Further downstream, the alveolar epithelium is more simplified, to allow an efficient gas exchange. It is formed by surfactant-producing alveolar epithelial type II cells (AECII), which are interspersed between thin squamous AEC type I cells (AECI) (Rackley and Stripp, 2012).

The epithelial barrier of the lungs is maintained through intercellular epithelial junctions between the different cell types. Those are composed of tight junctions, adherence junctions and desmosomes (Hallstrand *et al.*, 2014). Together they form a physical barrier that prevents invasion of the lung tissue by inhaled pathogens or particles (Soini, 2011). In addition, the lungs are protected by different chemical barriers (Fahy and Dickey, 2010). Goblet cells secrete highly glycosylated mucin proteins that form the macromolecular matrix of a viscoelastic mucus (Duncan F Rogers, 2007; Symmes *et al.*, 2018). The human and murine genomes encode for at least 19 different mucins, of which MUC5AC and MUC5B are predominantly involved in the formation of mucus (Clarke and Pavia, 1980; Symmes *et al.*, 2018). The mucus is essential to keep the pulmonary

epithelial surface hydrated, to entrap inhaled particles, and to preserve cilia functionality (Duncan F Rogers, 2007; Button *et al.*, 2012; Symmes *et al.*, 2018). Between 200-300 cilia can be found on the luminal surface of each pulmonary ciliated epithelial cell (Tilley *et al.*, 2015). Ciliary beating allows transport of mucus with dust, small particles, cellular debris and microbes towards the pharynx, where it can be removed by swallowing and coughing (Rokicki *et al.*, 2016a). This process is termed mucociliary clearance of the lungs (Symmes *et al.*, 2018). Another type of secretory cells in the cuboidal epithelium of the bronchioles are club cells (Rackley and Stripp, 2012) that contain secretory granules and have been shown to mainly secrete the protein uteroglobin (Antunes *et al.*, 2013). Its function is currently unclear, but it has been proposed that uteroglobin has immunosuppressive properties, by modulating the activity of cytokines, such as IFNγ or TNF-α (Hayashida *et al.*, 2000). Besides this, club cells also contribute to the renewal of the airway epithelial barrier, as they can serve as progenitor cells for ciliated epithelial cells (Rokicki *et al.*, 2016a). Altogether, the above described physical and chemical barriers constitute an effective first line of defense against inhaled substances and microorganisms (Rackley and Stripp, 2012; Brown *et al.*, 2017).

In contrast, the alveolar epithelial barrier exhibits a higher susceptibility for attachment and entry of pathogens, as it is devoid of the physical and chemical protection facilitated by ciliated epithelial cells, secretory club cells or mucus-producing goblet cells (French, 2009). However, for protection against invading microorganisms, alveolar epithelial type II cells (AECII) secrete large amounts of surfactant, which, besides preventing alveolar collapse during expiration, has potent antimicrobial properties (Wright, 2003). Some of its components, notably surfactant protein SP-A and SP-D, function as opsonins and have a direct antimicrobial activity (Wright et al., 2003). For further protection, tissue-resident immune cells operate as sentinel cells, which can quickly detect invading pathogens and initiate an immune response in coordination with epithelial cells (Maelfait *et al.*, 2016; Lloyd and Marsland, 2017; Lambert and Culley, 2017). Amongst these, AMs play a critical role in protection of the pulmonary alveoli due to their high phagocytic activity (Garbi and Lambrecht, 2017).

1.5.1.2. Pulmonary tissue-resident immune cells

Tissue-resident immune cells can be found in different anatomical compartments of the lungs during steady state (Pabst and Tschernig, 1995; Sun *et al.*, 2019). In the conducting airways, inhaled particles and microorganisms are removed through mucociliary clearance (Symmes *et al.*, 2018). However, when the physical and chemical barriers are breached, tissue-resident immune cells constitute the next line of defense, as discussed in section 1.5.2 (Lloyd and Marsland, 2017). However, during homeostasis, those immune cells play an important role in maintenance of the epithelial barrier (Lloyd and Marsland, 2017).

Different populations of tissue-resident lymphocytes are placed within the pulmonary epithelium or in the submucosa of the lungs (Stumbles *et al.*, 2003; Lloyd and Marsland, 2017). Those include intra-epithelial lymphocytes and other unconventional T cells, tissue-resident memory T cells (T_{RM}), and innate lymphoid cells (ILCs) (Fan and Rudensky, 2016). Their homeostatic function is usually mediated via cytokines. For instance, IL22 and amphiregulin produced by ILC subsets promote epithelial repair, whereas IL9 secreted by T cells enhances mucus production by goblet cells (Erle and Pabst, 2000; Fan and Rudensky, 2016). In addition to tissue-resident lymphocytes, the mucosa of the upper respiratory tract also contains phagocytic interstitial macrophages and DCs (Lloyd and Marsland, 2017), which together with pulmonary epithelial cells, remove debris from normal cellular turnover and thus prevent inflammation (Juncadella *et al.*, 2013; Grabiec and Hussell, 2016).

Although most particles are removed from the conducting airways by mucociliary clearance, some still reach the alveolar area and need to be cleared in a “silent” manner to avoid inflammation and interference with pulmonary gas exchange (Naeem *et al.*, 2019). For this, the alveolar lumen is lined by AMs, previously called “dust” cells, because of their high capacity to phagocytose inhaled dust particles (Wissinger *et al.*, 2009; Naeem *et al.*, 2019). Besides phagocytosis, a critical function of AMs in steady state is the maintenance of pulmonary immune tolerance, in order to prevent harmful, overreactive immune responses to innocuous substances (Lambrecht, 2006; Brown *et al.*, 2017). This is mainly mediated by active suppression of other immune cells through secretion

of IL10, TGFβ, nitric oxide and prostaglandins (Garbi and Lambrecht, 2017). At the same time, AMs are maintained in a minimal activated state through inhibitory effects of the pulmonary microenvironment. This is conveyed through binding of specific ligands to a set of inhibitory receptors expressed by AMs, including TGFβ receptors, IL10 receptors, CD200 receptors or the signal regulatory protein alpha (SIRPα) (Garbi and Lambrecht, 2017). In steady state another essential function of AMs is the catabolism of alveolar surfactant, which is continuously produced by type-II alveolar epithelial cells (AECII) (Garbi and Lambrecht, 2017). This prevents an elevated deposition of surfactant on the luminal surface of the alveoli, which could compromise an efficient gas exchange and lead to pulmonary diseases (Garbi and Lambrecht, 2017).

Besides their homeostatic function, tissue-resident immune cells positioned in the respiratory tract perform a sentinel function and are able to quickly detect harmful invading pathogens, in order to mount pro-inflammatory responses for elimination of those and to limit their spread.

1.5.2. Innate immune response to pathogens

1.5.2.1. Microbial recognition

Once pathogens are able to attach to epithelial cells and start to invade the pulmonary tissue, a rapid immune response is triggered by immune and non-immune cells, in order to clear the infection and preserve an efficient gas exchange (Rohmann *et al.*, 2011). Microbial recognition is the earliest response against invading pathogens. It is mediated by pulmonary non-immune cells and immune cells via pattern recognition receptors (PRRs) that sense specific, conserved microbial motifs, termed pathogen-associated molecular patterns (PAMPs) (Opitz *et al.*, 2010; Rohmann *et al.*, 2011). PRRs include Toll-like receptors (TLRs), cytosolic NOD-like receptor (NLRs), RIG-I-like receptors (RLRs) and cytosolic DNA sensors, located at strategic compartments of cells, where contact with microbes may occur (Takeuchi and Akira, 2010; Sellge and Kufer, 2015).

There are 11 different membrane-associated Toll-like receptors (TLRs) in humans and 13 in mice, which are located in the plasma membrane and/or in

vesicular compartments where they can engage with structures from extracellular or intracellular microorganisms (Opitz *et al.*, 2010; Rohmann *et al.*, 2011). TLRs recognize a wide diversity of PAMPS, including, for instance, peptidoglycan (TLR2), double-stranded RNA (TLR3), LPS (TLR4), flagellin (TLR5), or unmethylated CpG-rich DNA (TLR9) (Rohmann *et al.*, 2011; Medzhitov, 2017).

TLR signaling is mediated through the adaptor proteins MyD88 or TRIF and results in an NFκB-dependent expression of pro-inflammatory cytokines, chemokines, the costimulatory molecules CD40, CD80 and CD86, and major histocompatibility complex (MHC) molecules. Additionally, TLR signaling can result in an IRF3/7-dependent production of type I IFNs (O'Neill *et al.*, 2013; Medzhitov, 2017). Moreover, mammalian TLR signaling can lead to the production of antimicrobial peptides and nitric oxide that directly eliminate microbes (Thoma-Uszynski, 2001).

On the other hand, NOD-like receptors (NLRs) are cytosolic PRRs that recognize intracellular PAMPs of infected cells (Rohmann *et al.*, 2011). In humans 22 different NLRs (18 in mice) have been identified, of which NOD1 and NOD2 are best studied (Rohmann *et al.*, 2011; Corridoni *et al.*, 2014). While NOD1 recognizes mainly molecules related to bacterial peptidoglycan, NOD2 binds muramyl-dipeptide (MDP) and MurNac-L-Ala-D-*iso*-Gln of microorganisms (Rohmann *et al.*, 2011). In addition, some activated NLRs form intracellular oligomeric protein complexes, termed inflammasomes (Schroder and Tschopp, 2010; Rohmann *et al.*, 2011; Howrylak and Nakahira, 2017a). Those comprise, for instance, NLRP3 and NAIP5/NLRC4 (Howrylak and Nakahira, 2017b). The NLRP3 inflammasome detects various PAMPs, including bacterial cell wall components, microbial nucleic acids, and toxins (Opitz *et al.*, 2010). In contrast, NAIP5/NLRC4 inflammasomes specifically recognize bacterial flagellin (Opitz *et al.*, 2010). After activation, NLRP3 molecules assemble with the adaptor protein ASC to form supramolecular structures that mediate recruitment of the cysteine protease caspase-1 and its activation via autoproteolysis (Howrylak and Nakahira, 2017a; Pinkerton *et al.*, 2017). In contrast to this, NAIP5/NLRC4 inflammasomes can recruit caspase-1 independently of ASC (Opitz *et al.*, 2010). Activated caspase-1 can then cleave the premature forms of the cytosolic cytokines IL-1β

and IL18 into their active forms (Mascarenhas and Zamboni, 2017a; Pinkerton *et al.*, 2017). Besides this, inflammasome-mediated proteolytic activation of gasdermin-D results in cellular death by pyroptosis and in the release of the activated cytosolic cytokines into the extracellular milieu (Shi *et al.*, 2015; He *et al.*, 2015).

A third family of PRRs, which specifically sense short and long viral dsRNA are RIG-like receptors (RLRs). Those include the RNA helicase retinoic acid-inducible gene-I (RIG-I) and melanoma differentiation-associated gene 5 (MDA5) (Opitz *et al.*, 2010). Both proteins signal via the adaptor protein MAVS and promote the expression of type I-IFNs in an IRF7-dependent manner. Besides this, they can also induce the NFκB-dependent production of pro-inflammatory cytokines (Opitz *et al.*, 2010; Loo and Gale, 2011).

Lastly, cytosolic DNA sensor proteins can recognize viral and bacterial DNA. So far, the polymerase III-RIG-I pathway and the protein ZBP1 have been identified, both of which signal via the adaptor protein MAVS to induce expression of type I-IFNs (Vance, 2016; Abe *et al.*, 2019).

Expression of TLRs and other PRR is cell-specific, indicating a cellular division of labor in microbial recognition and response to pathogens. Sections 1.5.2.2-1.5.2.5 and 1.5.3 summary the contributions of specific cell populations to anti-microbial defenses (Takeuchi and Akira, 2010; Thompson *et al.*, 2011). All of the molecules, expressed after recognition of PAMPs via PRRs, are required to induce a strong immune response. This includes attraction of further immune cells from the circulation via chemokines as well as cytokine-induced activation resulting in stronger effector functions (Thompson *et al.*, 2011).

1.5.2.2. Pulmonary epithelial cells

Although pulmonary epithelial cells are not immune cells, microbial attachment and invasion result in PRR-mediated recognition of invading pathogens and in an early secretion of pro-inflammatory mediators that are fundamental for a rapid immune response. Currently, it is unknown how pulmonary epithelial cells distinguish between innocuous particles or microbes and harmful invading pathogens. However, it has been shown that epithelial cells in the gut are

polarized and express TLR5 only in the basolateral membrane (Gewirtz *et al.*, 2001). Therefore, it is likely that flagellin is not detected in the luminal pulmonary space, but rather only during inter-epithelial invasion. Another possibility may be that only higher concentrations of pathogens are able to sufficiently trigger PRR signaling before an immune response is mediated.

Upon activation, epithelial cells secrete different molecules that either attract and activate immune cells or have a direct microbiocidal effect. Different epithelial-derived chemokines are involved in the recruitment of immune cells to the sites of infection (Nicod, 2005). Those include CXCL1, -2, -5 and -8 (IL8), which play a major role in attraction of $CXCR2^{+}$ neutrophils (Arango Duque and Descoteaux, 2014). In addition, epithelial cells can also produce CXCL9, -10 and -11, which stimulate infiltration of DCs, NK cells and T cells, whereas MPC-1 secretion acts as an attractant for monocytes (Schmeck *et al.*, 2006; Arango Duque and Descoteaux, 2014).

Besides this, pulmonary epithelial cells release different cytokines upon stimulation that activate immune cells against invading pathogens. Those include IL6, TNFα, IL1β, IL1α and GM-CSF (Øvrevik *et al.*, 2009). While IL6 is mainly known to activate lymphocytes, GM-CSF plays a role in activation of DCs and neutrophils during infection (Øvrevik *et al.*, 2009; Hernández-Santos *et al.*, 2018). On the other hand, IL1β and IL1α can stimulate the production of other chemokines and cytokines by immune cells in an NFκB or AP-1-dependent manner (Øvrevik *et al.*, 2009). Lastly, TNF-α promotes activation of antigen-presenting cells (APCs), as well as ROS and RNS production by endothelial cells and myeloid cells (Mukhopadhyay *et al.*, 2006).

Finally, effector molecules secreted by epithelial cells include cathelicidins and defensins, which are cationic antimicrobial peptides that rupture negatively charged bacterial membranes (Leiva-Juárez *et al.*, 2018). Additionally, ciliated epithelial cells and alveolar epithelial type-II cells (AECII) can produce ROS, which have direct antimicrobial properties (Leiva-Juárez *et al.*, 2018).

1.5.2.3. Alveolar macrophages and other tissue-resident immune cells

Tissue-resident lymphocytes can become activated in a specific manner via their T cell receptor (TCR) (conventional and unconventional T cells) and/or in an innate-like manner by pro-inflammatory cytokines, such as IL12, IL18, IL23 or IL33 (Fan and Rudensky, 2016; Brembilla *et al.*, 2018). Either type of activation results in the release of similar cytokines depending on the expression of specific signature transcription factors. For instance, cytotoxic T lymphocytes (CTLs) and Th1 cells express T-bet, and innate or TCR-mediated activation of those cells will, in both cases, lead to IFNγ secretion (Bhat *et al.*, 2017; Yoshimoto *et al.*, n.d.). Another example is mucosa-associated invariant T (MAIT) cells, which secrete IFNγ and IL17 in an MR1-dependent manner (Le Bourhis *et al.*, 2011). IFNγ and IL17 promote anti-microbial defenses in the lungs, by activating several immune cells, as well as by promoting the production of further pro-inflammatory cytokines (Delves and Roitt, 1998; Tan and Rosenthal, 2013; Fan and Rudensky, 2016). In addition, subsets of tissue-resident lymphocytes also secrete TNFα, which is known to activate APCs during pulmonary infection (Sun *et al.*, 2019). Besides this, activated $CD8^+$ T cells and some unconventional T cells can directly induce cytolysis of infected target cells, via secretion of cytolytic granules (de la Roche *et al.*, 2016).

AMs can be directly activated by pathogens (Kopf *et al.*, 2015) or by pro-inflammatory cytokines produced by other cells, such as epithelial cells, other tissue-resident cells or inflammatory immune cells. As for other myeloid cells, AMs activation results in different effector mechanisms ranging from an increased phagocytic activity, an enhanced microbiocidal function via expression of ROS and RNS, to the production of chemokines and pro-inflammatory cytokines (Forman and Torres, 2002; Peake *et al.*, 2003; Nicod, 2005; Islam *et al.*, 2013). Cytokines secreted by AMs include IL1α, IL1β, IL6, IL12, IL18 and TNFα (Garc *et al.*, 1999; Rubins, 2003). IL18 and IL12 can jointly activate T cells or NK cells and stimulate production of IFNγ (Arango Duque and Descoteaux, 2014). Besides this, AMs secrete chemokines similar to those produced by pulmonary

epithelial cells including CXCL9 and -10 (Arango Duque and Descoteaux, 2014). In addition, they can secrete CCL5, which attracts T cells, basophils, eosinophils and DCs to the lungs and mediates an activation of NK cells (Arango Duque and Descoteaux, 2014). Similar to pulmonary epithelial cells, AMs can also produce lysozyme, defensins, ROS and RNS, which directly participate in the antimicrobial defense (Nicod, 2005; Kopf *et al.*, 2015).

Altogether, pulmonary epithelial cells and tissue-resident immune cells cooperate in order to remove invading pathogens and to promote the inflammatory immune response during pulmonary infection by recruiting and activating inflammatory immune cells (Herold *et al.*, 2011).

1.5.2.4. Inflammatory innate immune cells

During infection different inflammatory immune cells transmigrate from the blood circulation into the lungs, instructed by chemokines that are initially produced by lung-resident cells (Nicod, 2005; Schmeck *et al.*, 2006; Arango Duque and Descoteaux, 2014). Those inflammatory immune cells comprise mainly neutrophils, monocytes, and DCs. Neutrophils are short-lived phagocytic cells that make up to 40-70 % of all leukocytes in the circulation, where they patrol blood vessels for signs of inflammation (Borregaard, 2010; Actor and Actor, 2012; Amulic *et al.*, 2012). They are mainly attracted to infected tissues via the chemokines CXCL1, -2, -5 and -8 (IL8) (Amulic *et al.*, 2012; De Filippo *et al.*, 2013; Arango Duque and Descoteaux, 2014). Likewise, circulating dendritic cells (DCs) can be recruited via the chemokines CXCL9, -10 and -11 and monocytes in the circulation are attracted by MPC-1 (Arango Duque and Descoteaux, 2014).

In order to enter the tissue, circulating innate immune cells generally bind P-selectins and E-selectins on the surface of the pulmonary endothelium, as well as the integrins VCAM-1 and ICAM-1. Those interactions allow adhesion of the circulating cells to the endothelium ultimately leading to transmigration of those into the infected tissue (Schnoor, 2015).

Once, neutrophils reach the sites of infection, they can take up pathogens by receptor-mediated phagocytosis and efficiently kill them through phagolysosomal effector mechanisms, such as lysozyme, defensins, serine

proteases, ROS, RNS and an acidic pH (Segal, 2005; van Kessel *et al.*, 2014). However, neutrophils may also induce immunopathology, due to their high cytotoxic capacity causing morbidity and mortality, as it has been described for influenza infections (Wang, 2018).

Circulating monocytes can be further divided into two functional subsets, based on their differential expression of Ly6C (Ly6C^{low} and Ly6C^{high} monocytes) (Ginhoux and Jung 2014; Brown et al. 2017). Inflammatory Ly6C^{high} monocytes can be activated after they reach the sites of infection and may develop into monocyte-derived macrophages and dendritic cells, or more generally, monocyte-derived cells (MCs) (Brown *et al.*, 2017). Like other myeloid cells, MCs can directly kill pathogens by phagocytosis and production of ROS and RNS, as well as by secretion of a myriad of pro-inflammatory cytokines and chemokines (Atkinson *et al.*, 2000; Brown *et al.*, 2016; Paardekooper *et al.*, 2019).

Lastly, DCs can phagocytose pathogens and participate as APCs in the priming of naive T cells in secondary lymphoid organs, or reactivation of T cells in the lung during infection (Théry and Amigorena, 2001).

1.5.3. Adaptive immunity

Concomitant to the early innate immune response, an antigen-specific T- and B-cell response is initiated during pulmonary infections. However, this adaptive response is slower to become protective, due to a low frequency of antigen-specific naive T and B cells. Those cells first need to undergo activation-induced clonal expansion and differentiation in the draining lymph nodes and the spleen, before they are numerous enough to mediate protection in the infected lungs (Smith-Garvin *et al.*, 2009).

Naïve T cells recirculate between the blood and secondary lymphoid organs, where they scan the environment with their antigen-specific T cell receptors (TCR), in order to detect antigens presented by specialized antigen-presenting DCs (Smith-Garvin *et al.*, 2009). Recognition of pathogens by DCs via their PRRs results in an upregulation of CCR7 and CCR8 expression, which allows them to migrate to the draining lymph nodes, following a CCL19 and -22 gradient (Théry and Amigorena, 2001). Additionally, activated DCs endocytose

and process the detected pathogens into antigen-peptides, that may be presented on MHC class-I or MHC class-II molecules on their surface (Guermonprez *et al.*, 2002). Once the cells reach the lymph nodes, they provide three signals for activation of naïve T cells (Smith-Garvin *et al.*, 2009; Goral, 2011). The first signal involves interaction of DCs via peptide/MHC complexes with the T cell receptor (TCR) (Corthay, 2006). Naïve $CD4^+$ T cells recognize peptide/MHC class-II complexes, whereas naïve $CD8^+$ T cells mainly bind peptide/MHC class-I complexes (Punt, 2013; Zinkernagel, M Rolf, n.d.). The second signal is generated by binding of the costimulatory molecules CD86 and CD80 to CD28 expressed by T cells (Linsley *et al.*, 1990). Lastly, the third signal is provided by a polarizing cytokine that is released by mature DCs and binds to a corresponding receptor on T cells. Depending on the cytokine, differentiation of naïve $CD4^+$ T cells is directed towards distinct subsets, including Th1, Th2, Th17, T_{FH} and Tregs cells (Punt, 2013). During pulmonary infection those T cells can produce different effector cytokines, such as IFNγ, TNFα and IL2, IL4 or IL17A, that play an important role in the defense of intracellular pathogens and in the activation of further immune cells (Chen and Kolls 2013).

In addition, naïve $CD8^+$ T cells require a “confirmation” signal referred to as help from activated $CD4^+$ T helper cells (Bevan, 2004). The nature of this signal may be diverse, but both CD40-CD40L and IL15 have been identified (Grewal and Flavell, 1996; Greyer *et al.*, 2016). Upon stimulation, naïve $CD8^+$ T cells differentiate into cytotoxic effector T cells, which recognize specific peptide/MHC-I complexes on the surface of infected cells and induce apoptosis (Charles A Janeway *et al.*, 2001; Punt, 2013). This is mediated by different mechanisms, of which the most important are the perforin/granzyme system, FAS/FasL interaction, and TNF-mediated cell death (Harty *et al.*, 2000; Zhang and Bevan, 2011).

In addition to T cells, naïve B cells also circulate through secondary lymphoid organs until they encounter their specific antigen (Melchers and Andersson, 1984; Maddaly *et al.*, 2010; Kato *et al.*, 2013). Cross-linking of the B cell receptor (BCR) results in an internalization and intracellular processing of the antigen into peptides, by which some of them are bound to MHC class-II

molecules and presented on the cell surface (Kato *et al.*, 2013). Interaction with T helper cells via this peptide/MHC class-II complex and through CD40L and CD40 induces proliferation and differentiation of the B cells into antibody-secreting plasma cells (Kato *et al.*, 2013). This interaction can also stimulate B cells to undergo an antibody isotype switch, that results in the production of specific IgA, IgE or IgG antibodies with distinct roles in host defense (Xu *et al.*, 2012). Besides this, mature B cells undergo affinity maturation, where cells that bind their antigen with high affinity for the specific antigen survive, while those that bind it with low affinity get eliminated (Kepler and Perelson, 1993; Ersching *et al.*, 2017). The fully developed plasma cells can infiltrate infected tissues and provide antigen-specific protective antibodies for sterilizing immunity (Levinson, 2016).

1.6. The role of interleukin 18 in anti-microbial defense

Interleukin 18 (IL18) is a cytokine of the IL1 family (Dinarello, 2018). Although IL18 has multiple functions, it is best known for its ability to strongly induce IFNγ production by T cells and NK cells in the presence of IL12 (Dinarello *et al.*, 2013). Because of this, it was first described as 'IFNγ-inducing factor' when discovered in 1989 (Nakamura *et al.*, 1989). By inducing IFNγ, IL18 enhances microbial clearance by stimulating phagocytic cells to produce TNFα, ROS, and RNS (Nakanishi *et al.*, 2001).

IL18 is synthesized as a 24 kDa biologically inactive precursor (proIL18) that lacks a secretion signal peptide and, therefore, remains intracellular (Nakanishi *et al.*, 2001; Dinarello *et al.*, 2013). ProIL18 is constitutively expressed by immune cells such as macrophages, microglia, monocytes, and DCs as well as non-immune cells like osteoblasts, keratinocytes and intestinal and pulmonary epithelial cells (Nakanishi *et al.*, 2001; Lorey *et al.*, 2004). Following inflammasome activation, proIL18 is cleaved into its mature, biologically active form by the intracellular cysteine protease caspase-1 (Kaplanski, 2018). The mature protein is then released through an inflammasome- dependent cell death, likely via activation of gasdermin-D, as recently described for IL1ß (Man *et al.*, 2017; Dinarello, 2018; Tapia *et al.*, 2019). Inflammasome-independent release of

mature IL18 has also been reported, where Fas ligand (FasL) activation of Kupffer cells or splenic macrophages induces a caspase-1-independent but caspase-8-dependent release of active IL18 (Dinarello *et al.*, 2013; Kaplanski, 2018). Lastly, proIL18 can be released into the extracellular space from dying cells, where neutrophil proteases, such as proteinase-3, can process it into its mature form (Sugawara *et al.*, 2001; Dinarello *et al.*, 2013).

Active IL18 binds to the IL18 receptor, which consists of a ligand-binding IL18Rα chain (IL18R1 or CDw218a) and the coreceptor IL18Rβ (IL18R accessory protein; IL18RAP or CDw218b). Binding of IL18Rα with low affinity induces recruitment of IL18Rβ and allows the formation of a high-affinity trimeric complex. The IL18Rα chain is constitutively expressed by most lymphoid cells and in most tissues (Smeltz *et al.*, 2001; Kaplanski, 2018). In contrast, expression of the IL18Rβ chain is inducible by the pro-inflammatory cytokines IL12 and IL2 (Boraschi *et al.*, 2018).

IL18R activation by its ligand triggers recruitment of Myeloid differentiation primary response 88 (MyD88), Interleukin-1 receptor-associated kinases (IRAKs) and TNF receptor-associated factor 6 (TRAF-6), which ultimately induce nuclear translocation of NFκB by degradation of IκB (Novick *et al.*, 2013). In addition, it has been shown, that IL18R signaling leads to Signal transducer and activator of transcription 3 (STAT3) phosphorylation in NK cells and to an induction of the p38 MAP kinase pathway in neutrophils (Kaplanski, 2018). Both pathways result in expression of various pro-inflammatory cytokines including IFNγ (Tsutsumi *et al.*, 2014).

Besides its function in promoting IFNγ production, IL18R signaling has diverse effects on different cells. It has been shown to support proliferation of $CD4^+$ T cells after TCR engagement, Th1 differentiation as well as production of IL2 and GM-CSF (Dinarello, 1999; Ogura *et al.*, 2001; Ishikawa *et al.*, 2006; Doherty, n.d.). In addition, IL18 directly enhances the cytotoxic activity of NK cells and cytotoxic T cells by promoting FasL expression and release of perforin, thus inducing apoptosis of infected target cells (Nakanishi *et al.*, 2001; Biet *et al.*, 2002). In addition to its effect on lymphoid cells, IL18 can also induce IL8 expression by activated neutrophils, resulting in the recruitment of additional

neutrophils to the sites of inflammation (Leung *et al.*, 2001). Moreover, IL18R signaling in neutrophils results in the release of lactoferrin from intracellular granules, which is a potent bacteriostatic factor by sequestering essential iron (Leung *et al.*, 2001).

In addition to immune cells, IL18R signaling has been demonstrated to play a significant role in intestinal epithelial cells, where it influences maturation of goblet cells and may promote development of colitis (Nowarski *et al.*, 2015). Besides this, studies with epithelial cell lines have shown that IL18R signaling promotes the production of pro-inflammatory cytokines such as IL6, IL8, and IL1α (Lee *et al.*, 2004). Similarly, during bacterial infection of pulmonary epithelial A549 cells, IL18 triggers the production of anti-microbial proteins, such as cathelicidins, in synergy with IL12 (Yang *et al.*, 2018).

In *L. pneumophila* infected murine lungs, it has been shown that IL18 promotes the production of IFNγ by immune cells (Brieland et al. 2000). However, although clearance of *L. pneumophila* was compromised in mice lacking IFNγ, it was not compromised in mice lacking IL18 (Brieland *et al.*, 2000; Brown *et al.*, 2016). This indicates, that that IL18 is not essential for the defense against *L. pneumophila* (Brieland *et al.*, 2000; Brown *et al.*, 2016). In contrast to *L. pneumophila,* the impact of IL18 on the clearance of *L. longbeachae* is still unknown.

1.7. Animal models of Legionnaires' disease

Animal models have been widely used to study Legionnaires' disease *in vivo* (Brown, 2013). Early research utilized mainly guinea pigs to investigate the disease pathogenesis and to develop therapeutic strategies or protective antimicrobial treatments (Fitzgeorge *et al.*, 1983). In 1994 researchers started to use mouse models to further investigate the molecular and cellular immune responses against *Legionella* spp. (Brown, 2013). However, studies with *L. pneumophila* revealed that infection of most inbred mouse strains was self-limiting, including C57BL/6 and BALB/c (Yoshida and Mizuguchi, 1986; Brieland *et al.*, 1994). In contrast, A strain mice are strongly susceptible to infections with *L. pneumophila* and develop acute pneumonia that resembles disease

development in humans (Brieland *et al.*, 1994). There is evidence that this increased susceptibility is due to polymorphisms in the gene encoding for the neuronal apoptosis-inhibitory protein 5 (Naip5) (Wright *et al.*, 2003), which recognizes bacterial flagellin in the cytosol of infected host cells and assembles with NLRC4 to form an inflammasome complex that induces a pro-inflammatory response (Tenthorey *et al.*, 2017). In order to generate acute infections in inbred mouse strains, researchers often use aflagellated *L. pneumophila* strains (Brown *et al.*, 2017).

Contrary to *L. pneumophila*, infection studies with *L. longbeachae*, which naturally lacks a flagellum, demonstrated a high mortality for various mouse strains, including C57BL/6 (Gobin *et al.*, 2009; Massis *et al.*, 2017). It has been proposed, that this difference is due to the lack of flagella in *L. longbeachae*, and therefore, due to the lack of involvement of the Naip5/NLRC4 inflammasome in the clearance of the bacteria (Brown, 2013). In addition, flaA mutants of *L. pneumophila* are less infective as their wild type counterparts, contributing to the differences observed (Heuner and Steinert, 2003).

However, infection of mice with lower doses of *L. longbeachae* can be readily used to investigate innate immune responses and molecular mechanisms that are involved in the defense of the bacteria (Gobin *et al.*, 2009; Massis *et al.*, 2017).

1.8. Immune responses against *Legionella* spp.

Initially, *L. pneumophila* infection in mice is directly recognized via TLR2, TLR5 and TLR9. More specifically, TLR2 senses LPS from the outer membrane of *L. pneumophila* and promotes production of proinflammatory cytokines and chemokines, as well as the recruitment of neutrophils to the sites of infection (Hawn *et al.*, 2006; Brown, 2013). In contrast, TLR5 recognizes flagellin of *L. pneumophila* and also mediates an initial recruitment of neutrophils to the lungs (Hawn *et al.*, 2006). However, deficiency of TLR5 only has a moderate effect on the bacterial burden, as recruitment of neutrophils is restored after approximately 24 hours of infection (Hawn *et al.*, 2006). The role of TLR9 in the defense of *L. pneumophila* is less well known and there are conflicting studies about its

function during infection with the bacteria. However, TLR9 has been shown to be important for an early control of *L. pneumophila* and stimulates the production of the pro-inflammatory cytokines TNFα and IL12 during infection (Bhan *et al.*, 2008; Brown, 2013). In agreement with the involvement of those TLRs, deficiency in the adaptor molecule MyD88 results in systemic spread of *L. pneumophila* and increased mortality (Brown, 2013). In contrast to *L. pneumophila* the role of TLRs in the defense of *L. longbeachae* still remains to be fully elucidated.

Besides TLRs, the NAIP5/NLRC4 inflammasome plays an important role in detection of *L. pneumophila* flagellin in the cytosol, initiating an inflammatory response that results in the efficient clearance of the bacteria from the infected lungs (Cazalet *et al.*, 2010; Brown, 2013; Mascarenhas and Zamboni, 2017a). Interestingly, the adaptor protein ASC-dependent NLRC4 inflammasome activation is not required for protection (Mascarenhas and Zamboni, 2017b), indicating an ASC-independent role of NAIP5/NLRC4 in protection against *L. pneumophila* (Mascarenhas and Zamboni, 2017a). Unlike *L. pneumophila*, the NAIP5/NLRC4 inflammasome has no effect on the control of *L. longbeachae* during infection, which is likely because those bacteria do not encode for flagella (Pereira *et al.*, 2011). Similarly, signal transduction via caspase-1 has no effect on the clearance of *L. longbeachae* after inflammasome activation, suggesting that this protease is not critical for protection *against the bacteria* (Asare *et al.*, 2007; Pereira *et al.*, 2011).

AMs serve as a replicative niche for *L. pneumophila* (Newton *et al.*, 2010a). However, activated AMs are still able to restrict replication of this bacterial strain by undergoing pyroptotic cell death following flagellin-dependent activation of the NAIP5/NLRC4 inflammasome (Newton *et al.*, 2010a). Consistent with this, the number of AMs rapidly decreases after infection with *L. pneumophila* (Brown *et al.*, 2017). Although *L. longbeachae* is able to infect monocytic cell lines *in vitro* (Wood *et al.*, 2015), it is currently unknown which cell, if any, serves as a replicative niche for the bacteria *in vivo*.

After recognition of invading *Legionella* spp., a pro-inflammatory immune response is triggered that is characterized by a strong infiltration of immune cells into the infected pulmonary tissue. Early after infection with *L. pneumophila*,

mainly neutrophils and monocytes infiltrate the lungs, engulf the bacteria and degrade them, resulting in clearance of the infection (Gobin *et al.*, 2009; LeibundGut-Landmann *et al.*, 2011; Massis *et al.*, 2017). Consistently, depletion of neutrophils causes an increased bacterial burden in the lungs of *L. pneumophila*-infected mice (Brown *et al.*, 2017). The capacity of neutrophils to eliminate the bacteria efficiently has been demonstrated to rely mostly on the production of ROS, which is triggered through translocation of effector proteins by *L. pneumophila* (Ziltener *et al.*, 2016). Besides this, activated neutrophils release TNFα and IL17A during infection with *L. pneumophila*, which have an influence on IFNγ secretion by lymphoid cells (Cai *et al.*, 2016; Brown *et al.*, 2017). The released IFNγ can then stimulate killing of *L. pneumophila* by monocytes and MCs in the infected tissue (Brown *et al.*, 2017). However, the contribution of monocytes, including MCs and neutrophils, to the defense against *L. longbeachae* is unknown yet (Gobin *et al.*, 2009; Massis *et al.*, 2017).

In contrast to the above described inflammatory immune cells, the contribution of DCs in the defense against *L. pneumophila* during infection still remains to be elucidated. DCs infiltrate the lungs after infection and phagocytose the bacteria (Andrew S. Brown, van Driel, and Hartland 2013). They are key cells in the regulation of T cell activity (Steinman and Hemmi, 2006). Therefore, it is likely that DCs are responsible for T cell priming during infection with *L. pneumophila* (Brown *et al.*, 2017).

Besides innate immune responses against *L. pneumophila*, less is known about protective specific immune responses (Brown, 2013). $CD4^+$ T helper cells and cytotoxic T cells contribute to the late defense, as demonstrated in T cell depletion studies (Susa *et al.*, 1998; Brieland *et al.*, 2000). The $CD4^+$ T helper compartment is mainly composed of Th1 and Th17 cells during *L. pneumophila* infection. Th1 cells primarily secrete IFN-γ, which has been demonstrated to be essential for the clearance of *L. pneumophila* from the lungs (Brieland *et al.*, 2000; Brown *et al.*, 2016). Th2 cells secrete GM-CSF, which may play a role in further recruitment of myeloid cells to the infected lung. In contrast, the role of adaptive immunity in protection against *L. longbeachae* is unknown yet and remains to be elucidated in future studies (Zhang *et al.*, 2013).

1.9. Aims of this study

Legionnaires' disease is a severe form of pneumonia caused by *Legionella* spp., and has been mostly studied in the context of infections with *L. pneumophila*. However, the second most frequent causative agent for the disease are *L. longbeachae* bacteria, of which mainly genomic studies have been performed. In contrast, the cellular and molecular host responses against *L. longbeachae* are widely unknown yet. The main goal of this study was to identify cellular and molecular mechanisms that are important in the defense against *L. longbeachae* infection. For this, I investigated the following questions:

1. Which immune cell types infiltrate the lungs and internalize *L. longbeachae*?
2. Which specific immune cells types contribute to clearance of *L. longbeachae* from the lungs?
3. What is the role of IL18 and its corresponding receptor in the defense against *L. longbeachae*?
4. How does IL18 receptor signaling on immune and non-immune cells contribute to the clearance of *L. longbeachae*?

Uncovering the main cellular and molecular mechanisms against *L. longbeachae* will provide a basic understanding of host immunity during pulmonary bacterial pneumonia and deepen our knowledge on how bacteria may persist.

Chapter 2: Materials and Methods

2.1. Materials

2.1.1. Equipment

Equipment	Manufacturer
Amnis® ImageStream®X Mk II	Luminex, MV 's-Hertogenbosch, Netherlands
Autoclave	Belimed, Cologne, Germany
Biobeam2000 γ-Irradiator	MCP-STS, Braunschweig, Germany
Cell counting chamber	Neubauer improved, BLAUBRAND®, Wertheim, Germany
Centrifuge 5810R	Eppendorf, Hamburg, Germany
CM12 transmission electron microscope	Philips, Hamburg, Germany
FACS Canto II	Becton, Dickinson and Company, Franklin Lakes, NJ, USA
FACSAria™ Fusion	Becton, Dickinson and Company, Franklin Lakes, NJ, USA
FACSAria™ II	Becton, Dickinson and Company, Franklin Lakes, NJ, USA
FastPrep-24™ 5G Instrument	MP Biomedicals, Santa Ana, CA, USA
Freezer (-20 °C)	Liebherr, Biberach, Germany
Freezer (-80 °C)	Heraeus, Braunschweig, Germany
HERAcell 240 incubator	Heraeus, Braunschweig, Germany
HERAsafe workbench	Heraeus, Braunschweig, Germany
Infrafil red light bulb	Phillips, Hamburg, Germany
IVC mouse cages	Tecniplast, Hohenpeißenberg, Germany
Light microscope BMIL	Leica Biosystems, Nußloch, Germany
LSM 710 confocal microscope	Carl Zeiss Microscopy, Jena, Germany

LSM 880 confocal microscope with Airyscan-Technology	Carl Zeiss Microscopy, Jena, Germany
LSR Fortessa	Becton, Dickinson and Company, Franklin Lakes, NJ, USA
Luminex MAGPIX®	Luminex, MV ‘s-Hertogenbosch The Netherlands
Magnetic Plate Washer	Thermo Fisher Scientific, Waltham, MA, USA
MicroPulser Electroporator	Bio-Rad Laboratories, Feldkirchen, Germany
MicroVent Ventilator, Model 848	Harvard Apparatus, Cambridge, MA, USA
NanoDrop 2000	Thermo Fisher Scientific, Waltham, MA, USA
Perfect spin 24 table top centrifuge	Peqlab, Erlangen, Germany
Pipettes (10 µL, 100 µL, 200 µL, 1000 µL)	Thermo Fisher Scientific, Waltham, MA, USA
Pipetus pipette-boy	Hirschmann Labortechnik, Eberstadt, Germany
Preparation instruments	Labortec, Göttingen, Germany
Refrigerators (+4 °C)	Bosch, Stattgart and Liebherr, Biberach, Germany
Rodent laryngoscope Model LS-2-M	Penn Century, Wyndmoor, PA, USA
Tecan Safire^2 microplate reader	Tecan Trading AG, Männedorf, Switzerland
Tissue Lyser LT	Qiagen, Hilden, Germany
TW8 water bath (37 °C)	Julabo, Seelbach, Germany
Ultrospec 10 Cell Densitiy Meter	Biochrom, Berlin, Germany
Vortex Genie 2	Bender & Hobein, Ismaning, Switzerland

VT1000S vibrating-blade microtome (vibratome)	Leica Biosystems, Nußloch, Germany

2.1.2. Consumables

Consumables	**Company**
Aesculap® safety scalpels	VWR, Darmstadt, Germany
BD Discardit™ syringes, 1 mL, 2 mL, 5 mL, 10 mL and 20 mL	Becton, Dickinson and Company, Franklin Lakes, NJ, USA
BD Microlance injection needles, 27G, 25G, 20G	Becton, Dickinson and Company, Franklin Lakes, NJ, USA
Cryo-tubes, 2 mL	TPP Techno Plastic Products AG, Transadingen, Switzerland
Electroporation Cuvettes, 2 mm	VWR, Darmstadt, Germany
Epoxy Embedding Medium kit	Merck, Darmstadt, Germany
FACS tubes polystyrene, 5mL, 75 x 12 mm	Sarstedt, Nümbrecht, Germany
Falcon® 40 µm Cell Strainer	Corning, Corning, USA
Hypodermic needle 22G x 1”	BBraun, Melsungen, Germany
Inoculation loop, 10 µL	Greiner bio-one, Solingen, Germany
Mediware® TBC syringes, 1 mL	Servoprax GmbH, Wesel, Germany
Micro haematocrit tubes, L= 75 +/- 0,5 mm	Brand, Wertheim, Germany
Microtiter plates, 6, 12, 24 and 96-well, round and flat bottom	TPP, Trasadingen, Switzerland
Microtome blades, ultra-thin 0.076 mm	Ted Pella Inc., Redding, CA, USA
Parafilm ”M”	American National Can TM, Greenwich, USA
Pasteur pipettes, 150 mm and 230 mm	Roth, Karlsruhe, Germany
Petri dishes, 10 cm	Greiner bio-one, Solingen, Germany

Pipette tips, 10 µL, 200 µL and 1000 µL	Greiner bio-one, Solingen, Germany
Polypropylene tubes, 15 mL and 50 mL	Greiner bio-one, Solingen, Germany
Precellys® 2 mL Soft Tissue Homogenizing Ceramic Beads	Cayman Chemical, Michigan, USA
Reaction tubes, 1,5 mL and 2 mL	Eppendorf, Hamburg, Germany
Sieves, steel	University of Bonn, Department „Feinmechanik", Bonn, Germany
Stainless Steel Beads, 3mm	Qiagen, Hilden, Germany
UV-cuvettes 1.5-3 mL	Brand, Wertheim, Germany
Vasofix IV Safety Ported Cannula, 22G x 1"	BBraun, Melsungen, Germany

2.1.3. Chemicals and reagents

Reagent	**Company**
4',6-Diamidino-2phenylindole (DAPI)	BioLegend, San Diego, CA, USA
Acetone	Polysciences, Warrington, PA, USA
Agarose, low-temperature melting	Promega GmbH, Madison, WI, USA
Antigenfix	Diapath S.p.A., Martinengo, Bergamo, Italy
Bovine serum albumin fraction V (BSA)	Roth, Karlsruhe, Germany
Brain Heart Broth (BHI)	Sigma-Aldich, St. Louis, MO, USA
Buffered charcoal yeast extract agar (BCYE) plates	Oxoid Limited, Hampshire, United Kingdom
CaliBRITE™ Beads	Becton, Dickinson and Company, Franklin Lakes, NJ, USA

Clodronate liposomes	Liposoma B.V., Amsterdam, The Netherlands
Collagenase type III	Worthington Biochemical Corporation, Lakewood, NJ, USA
Collagenase type IV	Roche, Berlin, Germany
Digitonin	Sigma-Aldrich, St. Louis, MO, USA
Dimethylsulfoxide (DMSO)	Roth, Karlsruhe, Germany
Disodiumhydrogenphosphate (Na_2HPO_4)	Merck, Darmstadt, Germany
DNAse I	Roche, Mannheim, Germany
Donkey gamma globulin	Jackson ImmunoResearch, Ely, UK
Dulbecco´s modified eagle medium (DMEM)	Sigma-Aldrich, St. Louis, MO, USA
Ethylene diamine tetra acetic acid (EDTA)	Merck, Darmstadt, Germany
Fetal calf serum (FCS)	Life Technologies, Carlsbad, CA, USA
Fixable Viability Dye eFluor® 506	eBioscience, San Diego, CA, USA
Fixable Viability Dye eFluor® 780	eBioscience, San Diego, CA, USA
Foxp3 / Transcription Factor Staining Buffer Set	eBioscience, San Diego, CA, USA
Gelatin from cold water fish skin (CWFG)	Sigma-Aldrich, St. Louis, MO, USA
GeneBLAzer™ *In Vivo* Detection Kit	Thermo Fisher Scientific, Waltham, MA, USA
Gentamicin	Thermo Fisher Scientific, Waltham, MA, USA
Glutaraldehyde 2.5 % in 0.1 M Sodium Cacodylate Buffer, pH 7.4	Ladd Research, Williston, VT, USA
Glutaraldehyde 25 %	Merck, Darmstadt, Germany

Glycine	Sigma-Aldrich, St. Luis, MO, USA
Goat gamma globulin	Jackson ImmunoResearch, Ely, UK
Hoechst 33528	Sigma-Aldrich, St. Louis, MO, USA
Isoflurane	AbbVie, North Chicago, IL, USA
Ketamine 10 %	WDT, Garbsen, Germany
Lead citrate, 3 %	Science Services GmbH, München, Germany
Liquid nitrogen (LN_2)	Linde, Wiesbaden, Germany
L-lysine monohydrate	Merck, Darmstadt, Germany
Mouse gamma globulin	Jackson ImmunoResearch, Ely, UK
Mouse MUC5AC ELISA Kit (Colorimetric)	Novus Biologicals, Centennial, CO, USA
Mouse MUC5B ELISA Kit (Colorimetric)	Novus Biologicals, Centennial, CO, USA
Octagam® 10 % normal human IgG	Octapharma, Langenfeld, Germany
Osmium tetroxide 4 %	Merck, Darmstadt, Germany
Paraformaldehyde 16 % (PFA), methanol-free	Thermo Fisher Scientific, Waltham, MA, USA
PBS liposomes	Liposoma B.V., Amsterdam, The Netherlands
Penicillin/Streptomycin	Merck, Darmstadt, Germany
Permeabilization buffer (x10)	eBioScience™; San Diego, CA, USA
Phorbol 12-myristate 13-acetate (PMA)	Sigma-Aldrich, St. Louis, MO, USA
Phosphatase Inhibitor Cocktail Set II	Merck, Darmstadt, Germany
Phosphate buffered saline (PBS)	Life Technologies, Carlsbad, CA, USA
ProcartaPlex Mouse Basic Kit	Thermo Fisher Scientific, Waltham, MA, USA

ProcartaPlex Simplex Kits	Thermo Fisher Scientific, Waltham, MA, USA
Propidium iodide (PI)	Sigma-Aldrich, St. Louis, MO, USA
Rat gamma globulin	Jackson ImmunoResearch, Ely, UK
Recombinant mouse IL-18	BioLegend, San Diego, CA, USA
RNeasy Plus Micro Kit (50)	Qiagen, Hilden, Germany
Rompun 2 % (Xylazin)	Bayer, Leverkusen, Germany
Roswell park memorial institute medium 1640 (RPMI)	Invitrogen, Darmstadt, Germany
RPMI 1640 medium, GlutaMAX	Invitrogen, Darmstadt, Germany
Saponin	Sigma-Aldrich, St. Louis, MO, USA
Sodium azide (NaN_3)	Roth, Karlsruhe, Germany
Sodium cacodylate trihydrate	Merck, Darmstadt, Germany
Sodium chloride (NaCl)	Sigma-Aldich, St. Louis, MO, USA
Sodium dihydrogen phosphate (NaH2PO4)	Merck, Darmstadt, Germany
Sodium hydroxide (NaOH)	Thermo Fisher Scientific, Waltham, MA, USA
Sodium periodate ($NaIO_4$)	Sigma-Aldrich, St. Luis, MO, USA
Triton-X 100	Sigma-Aldich, St. Louis, MO, USA
Trizma® hydrochloride (Tris HCl)	Sigma-Aldich, St. Louis, MO, USA
Trypan blue (0.4 %)	Lonza, Cologne, Germany
Tween® 20	Roth, Karlsruhe, Germany
Uranyl Acetate	Electron Microscopy Sciences, Hatfield, PA, USA

2.1.4. Buffers, media and solutions

Buffer	Reagents
ACK Lysis Buffer	Double distilled H_2O (ddH_2O), 150 mM NH_4Cl, 10 mM $KHCO_3$, 0.1 mM EDTA
BHI Medium	ddH_2O, 37 g/L BHI (w/v)

Cell Lysis Buffer	ddH_2O, 10 µg/mL Digitonin (w/v)
Confocal Blocking Buffer	PBS, 1 % CWFG (w/v), 1 % FCS (v/v), 0.3 % Triton-X 100 (v/v), containing a relevant blocking Ig
FACS Blocking Buffer	PBS, 3 % (v/v) FCS, 0.1 % (v/v) NaN_3, 0.05 % Octagam® normal IgG
FACS Buffer	PBS, 3 % (v/v) FCS, 0.1 % (v/v) NaN_3
P Buffer	ddH_2O, 0.2 M NaH_2PO_4 (w/v), 0.2 M Na_2HPO_4 (w/v); adjust to pH 7.4
PLP Buffer	P buffer 0.1 M, 4 % PFA (v/v), 0.2 M L-lysine (v/v), 1 M NaOH (v/v), 0.01 M $NaIO_4$ (w/v)
RPMI Buffer	RPMI Glutamax, 1 % (v/v) FCS, 15 µg/mL Gentamicin (v/v)
Washing Buffer	PBS, 0.05 % Tween® 20 (v/v)

2.1.5. Antibodies

2.1.5.1. Antibodies for flow cytometry analysis

The following fluorochrome-conjugated antibodies were used for flow cytometric analysis of murine antigens:

Antigen	**Clone**	**Company**
CD103	2E7	BioLegend, San Diego, CA, USA
CD11b	M1/70	BioLegend, San Diego, CA, USA
CD11c	N418	BioLegend, San Diego, CA, USA
CD19	6D5, 1D3	BioLegend, San Diego, CA, USA
CD19	1D3	BD Biosciences, Franklin Lakes, NJ, USA
CD218a	BG/IL18RA	BioLegend, San Diego, CA, USA
CD218a	P3TUNYA	eBioscience, San Diego, CA, USA
CD31	MEC 13.3, 390	BioLegend, San Diego, CA, USA
CD326	G8.8	BioLegend, San Diego, CA, USA
CD3e	145-2C11	BioLegend, San Diego, CA, USA

CD4	GK1.5	BioLegend, San Diego, CA, USA
CD44	IM7	BioLegend, San Diego, CA, USA
CD45	30-F11	BioLegend, San Diego, CA, USA; BD eBioscience, Franklin Lakes, NJ, USA
CD45.1	A20	BioLegend, San Diego, CA, USA
CD45.2	104	BioLegend, San Diego, CA, USA
CD64	X54-5/7.1	BioLegend, San Diego, CA, USA
CD8a	53-6.7	BioLegend, San Diego, CA, USA
CD8b	YTS 156.7.7	BioLegend, San Diego, CA, USA
CD90.1	OX-7	BD Biosciences, Franklin Lakes, NJ, USA
CD90.2	53-2.1	BioLegend, San Diego, CA, USA
F4/80	BM8	BioLegend, San Diego, CA, USA
I-A/I-E	M5/114.15.2	BioLegend, San Diego, CA, USA
L. longbeachae	Rabbit polyclonal serum	Provided by Prof. Hartland, Hudson Institute of Medical Research
Ly6C	HK1.4	BioLegend, San Diego, CA, USA
Ly6G	1A8	BioLegend, San Diego, CA, USA; BD Biosciences, Franklin Lakes, NJ, USA
NK1.1	PK136	BioLegend, San Diego, CA, USA; BD Biosciences, Franklin Lakes, NJ, USA
NKp46	29A1.4	eBioscience, San Diego, CA, USA
Rabbit IgG	polyclonal	Thermo Fisher Scientific, Waltham, MA, USA
Siglec-F	E-50-2440	BD Biosciences, Franklin Lakes, NJ, USA
TCRβ	H57-597	BioLegend, San Diego, CA, USA
TCRγ/δ	GL3	BioLegend, San Diego, CA, USA
TCRγ/δ	UC7-13D5	BioLegend, San Diego, CA, USA
TER-119	TER-119	BioLegend, San Diego, CA, USA

The following antibodies were used for confocal microscopy analysis of murine lung slices:

2.1.5.2. Antibodies for confocal microscopy

Antigen	Label	Species/Isotype	Clone	Company
Acetylated Tubulin	-	Mouse IgG2b	6-11B-1	Sigma-Aldrich, St. Louis, MO, USA
Actin α-Smooth Muscle	-	Mouse IgG2a	1A4	Sigma-Aldrich, St. Louis, MO, USA
Aquaporin 5	-	Rabbit IgG	Polyclonal	Abcam, Cambridge, UK
Aquaporin 5	AF488	Rabbit IgG	Polyclonal	Bioss Antibodies, Boston, USA
CD31	AF488	Rat IgG2a	MEC13.3	BioLegend, San Diego, CA, USA
CD326 (EpCAM)	AF647	Rat IgG2a	G8.8	BioLegend, San Diego, CA, USA
CD45	BV421	Rat IgG2b	30-F11	BioLegend, San Diego, CA, USA
CD45.2	AF488	Mouse IgG2a	104	BioLegend, San Diego, CA, USA
Mouse IgG2a	AF488	Goat IgG	Polyclonal	Jackson ImmunoResearch, Ely, UK
Mouse IgG2b	DL405	Goat IgG	Polyclonal	Jackson ImmunoResearch, Ely, UK
Prosurfactant Protein C	-	Rabbit IgG	07-647	Merck, Darmstadt, Germany

Rabbit IgG	DL405	Donkey IgG	Polyclonal	Jackson ImmunoResearch, Ely, UK
Rabbit IgG	AF647	Donkey IgG	Polyclonal	Jackson ImmunoResearch, Ely, UK
Uteroglobin	-	Rabbit IgG	EPR19846	Abcam, Cambridge, UK

2.1.5.3. Antibodies for *in vivo* cell depletion

In vivo depletion of different immune cell populations was performed using the following mAb:

Antigen	Clone	Species/Isotype	Company
CD4	GK1.5	Rat, IgG2b	BioXCell, Lebenon, NH, USA
CD8a	YTS 169.4	Rat, IgG2b	BioXCell, Lebenon, NH, USA
Ly6G	1A8	Rat, IgG2a	BioXCell, Lebenon, NH, USA
NK1.1	PK136	Mouse, IgG2a	BioXCell, Lebenon, NH, USA

The following irrelevant isotype-matched mAbs were used as negative controls:

Antigen	Clone	Species/Isotype	Company
KLH	LTF-2	Rat, IgG2b	BioXCell, Lebenon, NH, USA
Phycoerythrin	2A3	Rat, IgG2a	BioXCell, Lebenon, NH, USA
Unknown	C1.18.4	Mouse, IgG2a	BioXCell, Lebenon, NH, USA

2.1.6. Vectors

Name	Plasmid	Company
pON.mCherry	84821	Addgene, Watertown, MA, USA

2.1.7. Mouse strains

C57BL/6 (B6) wild-type mice were bred under specific pathogen-free (SPF) conditions and in accordance with institutional animal guidelines in the animal facilities (House of Experimental Therapie, HET; Bio21 Institute) of the University of Bonn and the University of Melbourne. Experiments were performed with mice 8-12 weeks of age. All mice were backcrossed to the B6 background for at least 10 generations. The following mice were used:

Mouse strain	Description
BL6	C57BL/6J. Non-transgenic wild-type (WT) mice.
Ccr2$^{-/-}$	B6.129S4-*Ccr2tm1Ifc*/J. Mice lacking the gene encoding chemokine C-C motif receptor type 2 (CCR2). These mice consequently have reduced numbers of cells that are dependent on CCR2 (Boring *et al.*, 1997).
CD45.1	B6.SJL-*Ptprc*^{a} *Pepc*^{b}/BoyJ. Mice expressing the congenic pan-leucocyte marker CD45.1 (Mardiney and Malech, 1996).
Cd4-cre	Tg(Cd4-cre)1Cwi/BfluJ. In this mice expression of a cre recombinase is under control of the gene for CD4 from T cells, allowing application of the cre/loxP system. (Sawada *et al.*, 1994)
Il18$^{-/-}$	B6.129P2-*Il18*^{tm1Aki}/J. These mice lack the ability to produce the cytokine IL-18 (Takeda *et al.*, 1998).
Il18r$^{-/-}$	B6.129P2-*Il18r1*^{tm1Aki}/J. These mice do not express the receptor for the cytokine IL-18 (Hoshino *et al.*, 1999)
IL18R1-tdTomato	Unpublished. Knock-in reporter mice generated by Ozgene (Australia) for Prof. Kastenmüller (University of Würzburg). In these mice tdTomato expression is under the control of the endogenous *Il-18r1* promotor.
IL18R$^{flx/flx}$	Unpublished. Mice were generated by Prof. Kastenmüller (University of Würzburg). In these mice the gene for the IL-18R is flanked by two loxP sites, allowing cell-specific Cre-mediated recombination.

A maximum of 5 mice were kept under pathogen-free conditions (SPF) in one individual ventilated cage (IVC). Ventilation was constant with 22 °C and 50-60 % air humidity. The animals were kept in a 12-hour light-dark cycle. Cages and beddings were exchanged weekly by qualified animal caretakers and the mice received autoclaved water and food. One week before an experiment, animals were transferred to the laboratory rooms, exhibiting the same conditions as described before.

2.1.8. Pathogens

Pathogen	Description
L. longbeachae pXDC61 BlaM	Genetically modified *L. longbeachae* NSW150 expressing the empty vector pXDC61 BlaM
L. longbeachae-mCherry	Genetically modified *L. longbeachae* NSW150, expressing mCherry
L. longbeachae pXDC61 RalF-BlaM	Genetically modified *L. longbeachae* strain NSW150 containing the vector pXDC61 RalF-BlaM
Legionella longbeachae	Strain NSW150; clinical isolate
Legionella pneumophila	Strain JR32 *ΔflaA* with a deletion of the *flaA* gene, resulting in non-flagellated *L. pneumophila.*

2.1.9. Software

Software	Company
FACS Diva V8.01	Becton, Dickinson and Company, Franklin Lakes, NJ, USA
FlowJo V10.1	Tree Star, Ashland, OR, USA
Illustrator CC2018	Adobe Systems, San Jose, CA, USA
ImageJ/Fiji v.152i	Open Source

Imaris 7.6.3	Bitplane, Zurich, Switzerland
MS Office 2016	Microsoft, Redmond, WA, USA
Photoshop CC2018	Adobe Systems, San Jose, CA, USA
Prism 8.0.2	GraphPad Software, La Jolla, CA, USA
ZEN V	Carl Zeiss Microscopy GmbH, Jena, Deutschland
Zotero 5.0.74	Open Source

2.2. Methods

2.2.1. Bacterial culture

Legionella bacteria were exponentially grown on buffered charcoal yeast extract (BCYE) agar plates at as previously described (Massis *et al.*, 2017). Briefly, bacteria stored at -80 °C in 50 % (v/v) glycerol/BHI solution were plated on BCYE agar plates by using the streak plate method. After approximately 72 h at 37 °C, 3-5 colonies were pooled and resuspended in PBS for intranasal infection.

2.2.2. Generation of mCherry-expressing *L. longbeachae*

L. longbeachae was grown on BCYE agar plates as described in section 2.2.1. Five colonies were picked and resuspended in 200 µL ddH_2O containing 10 ng pON.mcherry plasmid. Bacteria were then electroporated in 2 mm cuvettes at 2.5 kV, 200 Ω and 25 µV for 4 ms and 100 µL bacterial suspension was plated on BCYE agar plates. Three days after incubation at 37 °C violet colonies were picked and stored in 50 % (v/v) glycerol/BHI solution at -80 °C until further use.

mCherry expression was confirmed by flow cytometric analysis of *L. longbeachae*-mCherry in 3-5 pooled colonies. Stable mCherry expression was confirmed by visual evaluation of *L. longbeachae* colonies grown in BCYE plates after 5 serial passages of single colonies over a period of 15 days in the absence of selection for the pON.mCherry plasmid.

2.2.3. Intranasal infection of mice with Legionella

Mice were infected with Legionella intranasally, as previously described (Brown et al. 2016). Briefly, bacteria were grown on BCYE agar plates as described in

section 2.2.1. 3-5 colonies were resuspended in PBS and the absorbance at an optical density of 600 nm (OD_{600}) was adjusted to 1, corresponding to $1x10^9$ CFU/mL *L. longbeachae* or *L. pneumophila*. The infection dose was then adjusted by dilution in PBS. Mice were anesthetized with 2 % isoflurane/O_2 (v/v) and 50 µL PBS, containing the indicated bacterial dose, was slowly administered dropwise into the nostrils of mice kept in supine position. The infection dose used in each experiment was confirmed by retrospective CFU quantification.

For *L. longbeachae* studies conducted in Melbourne, mice were infected with $2.5x10^5$ CFU i.n. However, that dose proved to be lethal for the same mouse strain in Bonn. Therefore, mice in Bonn were infected with 10^4 CFU i.n. Importantly, infected mice at both locations underwent similar weight loss and harbored comparable numbers of CFU in the lungs 3 and 5 days after infection with their respective doses.

All infections with *L. pneumophila* were conducted in Melbourne using $2.5x10^5$ CFU per mouse.

2.2.4. Quantification of Legionella CFU in infected organs

At the indicated times after infection with Legionella, mice were killed by CO_2 asphyxiation. The right lung excluding trachea, the bronchia external side, and mediastinal lymph nodes, was then collected into 2 mL Eppendorf tubes containing 2 stainless steel beads in 1 mL PBS and homogenized using the Tissue Lyser LT (Qiagen) at 50 oscillations/s. After 30 min, cells were lysed by adding 1 mL PBS containing 0.1 % saponin for further 30 min at 37 °C. The lung homogenate was serially diluted 1/10 in PBS (1 mL final volume) and 100 µL (*L.pn.*) or 25 µL (*L.lo.)* of each dilution was plated in duplicates on BCYE agar plates using the streak plate method. Colonies were manually counted after 3 days of culture at 37 °C. The CFU was calculated by using the following formulae:

$CFU / lung = n \times DF_a \times DF_b \times DF_c$

Where:

n = average number of colonies from duplicate plates

DF_a = 2 (for total lung -right and left lobes)

DF_b = factor for sample dilution

DF_c = Factor for plating dilution; DF_c = 10 or 4 for *L. pneumophila* or *L. longbeachae*, respectively.

2.2.5. *In vivo* cell depletion

Neutrophils and NK cells were depleted *in vivo* to identify their specific role in the defense against *L. longbeachae* following established protocols.

Depletion of neutrophils was accomplished by i.p. injection of 200 µl PBS containing 200 µg anti-Ly6G mAb (clone 1A8) every third day (Daley *et al.*, 2008) , starting one day before infection. Control mice were similarly treated with an equivalent amount of irrelevant, isotype-matched antibody (rat IgG2a, clone 2A3) directed against phycoerythrin.

Depletion of NK cells was accomplished by i.p. injection of 200 µl PBS containing 200 µg anti-NK1.1 mAb (clone PK136) every third day, starting one day before infection (Hochweller *et al.*, 2009). Control mice were similarly injected with an equivalent amount of an irrelevant, isotype-matched antibody (mouse IgG2a, clone 2A3).

Cell depletion was confirmed by flow cytometry in the blood and lungs for each experiment.

2.2.6. Intravascular leukocyte staining

Mice were anesthetized with 10 mg/kg body weight (bw) Xylazine and 100 mg/kg bw Ketamine. Afterwards, 100 µL PBS containing 5 µg of AlexaFluor 488-labeled anti-CD45.2 antibody was injected i.v. into the lateral tail vein. Exactly 5 min later, excess antibody in the pulmonary circulation was removed via intracardial perfusion with PBS through the right ventricle. Lungs were then removed and processed for flow cytometry (Section 2.2.7 and 2.2.8).

2.2.7. Cell isolation for flow cytometry

Mice were painlessly killed as described in Section 2.2.1 or 2.2.8. Pulmonary blood was removed by perfusion as described in Section 2.2.8, or by severing the lower aorta.

Lungs were dissected out excluding trachea, external part of bronchi and lymph nodes, injected with 1 mL ice-cold digestion buffer and incubated in a total volume of 4 mL digestion buffer. After 5 min at room temperature (RT), lungs were disrupted with surgical forceps and incubated in 15 mL tubes for further 30 min at 37 °C with occasional mixing by pipetting, resulting in complete digestion. Cell suspensions were then filtered through a 100 µm cell strainer and washed with 10 mL ice-cold PBS at 1500 rpm for 5 min at 4 °C. Cells were resuspended in 1- or 2-mL ice-cold PBS and kept at 4 °C until further use.

For taking cells in the bronchoalveolar space, tracheas were exposed by removing the surrounding skin, tissue, and muscles. Tracheas were then cannulated with a 22G x 1” hypodermic needle attached to a 2 cm polyethylene tubing with a diameter of 0.85 mm. Cells were collected by three washes with 1 mL PBS containing 5 mM EDTA at RT, centrifuged at 1500 rpm for 5 min at 4 °C, resuspended in 1 mL ice-cold PBS, and kept at 4 °C until further use.

Spleens were dissected and passed through a 100 µm cell strainer to make single-cell suspensions in ice-cold PBS. Cells were then centrifuged at resuspended in 1 mL ice-cold PBS and kept at 4 °C until further use.

For isolation of peripheral blood leukocytes, blood from the facial or tail vein was collected into 2 heparinized 70 µL micro-hematocrit capillaries and pooled. Red blood cells (RBC) were lysed in 500 µL ACK Lysis Buffer for 12 min at RT. Lysis was stopped by adding 500 µL ice-cold PBS containing 3 % FCS. Cells were centrifuged at 1500 rpm for 5 min at 4 °C, resuspended in ice-cold PBS and kept at 4 °C until further use.

2.2.8. Flow cytometry

Depending on the organ of origin, 0.5-2x10^6 cells were transferred to 96-well U-bottom plates. Staining of antigens expressed on the cell surface was performed in 50 µL of a mAb cocktail in FACS Blocking Buffer for 30 min at 4 °C in the dark. Cells were then washed twice with 200 µL ice-cold PBS at 1500 rpm and stained with the Fixable Viability Dye eFluor 780 or eFluor 506 according to the manufacturer´s instructions in order to exclude dead cells during flow cytometry analysis. After washing 3 times in PBS, cells were fixed in 200 µL PBS containing

2 % PFA for 30 min at RT. Cells were further washed in 200 µL FACS buffer and resuspended in 200 µL FACS buffer containing 2 x 10^4 fluorochrome-labelled CaliBRITE™ Beads for quantification of cell numbers by flow cytometry.

When stated, *L. longbeachae* bacteria were intracellularly stained with an anti-*L. longbeachae* antibody. Following staining of surface antigens and dead cells as described above, cells were incubated in Fixation/Permeabilization Buffer (Foxp3/Transcription Factor Staining Buffer Set, eBioscience) for 30 min at 4 °C. Afterwards, cells were washed with Permeabilization Buffer (Foxp3/Transcription Factor Staining Buffer Set, eBioscience) for 5 min at 1200 rpm. The cells were resuspended in 50 µL Permeabilization Buffer containing rabbit anti-*L. longbeachae* polyclonal serum diluted 1/500 for 30 min at RT in the dark. Following this, cells were washed with Permeabilization Buffer for 5 min at 1200 rpm. Cells were then resuspended in 50 µL Permeabilization Buffer containing AlexaFluor488-labeled anti-rabbit antibody for 30 min at RT. Cells were washed with 1 mL Permeabilization Buffer (Foxp3/Transcription Factor Staining Buffer Set, eBioscience) at 1200 rpm and finally resuspended in 200 µL FACS buffer.
Cells were acquired on an LSRFortessa or sorted via the FACSAria fusion or FACSAria II using FACSDiva version 8.01 for data-acquisition and FlowJo version 10.1 for data analysis.

2.2.9. Quantification of Legionella RalF translocation

For the RalF translocation assay, mice were infected i.n. with 2.5x10^5 CFU *L. longbeachae* pXDC61 RalF-BlaM or *L. longbeachae* pXDC61 BlaM as described in section 2.2.3. Mice were painlessly killed with CO_2 asphyxiation 2 days after infection, and cell suspensions were generated from the spleen and lungs as described in section 2.2.7. After staining surface antigens and dead cells as described in section 2.2.8, cells were loaded with the β-lactamase substrate CCF2-AM from the GeneBLAzer™ *In Vivo* Detection Kit following the manufacturer´s instructions.

The RalF translocation assay works as follows: *L. longbeachae* pXDC61 RalF-BlaM expresses the effector molecule RalF as fusion protein together with ß-lactamase (BlaM), which can be translocated into the host cell cytosol via the

bacterial Dot/Icm type IV secretion system (Wood *et al.*, 2015). The ß-lactamase substrate CCF2-AM reaches the cytosol when added exogenously and contains the two fluorophores hydroxycoumarin and fluorescein. In the absence of the translocated RalF-BlaM in the cytosol, excitation of hydroxycoumarin leads to an energy transfer through FRET to the acceptor molecule fluorescein. This results in an emission of green light in a wavelength of 530 nm. However, translocated RalF-BlaM hydrolyzes CCF2-AM producing 3-fluorescein and causing a shift in the emission wavelength from 530 nm to 460 nm (Jones and Padilla-Parra, 2016). This change in emission can then be readily detected via FACS analysis.

2.2.10. Identification of immune cells containing viable Legionella

Cells were isolated from the lungs of mice infected with either *L. pneumophila* or *L. longbeachae* as described in section 2.2.6 and stained for cell sorting as stated in section 2.2.7. Single viable Hoechst^{-}CD45^{+} cells were FACS sorted into PBS at 4-°C. Single viable neutrophils were FACS sorted as Hoechst^{-} CD45^{+}CD11b^{+}Ly6G^{+}Ly6C$^{+/-}$ cells into PBS at 4 °C. Single viable monocytes were FACS sorted as Hoechst^{-}CD45^{+}CD11b^{+}Ly6G^{-}Ly6C^{+} cells. Single viable AMs were FACS sorted as Hoechst^{-}CD45^{+}SiglecF^{+}CD11c^{+} cells. Cells in each sorted population was immediately lysed in 200 µL Cell Lysis Buffer for 5 min at RT and kept on ice until plating on BCYE agar plates. 100 µL of the lysates containing 10^4 cells were each plated in duplicates and incubated at 37 °C for 3 days.

2.2.11. Imaging flow cytometry

Hoechst^{-}CD45^{+} cells were sorted as described in section 2.2.10. Cells were then visualized using an Amnis® ImageStream$^{®X}$ Mk II machine.

2.2.12. *L. longbeachae* killing assay

The ability of neutrophils to kill *L. longbeachae* was analyzed using an *ex vivo* killing assay. For this, neutrophils containing *L. longbeachae* were FACS sorted from the lungs of mice, that were infected with 10^4 CFU *L. lo.*-mCherry 3 days earlier, as Hoechst^{-}CD45^{+}CD11b^{+}Ly6G^{+} mCherry^{+} cells into RPMI Buffer at 4 °C. The sorted population was split into two equal aliquots in 1.5 mL microcentrifuge

tubes and centrifuged at 1200 rpm for 5 min at 4 °C. The cell pellet of one aliquot (referred to as T=0 min) was immediately lysed in 200 µL Cell Lysis Buffer for 5 min at RT and kept on ice until plating on BCYE agar plates. The cell pellet of the other aliquot (T=30 min) was resuspended in 200 µL RPMI Buffer supplemented with 1 % FCS and incubated for 30 min at 37 °C to allow for *ex vivo* bacterial killing. Cells were then lysed as their T= 0 min counterparts. 100 µL of cell lysate was then plated on BCYE agar plates for quantification of *L. longbeachae* CFUs as described in section 2.2.4.

2.2.13. Cytokine profiling

Bronchoalveolar lavage fluid (BALF) was isolated from mice as described before but with only 500 µL PBS. Afterwards, the sample was centrifuged at 1200 rpm and 4 °C for 5 min. The concentration of IFNγ and IL18 in 25 µL of undiluted BALF was measured using the ProcartaPlex Mouse Basic Kit and ProcartaPlex Simplex Kits for IFNγ and IL18 (Thermo Fisher Scientific). The assay was performed using the manufacturer's instructions and the analysis was done with the Luminex 200 system. Briefly, 50 µL of magnetic beads coated with anti-IL18 or -IFNγ mAbs were added to each well of a 96-well microtiter plate. The plate was secured on a hand-held Magnetic Plate Washer and washed with 150 µL Wash Buffer. Afterwards, 25 µL of PBS were combined with 25 µL of each sample or diluted standard before they were added to the appropriate wells and incubated for 60 min at RT, shaking at 500 rpm. After washing, 25 µL Detection Antibody Mixture containing biotinylated anti-IL18 or -IFNγ mAbs, was added to each well and the plate was incubated for 30 min at RT, shaking at 500 rpm. Subsequently, the plate was washed 3 times before 50 µL Streptavidin-PE solution (SAPE) was added to each well. After shaking at 500 rpm for period for 30 min at RT, the plate was washed and 120 µL Reading Buffer were added to each well. The analysis was performed using a Luminex MAGPIX® instrument.

2.2.14. MUC5AC and MUC5B ELISA

WT, *Il18*$^{-/-}$ or *Il18r*$^{-/-}$ mice were infected with *L. longbeachae* as described in section 2.2.3. Three days after infection lungs were collected into 500 µL PBS

and homogenized using ceramic beads for 3 min. Homogenates were centrifuged at 13000 rpm and 4 °C for 5 min and the supernatant was transferred into fresh 1.5 mL tubes. Detection of MUC5AC and MUC5B was performed using the mouse MUC5AC or MUC5B ELISA kits, according to the manufacturer's instructions. Briefly, a 96-well microtiter plate containing 100 µL Capture Antibody Solution with 0.5-4 µg/mL anti-MUC5AC or anti-MUC5B mAbs was incubated overnight at 4°C, washed with 400 µL Wash Buffer (1 X PBS containing 0.05 % v/v Tween-20) and blocked with 300 µL Reagent Diluent (1 X PBS with 1% BSA w/v) for 60 min at RT. After washing, 100 µL of diluted samples and standards were added to the appropriate wells and incubated for 2 h at RT. Subsequently, the plate was washed and incubated with 100 µL Detection Antibody Solution, containing 0.25-2 µg/mL anti- MUC5AC or MUC5B mAbs, for 2 h at RT, before another washing step was performed. Next the plate was incubated with 100 µL added Substrate Solution, containing 50-250 ng/mL horseradish peroxidase **(**HRP)-conjugated streptavidin, for 30 min. After color development 50 µL of Stop Solution was added and the absorbance was measured immediately using the Tecan Safire^2 microplate reader.

2.2.15. Transmission electron microscopy

Hoechst$^-$CD45$^+$CD11b$^+$Ly6G$^+$Ly6C$^{+/-}$ *L. longbeachae*$^+$ neutrophils were sorted as described in section 2.2.10. Cells used for transmission electron microscopy were processed using standard methods. Briefly, cells were fixed with 2.5 % glutaraldehyde in 0.1 M sodium cacodylate buffer (pH 7.4) for 1 h and at 37 °C. After fixation cells were pelleted and washed in sodium cacodylate buffer. Cells were then incubated in 2.5 % osmium tetroxide for 1 h, followed by dehydration in a graded acetone series. The pellet was embedded using the epoxy medium embedding kit (Merck). Thin (0.5 µm) sections were stained with 10 % uranyl acetate and 3 % lead citrate before visualizing under a Philips CM12 transmission electron microscope at 60 kV.

2.2.16. Confocal microscopy

Confocal microscopy was performed on 100 µm tick vibratome sections, in order to preserve the tissue structure (Holland *et al.*, 2018). Briefly, mice were anesthetized with 10 mg/kg bw Xylazine and 100 mg/kg bw Ketamine and exsanguinated by cutting the aorta. Immediately after this, lungs were kept in the inspiration phase by instilling 2 mL of 2 % low-temperature melting agarose at 37 °C i.t. Cold PBS was poured over the lungs to polymerize the agarose. Afterwards, the lungs were quickly dissected out and kept at 4 °C for 30 min to further solidify the agarose. Subsequently, lung lobes were embedded in 4 % low-temperature agarose and cut with a VT1000S vibrating-blade microtome at a frequency of 10 Hz and a speed of 5-7 µm/s. Sections were placed in ice-cold PBS for a maximum of 30 min. and were then fixed with PLP Buffer or with Antigenfix for 30 min. at 4 °C. Afterwards, sections were washed and incubated in Confocal Blocking Buffer for 30 min at 4 °C, which contained 5 µg/mL purified Ig of either the same species and isotype as the directly fluorochrome-conjugated primary antibody, or as the secondary antibody. Sections were then stained with a mAb cocktail in Confocal Blocking Buffer overnight at 4 °C with mild shaking in the dark. Slices were washed 3 times in ice-cold Washing Buffer and, when necessary, incubated for 2 h at room temperature in Blocking Buffer containing fluorochrome-labeled secondary antibody diluted 1/500. Sections were washed 5 times in ice-cold Washing Buffer and mounted in PBS on microscopy slides. When indicated, DAPI was used to counterstain nuclei.

Imaging was performed with a Zeiss LSM 710 confocal microscope equipped with a 20x lens (Zeiss, plan-apochromat 20x/0.8) using the lambda mode of acquisition and spectral imaging with linear unmixing in order to remove autofluorescence and avoid overlapping of fluorescence signals when using 4 or 5 different fluorochromes. When indicated, a Zeiss LSM 880 confocal microscope equipped with AiryScan detector and a 63x lens (Zeiss plan-apochromat 63x/1.4) was used. Images were acquired using Zen V and analyzed using either the ImageJ/Fiji v 1.52p or Imaris software version 7.6.3.

2.2.17. Data processing and statistical analysis

Processing of raw data was done with Microsoft Excel v2016, FlowJo v10.1 and ImageJ/Fiji v1.52p or Imaris v7.6.3. Statistical significance was determined using the Prism v8.0.2 software. A two-tailed unpaired Student´s *t*-test was used when two groups were compared or (repeated-measurements) one-way ANOVA with Bonferroni post-test were used when three groups or more were compared. A two-way ANOVA was used when two or more groups with two independent variables were compared. Statistical significance was set at $*P < 0.05$ and indicated as $*P < 0.05$; $**P < 0.01$; $***P < 0.001$.

Chapter 3: Cellular mechanisms in the defense against pulmonary *L. longbeachae* infection in mice

3.1. Introduction

Legionella spp. are facultative intracellular bacteria that cause a severe and often fatal form of pneumonia, termed Legionnaire's disease (Brown *et al.*, 2017). In humans, *L. pneumophila* and *L. longbeachae* are the most common causative agents for this disease (Percival and Williams, 2014). While the cellular immune response against *L. pneumophila* has been widely studied, the defense mechanisms against *L. longbeachae* are far less well understood. Once *L. pneumophila* is phagocytosed by tissue-resident alveolar macrophages (AMs) upon infection, it translocates over 300 different effector molecules into the host cell cytosol (Newton *et al.*, 2010a), leading to inhibition of phagolysosomal fusion and vesicular remodeling to form the so-called LCV (Zhan *et al.*, 2015). Within the LCV, *L. pneumophila* is able to replicate until the bacteria egress from infected cells (Molmeret *et al.*, 2004). In contrast, it is currently unknown whether or not a specific cell population serves as a replicative nice for *L. longbeachae*.

Other immune cell populations have been shown to contribute to the clearance of *L. pneumophila* from the lungs. Those include, neutrophils, monocytes, dendritic cells (DCs), NK cells and T cells. Early during infection with *L. pneumophila*, neutrophils infiltrate the lungs, where they engulf the bacteria and eliminate them via production of ROS (Gobin et al. 2009; Massis et al. 2017; Brown et al. 2013). Similarly to infections with *L. pneumophila*, neutrophils infiltrate the lungs during pulmonary infections with *L. longbeachae* (Gobin *et al.*, 2009). However, their contribution to the clearance of this strain of bacteria still requires further investigation. DCs are also able to take up *L. pneumophila* and control bacterial replication through caspase-1-dependent pryoptosis and classical cell death pathways (Schuelein *et al.*, 2011). Most likely DCs also play a role in promoting T cell activation via presentation of Legionella antigens (Brown *et al.*, 2017). Whether DCs take up *L. longbeachae* and their role in clearance of those bacteria have not been investigated.

T cells and NK cells are amongst the main contributors of IFN-γ after activation, which is essential for the clearance of *L. pneumophila* from mouse lungs (Brieland *et al.*, 2000; Brown *et al.*, 2016) by activating monocyte-derived cells (MCs) (Brown *et al.*, 2016). Besides this, MAIT cells have been described to contribute to the clearance of *L. longbeachae* in an IFNγ-dependent manner after 10 days of infection (Wang *et al.*, 2018). However, the role of T cells, NK cells, and monocytes as well as the defense mechanisms against *L. longbeachae* are still not well understood. Therefore, the overall aim of this chapter is to investigate the infection kinetics of *L. longbeachae* and the contribution of different immune cell populations to protection. For this, we have generated a novel fluorescent *L. longbeachae* reporter strain and employed established mouse models for cell-specific depletion.

3.2. Results

3.2.1. Generation of genetically modified *L. longbeachae*

In order to identify cells that take up *L. longbeachae in vivo*, bacteria were genetically modified with the vector pON.mCherry to constitutively express the red fluorescent protein mCherry. After electroporation and growth on BCYE agar plates, mCherry expression was evaluated by flow cytometry and confocal microscopy (Fig. 1A-B). About 94 % of *L. longbeachae* bacteria expressed a high level of mCherry that was readily detected by flow cytometry (Fig. 1A) and confocal microscopy (Fig. 1B). Colonies of mCherry-expressing *L. longbeachae* appeared violet on BCYE agar plates, which allowed us to visually investigate whether mCherry expression was stable over time. Serial plating of *L. longbeachae*-mCherry over a period of 12 days demonstrated stable expression, since all colonies maintained the violet color (Fig. 1C).

Next, we tested whether mCherry expression was also stable during *in vivo* infection of mice. For this, lung homogenates from *L. longbeachae*-mCherry infected mice were plated on BCYE agar plates 5 days after infection. All

recovered bacterial colonies had the characteristic violet color (Fig. 1D), indicating that mCherry expression was stable.

Altogether, these results demonstrate a successful generation of genetically modified *L. longbeachae* bacterial that stably express mCherry for detection by flow cytometry and confocal microscopy.

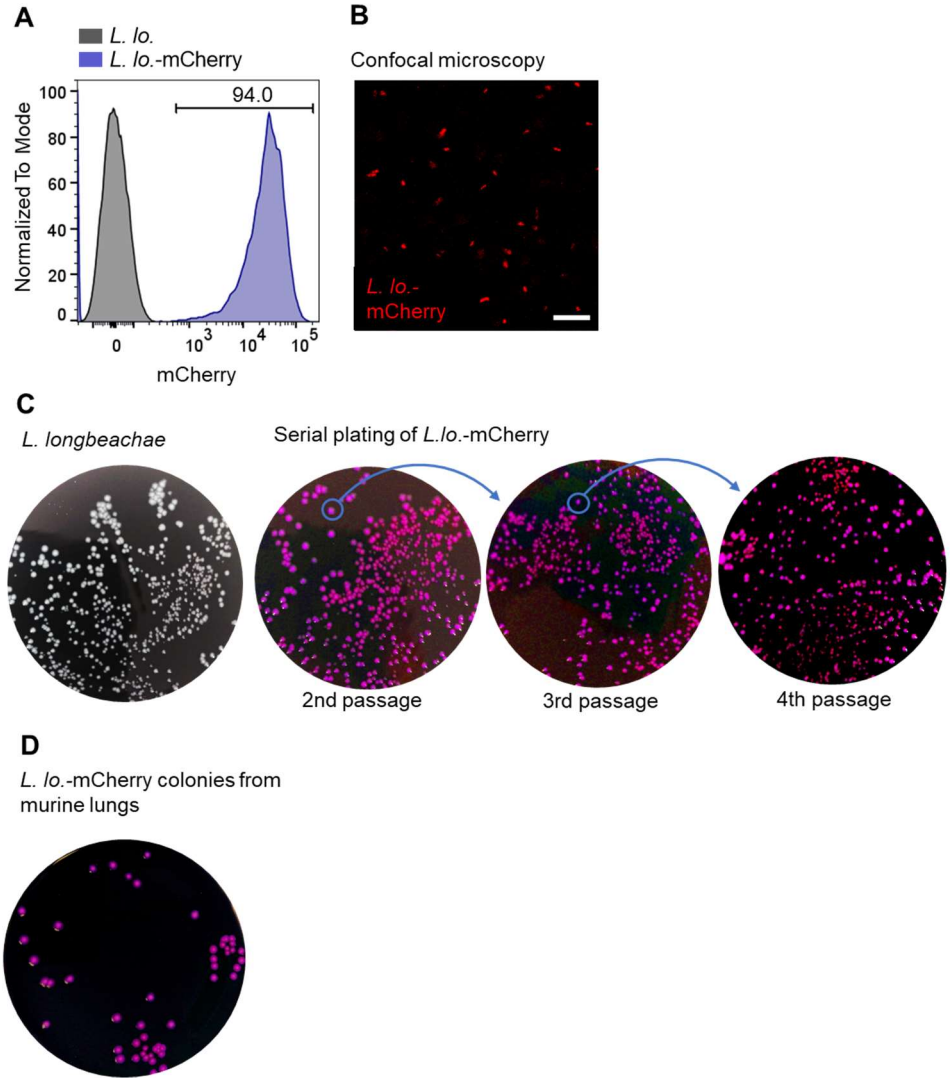

Figure 1: Stable mCherry expression by genetically-modified *L. longbeachae*-mCherry. (A) Representative flow cytometric histogram of mCherry expression by *L. longbeachae*-mCherry grown *in vitro* and **(B)** visualization of *L. longbeachae*-mCherry grown *in vitro* by confocal microscopy. Bacteria used in **(A, B)** were pooled from 10 randomly picked colonies. Bar, 10 µm. **(C)** Violet colonies of *L. longbeachae*-mCherry or white colonies of native *L. longbeachae* on BCYE agar plates after serial plating of single colonies as indicated. Plates were grown for 3 days. **(D)** Violet colonies of *L. longbeachae*-mCherry (white arrowheads) derived from a mouse lung 5 days after infection. Shown is a representative of 2 independent experiments. *L. lo., L. longbeachae*.

3.2.2. Internasal inoculation of *L. longbeachae* establishes severe pulmonary infection in mice

Intranasal inoculation of bacteria is a common route to induce pulmonary infection in mice (Ang *et al.*, 2012). We infected WT mice with a dose of 2.5 x 10^5 CFU *L. longbeachae* to characterize the infection kinetics *in vivo,* since this dose has been widely used for *L. pneumophila* (Davis *et al.*, 1983; Brown *et al.*, 2016). *L. longbeachae*-infected mice showed a transient decrease in body weight that reached a maximum of 20 % at day 4 after infection*,* while *L. pneumophila* infected mice showed a maximal decrease in body weight of only 13 % peaking 3 days after infection (Fig. 2A). These results confirm previous studies, indicating that *L. longbeachae* induces more severe symptoms in mice than *L. pneumophila* (Massis *et al.*, 2017).

The bacterial burden in lungs and spleen was quantified on BCYE agar plates. Three days after infection, lungs contained over 100-fold more *L. longbeachae* CFUs than the inoculum initially used for infection, whereas *L. pneumophila* CFU counts were similar to those used for infection (Fig. 2B). This suggests that *L. longbeachae* replicated more rapidly following pulmonary infection. However, independently of the *Legionella* spp. used, CFU counts declined steadily beyond day 3 after infection (Fig. 2B), suggesting the induction of a protective immune response. During infection, *L. longbeachae* spread systemically and could be detected in the spleen (Fig. 2B), although the bacterial burden was very low and close to detection limit. In addition, systemic spread was observed in only about half of all the experiments performed for this thesis (data not shown).

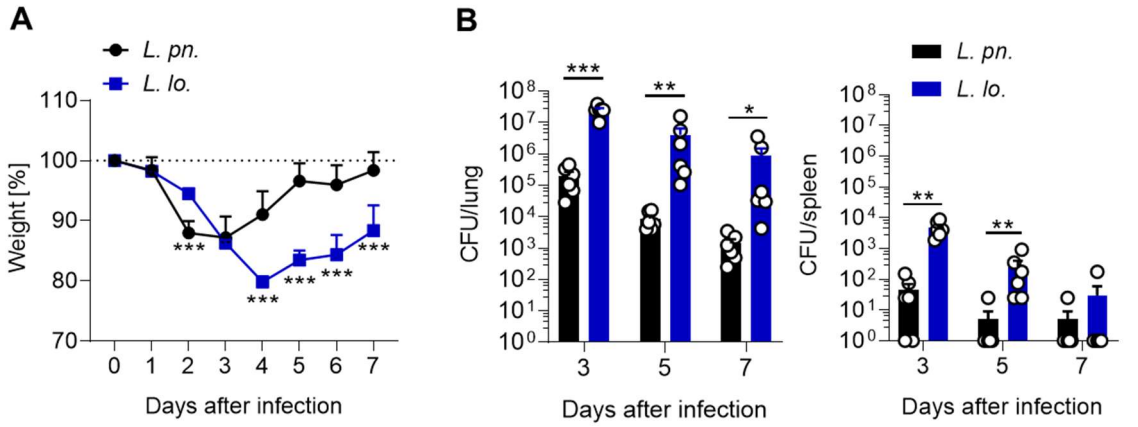

Figure 2: *L. longbeachae* establishes a productive pulmonary infection in mice. Mice were infected i.n. with 2.5 x 10^5 CFU of the indicated *Legionella* spp. and infection kinetics were compared between both species. **(A)** Weight of infected mice as a percentage of weight on day of infection (day 0). **(B)** Legionella CFU in the lungs (left panel) or spleen (right panel) 3, 5 and 7 days after infection. Data are shown as mean ± SEM of 2 pooled experiments (n = 3 mice per group and experiment). **P* < 0.05; ***P* < 0.01; ****P* < 0.001 (Two-way ANOVA). *L. pn.*, *L. pneumophila*; *L. lo., L. longbeachae*; CFU, colony-forming unit.

We next analyzed the distribution of *L. longbeachae* within the lung tissue. For this, WT mice were infected with *L. longbeachae*-mCherry and lungs were analyzed 2 days later by confocal microscopy. Infected lungs exhibited a high number of $CD45^+$ leukocytes that clustered together with red fluorescent *L. longbeachae*-mCherry in the alveolar area close to pulmonary bronchioles (Fig. 3A). Those clusters were likely infection foci, since most of the $CD45^+$ staining resulted from leukocyte debris, as evidenced by lack of a clear cellular shape and nuclear staining (Fig. 3A). Outside of those infection foci, *L. longbeachae* could be detected within leukocytes, demonstrating bacterial uptake by immune cells (Fig. 3B).

Altogether, these results demonstrate that i.n. *L. longbeachae* administration establishes a productive infection in the pulmonary alveolar region.

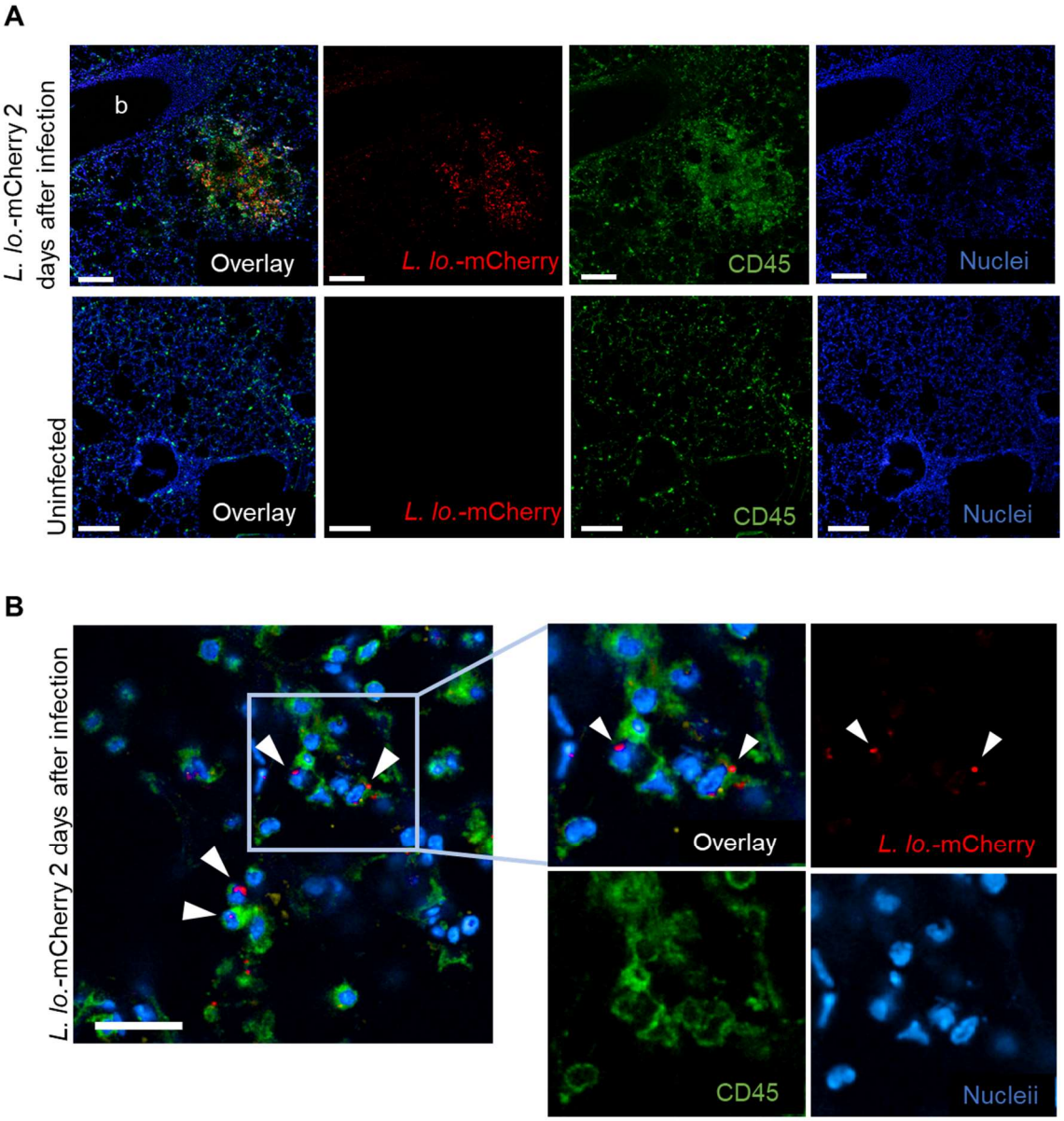

Figure 3: Detection of *L. longbeachae* in the lungs by confocal microscopy. Vibratome lung sections were analyzed by confocal microscopy 2 days after i.n. infection of WT mice with 2.5×10^5 CFU *L. longbeachae*-mCherry. **(A)** Representative confocal microscopy images showing a cluster of bacteria and leukocyte debris in the alveolar region close to a bronchiole (b). Bar, 200 µm. **(B)** Representative confocal microscopy image showing *L. longbeachae*-mCherry (white arrowheads) internalized by $CD45^+$ leukocytes. Bar, 30 µm. Similar results were obtained in 5 independent experiments. *L. lo., L. longbeachae*.

3.2.3. Neutrophils dominate the inflammatory response during acute *L. longbeachae* infection

Specific immune cell types present in the lung of non-infected mice and after i.n. infection with 2.5 x 10^5 CFU *L. longbeachae* were identified via flow cytometry (Fig. 4 and Fig. 5, respectively). A transient infiltration of immune cells into the lungs was observed peaking 5 days after infection, with a 75-fold increase compared to uninfected mice (Fig. 6A, B). Independently of the time point analyzed after infection, neutrophils dominated the immune cell infiltrate, both in percentage of immune cells (Fig. 6C) and number (Fig. 6D). Accordingly, neutrophils comprised 81 %, 70 % and 53 % of the leucocyte fraction 3, 5 and 7 days after infection, respectively (Fig. 6C). The second most frequent cell population in *L. longbeachae*-infected lungs were monocytes, comprising in average 15 % of the infiltrating leukocytes (Fig. 6C, D). Numbers of DCs and of the investigated lymphoid cells also increased during infection, although together they contribute less (about 0,4 %) than neutrophils and monocytes (together 99,4 %) to the total infiltrate between day 3 and day 5 after infection (Fig. 6D). Seven days after infection we observed an increase in the infiltration of lymphocytes, particularly $CD4^+$ T cells (18.4 % of all immune cells), which may suggest on-going adaptive immune responses in the late phase of *L. longbeachae* infection (Fig. 6C, D).

Overall, these results demonstrate an early infiltration of innate immune cells into the lungs of *L. longbeachae*-infected mice dominated by neutrophils and, to a lesser extent, monocytes followed by an increase in T cell counts during later stages of infection.

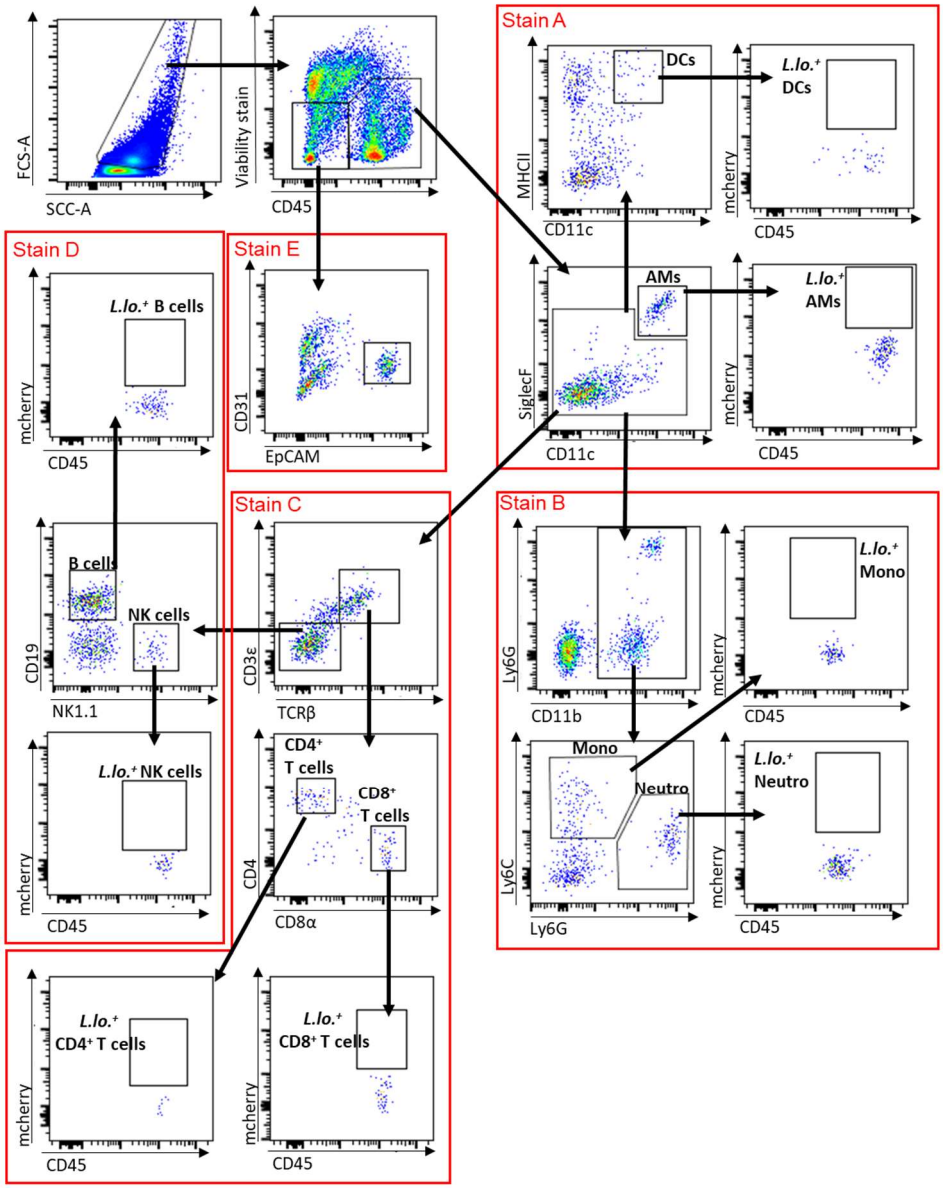

Figure 4: Gating strategy for identification of different cell types in the naive lung. Single-cell suspensions of collagenase IV-digested lungs were stained and analyzed by flow cytometry. Cell types were identified as follows:
Alveolar macrophages (**AMs**) as Live CD45$^+$Siglec-F$^+$CD11c$^+$ cells.
Dendritic cells (**DCs**) as live CD45$^+$Siglec-F$^-$CD11c$^+$MHC-II$^+$ events.
Neutrophils (**Neutro**) as live CD45$^+$CD11c$^-$CD11b$^+$Ly6G$^+$Ly6C$^{-/+}$ events.
Monocytes (**Mono**) as live CD45$^+$CD11c$^-$CD11b$^+$Ly6G$^-$Ly6C$^+$ events.
B cells as live CD45$^+$CD11c$^-$CD3ε$^-$TCRβ$^-$NK1.1$^-$CD19$^+$ events.
NK cells as live CD45$^+$CD11c$^-$CD3ε$^-$TCRβ$^-$NK1.1$^+$CD19$^-$ events.
CD4$^+$ T cells as live CD45$^+$CD11c$^-$CD3ε$^+$TCRβ$^+$CD4$^+$CD8α$^-$ events.
CD8$^+$ T cells as live CD45$^+$CD11c$^-$CD3ε$^+$TCRβ$^+$CD4$^-$CD8α$^+$ events.
Epithelial cells (**EpCs**) as live CD45$^-$EpCAM$^+$CD31$^{-/lo}$ events.
Only single cells were quantified by standard SSC-width versus SSC-area gating for each specific cell population (not shown for simplicity reasons).

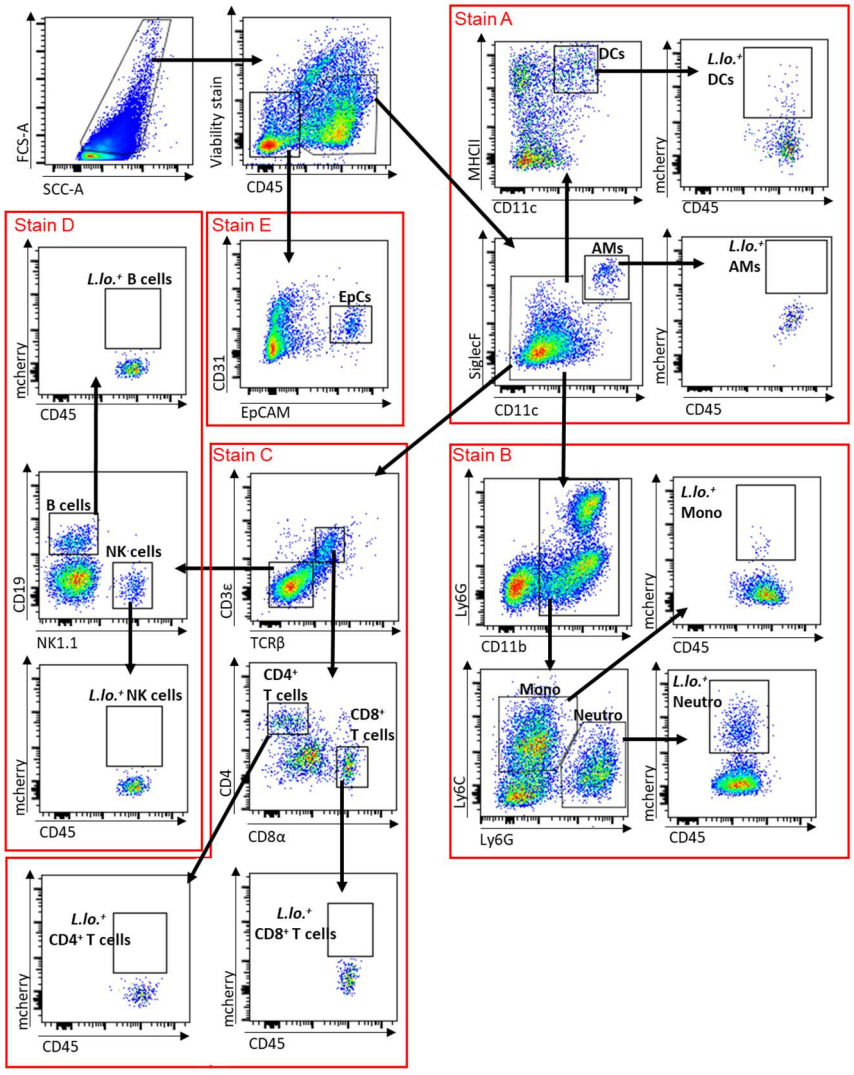

Figure 5: Gating strategy for identification of different cell types in the lung following *L. longbeachae* infection. 5 days after i.n. infection with 10^4 CFU *L. longbeachae*-mCherry, single-cell suspensions of collagenase IV-digested lungs were stained and analyzed by flow cytometry. Cell types were identified as follows:
Alveolar macrophages (**AMs**) as Live CD45$^+$Siglec-F$^+$CD11c$^+$ cells.
Dendritic cells (**DCs**) as live CD45$^+$Siglec-F$^-$CD11c$^+$MHC-II$^+$ events.
Neutrophils (**Neutro**) as live CD45$^+$CD11c$^-$CD11b$^+$Ly6G$^+$Ly6C$^{-/+}$ events.
Monocytes (**Mono**) as live CD45$^+$CD11c$^-$CD11b$^+$Ly6G$^-$Ly6C$^+$ events.
B cells as live CD45$^+$CD11c$^-$CD3ε$^-$TCRβ$^-$NK1.1$^-$CD19$^+$ events.
NK cells as live CD45$^+$CD11c$^-$CD3ε$^-$TCRβ$^-$NK1.1$^+$CD19$^-$ events.
CD4$^+$ T cells as live CD45$^+$CD11c$^-$CD3ε$^+$TCRβ$^+$CD4$^+$CD8α$^-$ events.
CD8$^+$ T cells as live CD45$^+$CD11c$^-$CD3ε$^+$TCRβ$^+$CD4$^-$CD8α$^+$ events.
Epithelial cells (**EpCs**) as live CD45$^-$EpCAM$^+$CD31$^{-/lo}$ events.
Only single cells were quantified by standard SSC-width versus SSC-area gating for each specific cell population (not shown for simplicity reasons).

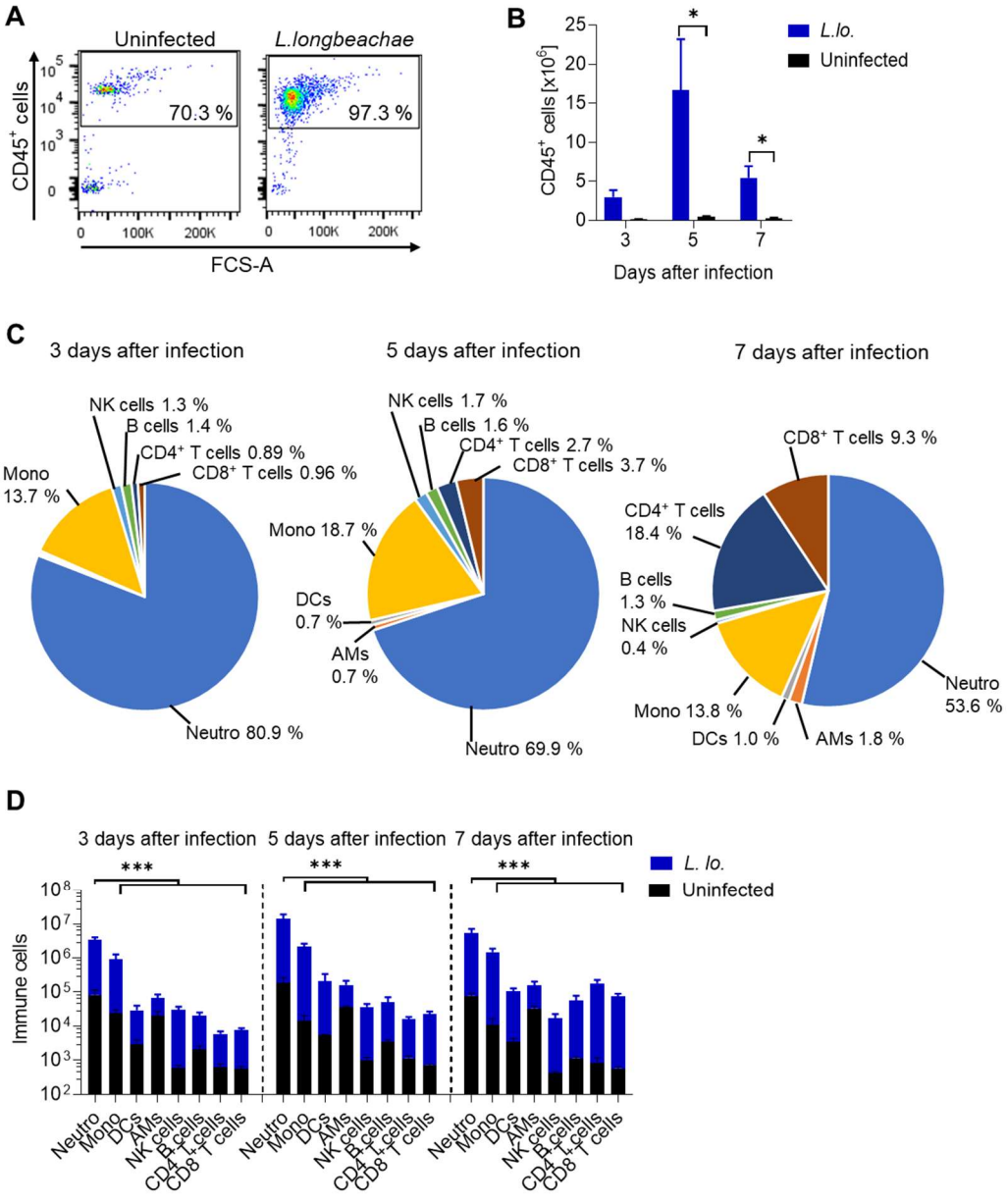

Figure 6: Neutrophils dominate the cellular infiltrate in the lung during *L. longbeachae* pulmonary infection. Mice were infected i.n. with 2.5 x 10^5 CFU *L. longbeachae* and lung cell suspensions were analyzed by flow cytometry on the indicated days after infection. **(A)** Representative flow cytometric dot plot of viable cells from the indicated mice 3 days after infection. **(B)** Number of viable CD45$^+$ leukocytes in the lungs of the indicated mice. **(C)** Proportion of immune cells types within the viable CD45$^+$ leucocyte fraction on the indicated days after infection. **(D)** Number of immune cell types in the lung on the indicated days after infection. The indicated cell populations were identified as illustrated in Fig. 4 and 5. Data shown in (B) and (D) represent the mean ± SEM. Data in (C) represent the mean percentage. All data are from 2 pooled experiments (n = 3 mice per group and experiment). In (B) $*P < 0.05$; (Two-way ANOVA) and in (D) $***P < 0.001$ (One-way ANOVA). *L. lo.*, *L. longbeachae*.

3.2.4. Neutrophils are the major cell type that phagocytosed *L. longbeachae*

We investigated the cell types that took up *L. longbeachae* in the lung during infection via flow cytometry. WT mice were infected with 10^4 CFU *L. longbeachae*-mCherry. As detailed in Section 2.2.3, we used a lower dose of bacteria in Bonn (10^4 CFU) than in Melbourne (2.5×10^5 CFU) due to a different susceptibility of BL6 mice between the two locations. Infection with non-fluorescent *L. longbeachae* was used as a negative control for the mCherry signal. *L. longbeachae*-mCherry was taken up almost entirely by $CD45^+$ immune cells independently of the time point after infection (Fig. 7A; shown for 3 dpi, similar results for 5 dpi and 7 dpi). Bacterial uptake by immune cells was further confirmed by imaging flow cytometry (Fig. 7B). Consistent with a decrease in CFU over time (Fig. 2B), the number of immune cells with internalized *L. longbeachae*-mCherry progressively declined (Fig. 7C). Most of the red fluorescent bacteria were taken up by neutrophils followed by monocytes and DCs (Fig. 7D). Overall, neutrophils were the largest fraction of the whole cell compartment containing *L. longbeachae*-mCherry 3 and 5 days after infection (Fig. 7D). On day 3, about 70 % of immune cells having internalized *L. longbeachae*-mCherry were neutrophils, while at day 5 after infection about 60 % neutrophils contained the bacteria (Fig. 7D). Seven days after infection, however, most of the cells containing *L. longbeachae* were DCs (Fig. 7D), although the total number of cells positive for the bacteria at day 7 was negligible compared to days 3 and 5 after infection (Fig. 7C). The contribution of other cells such as epithelial cells and lymphocytes was minimal (Fig. 7D).

In addition, AMs comprised about 0.7 % of the total immune cell fraction containing *L. Longbeachae*-mCherry at day 3 and 5 after infection (Fig. 7D). These results were surprising because AMs act as a replicative niche for *L. pneumophila* that is important to establish infection (Newton *et al.*, 2010a). In order to investigate whether there was a higher frequency of AMs containing *L. longbeachae*-mCherry earlier during infection, we quantified internalization of *L. longbeachae*-mCherry 1 day after pulmonary infection. Again, AMs

represented less than 1 % of the total *L. longbeachae*-containing immune cell fraction (Fig. 7E).

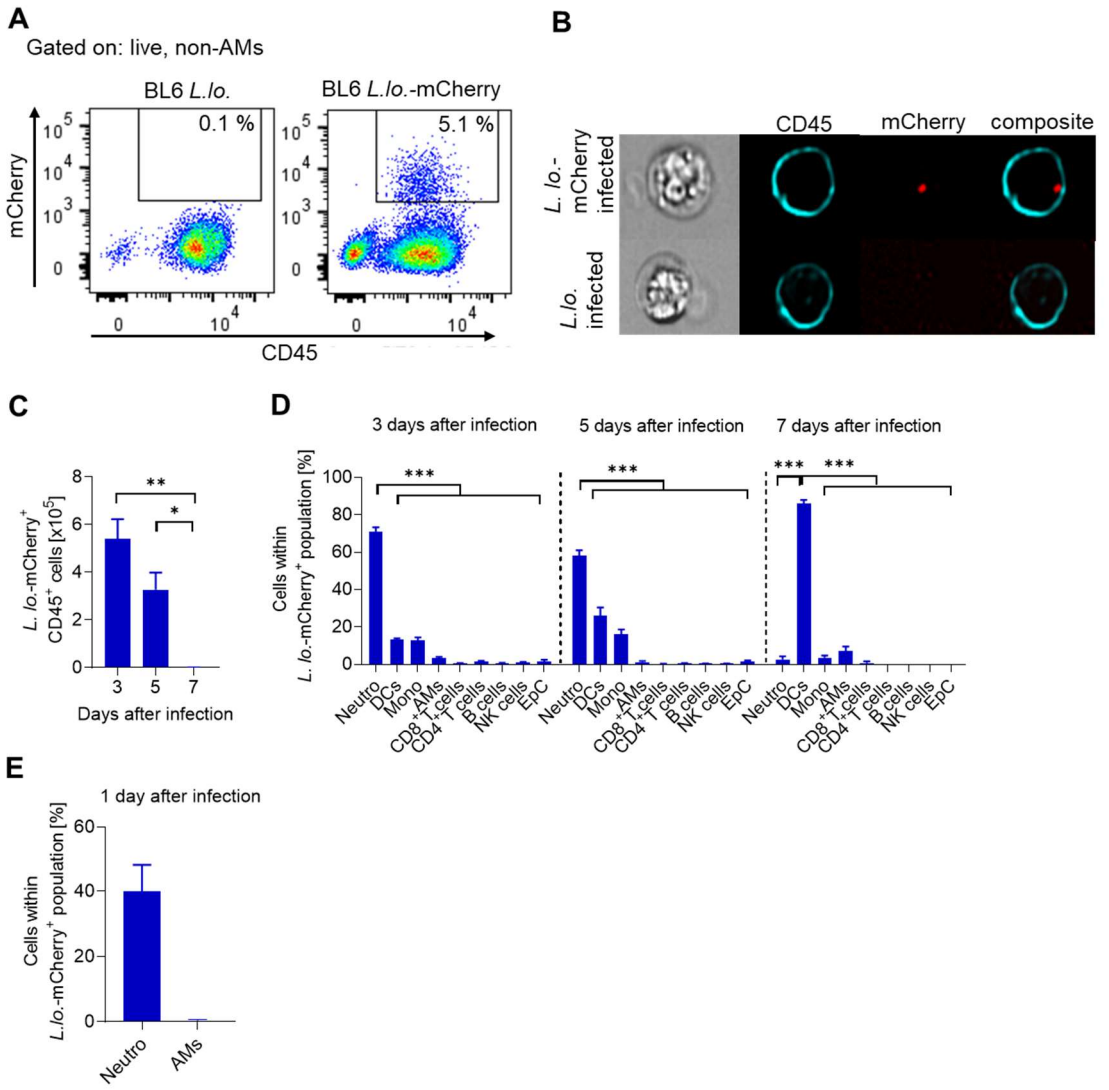

Figure 7: Neutrophils are the major cell type that phagocytosed *L. longbeachae*. WT mice were infected i.n. with 10^4 CFU *L. longbeachae*-mCherry and lung cell suspensions were analyzed by flow cytometry at the indicated days after infection. **(A)** Representative flow cytometric dot plot of viable $CD45^+$ cells from the indicated mice 3 days after infection. **(B)** Representative ImageStream picture of *L. longbeachae* mCherry-containing $CD45^+$ cells 3 days after infection. **(C)** Number of $CD45^+$ cells in the lungs containing *L. longbeachae*-mCherry on the indicated time-points. **(D, E)** Proportion of cells within the total *L. longbeachae*-$mCherry^+$ cell fraction on the indicated days after infection. Data shown in (C-E) represent the mean ± SEM of 2 pooled experiments (n = 5 mice per group and experiment). $^*P < 0.05$; $^{**}P < 0.01$; $^{***}P < 0.001$ (One-way ANOVA). *L. lo., L. longbeachae*.

Having identified the immune cells taking up *L. longbeachae*, we investigated the efficiency at which each cell type took up *L. longbeachae*-mCherry by quantifying the percentage of cells with bacteria within each specific cell population (Fig. 8A). Again, neutrophils comprised the highest fraction, with about 11 % of them being mCherry^{+} (Fig. 8B). In contrast, the percentage of AMs containing bacteria was about 1 % (Fig. 8A, B). Although a very small fraction of AMs took up *L. longbeachae,* those that internalized them had higher mCherry MFI than the other cell types, indicating more bacteria on a per-cell basis (Fig. 8C).

Altogether, these results demonstrate a dynamic uptake of *L. longbeachae* by different myeloid immune cell types with a predominance of neutrophils, most likely reflecting distinct phases of the immune response.

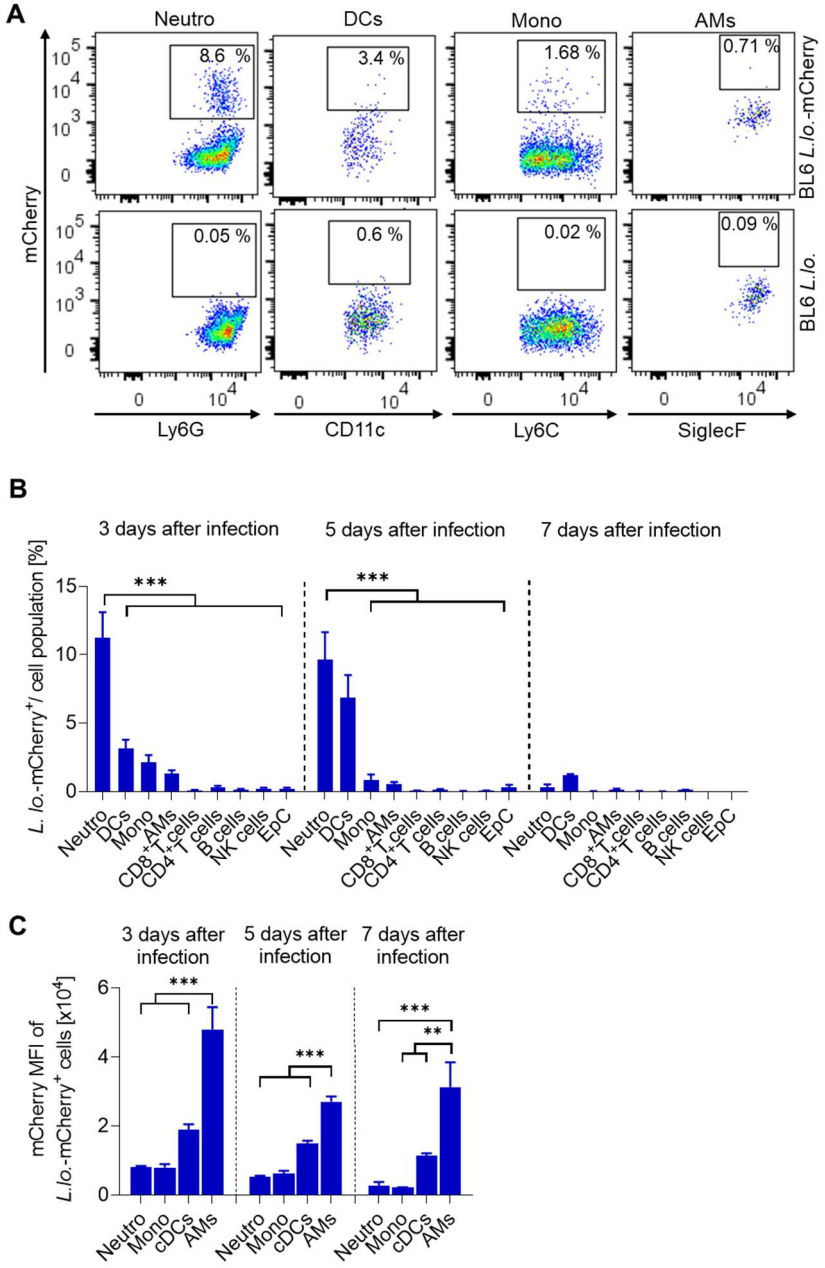

Figure 8: Neutrophils efficiently take up *L. longbeachae* during infection. Mice were i.n. infected with 10^4 CFU *L. longbeachae*-mCherry or *L. longbeachae* and lung cell suspensions analyzed by flow cytometry. **(A)** Representative flow cytometric dot plots of the indicated immune cell populations 3 days after infection. **(B)** Frequency of mCherry$^+$ cells within the indicated populations. **(C)** mCherry mean fluorescence intensity (MFI) of the indicated *L. longbeachae*$^+$ cells. The indicated cell populations were identified as illustrated in Fig. 4 and 5. Data shown represent the mean ± SEM of 2 pooled experiments (n = 5 mice per group and experiment). Data shown in (B) and (C) represent the mean ± SEM of 2 pooled experiments (n = 5 mice per group and experiment). $^{**}P < 0.01$ $^{***}P < 0.001$ (One-way ANOVA). *L. lo., L. longbeachae.*

3.2.5. Most viable *L. longbeachae* reside in neutrophils after infection of mice

We quantified how many viable bacteria were contained in different immune cell populations. For this, WT mice were infected with 10^4 CFU *L. longbeachae*, and 2 days later different immune cell populations were FACS-sorted, lysed and plated on BCYE agar plates. Consistently with our results on *L. longbeachae* internalization (Fig. 7D; Fig.8B), neutrophils contained the highest number of viable bacteria followed by monocytes and AMs (Fig. 9A).

L. pneumophila can establish a LCV following translocation of bacterial effectors into the host cytosol, which is essential for its survival and replication (Newton *et al.*, 2010a). Similarly, to *L. pneumophila* we observed a double-membrane vacuole containing *L. longbeachae* in infected neutrophils (Fig. 9B). However, unlike the *L. pneumophila* LCV this vacuole was not studded with ribosomes (Fig. 9B). To investigate the ability of *L. longbeachae* to inject effectors into the cytosol of different immune cells, we next performed a *L. longbeachae*-encoded RalF β-lactamase translocation assay. Translocation of RalF was detectable in myeloid cells by a shift in the emission wavelength of the β-lactamase substrate CCF2 from 530 nm to 460 nm (Fig. 9C). All cell subpopulations tested harboring *L. longbeachae* supported effector translocation, albeit at a different degree (Fig. 9C, D). Consistent with our results on a dominant uptake of *L. longbeachae* by neutrophils (Fig. 7D and Fig. 8B), about 60 % of all cells with translocated RalF were neutrophils (Fig. 9E).

Altogether these results demonstrate that all infected myeloid cells contain viable bacteria, with a predominance of the neutrophil compartment. Similarly, all infected myeloid cells also support translocation of *L. longbeachae* effectors, which are likely to mediate the generation of an LCV-like vacuole.

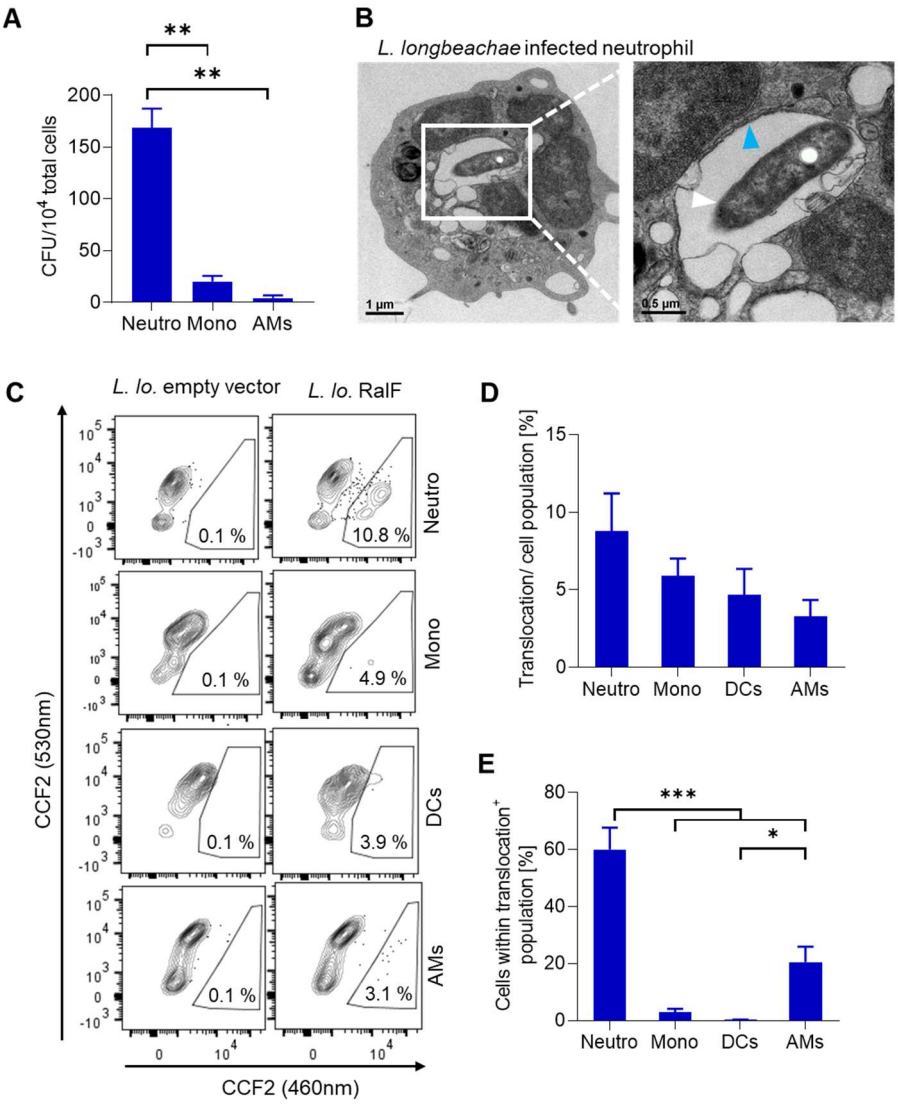

Figure 9: *L. longbeachae* translocates virulence effector molecules into myeloid host cells. (A) Quantification of viable *L. longbeachae* CFU in the indicated cell populations isolated from the lungs 2 days after i.n. infection with 10^4 CFU *L. longbeachae*-mCherry. **(B)** Electron microscopy image of a neutrophil containing *L. longbeachae* (white arrowhead) within a vacuole exhibiting a double membrane (blue arrowhead) 2 days after infection. **(C)** Representative flow cytometric dot plots showing translocation of RalF in the indicated immune cells 2 days after infection with 2.5 x 10^5 CFU *L. longbeachae*-RalF or *L. longbeachae* containing an empty vector as indicated. **(D, E)** Frequency of cells with translocated RalF within each cell subpopulation (D) or within the total cell fraction with translocated RalF (E). Immune cells were identified as illustrated in Fig. 4 and Fig. 5. Data shown in (A) represent the mean ± SEM from a representative (n = 3 mice per group) of 3 independent experiments or of 3 pooled experiments (n = 3 mice per group and experiment) (D, E). **P* < 0.05; ***P* < 0.01; ****P* < 0.001 (One-way ANOVA). *L. lo., L. longbeachae.*

3.2.6. The role of myeloid cells in the clearance of *L. longbeachae*

3.2.6.1. The role of neutrophils in *L. longbeachae* clearance

We investigated the role of neutrophils in *L. longbeachae* clearance from lungs by antibody-mediated neutrophil depletion starting from 1 day before infection with 10^4 CFU *L. longbeachae* (Fig. 10A). Neutrophils were efficiently depleted in the lungs 3 days after infection (about 98 % depletion) (Fig. 10B, C). Depletion of neutrophils from infected mice resulted in a severe weight loss compared to non-depleted mice (about 20 % and 10 %, respectively, at day 5 after infection) (Fig. 11A), suggesting that *L. longbeachae* infection is more virulent in absence of neutrophils. Consistently with this, the bacterial burden in the lungs of neutrophil-depleted mice was over 10- and 1000-fold higher than in their non-depleted counterparts at day 3 and 5 after infection (Fig. 11B).

During infection we observed an increase in monocyte infiltration into the infected lungs of neutrophil-depleted mice that, in addition, took up more bacteria than those of their non-depleted counterpart (Fig. 11C and Fig. 11D, respectively). These results may be explained as a compensatory mechanism for the lack of neutrophils resulting in higher bacterial burden (Fig. 11B).

Altogether, these results demonstrate that neutrophils are necessary for the control of *L. longbeachae* infection and no other immune cell can fully compensate for their absence.

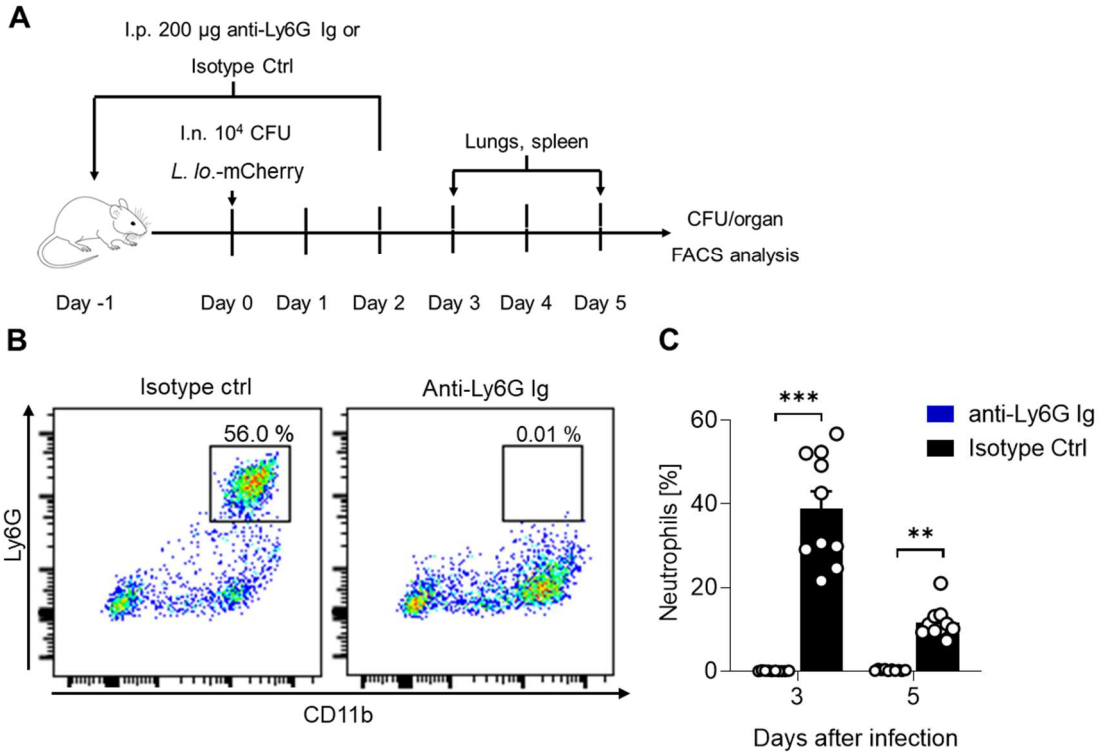

Figure 10: Depletion of neutrophils form *L. longbeachae* infected lungs. (A) Cartoon illustrating the experimental plan. **(B)** Representative flow cytometric dot plots of viable, $CD45^{+}Ly6G^{+}CD11b^{+}$ neutrophils from the lungs of WT mice after 3 days of infection (A) treated with an isotype control or with depleting antibodies. **(C)** Percentage of neutrophils at the indicated time-points after infection. Data shown in (C) represent the mean ± SEM of 2 pooled experiments (n = 5 mice per group and experiment). In (C) $^{**}P < 0.01$; $^{***}P < 0.001$ (Two-way ANOVA). Ig, Immunoglobulin; Ctrl, control; *L. lo.*, *L. longbeachae*; CFU, colony-forming unit.

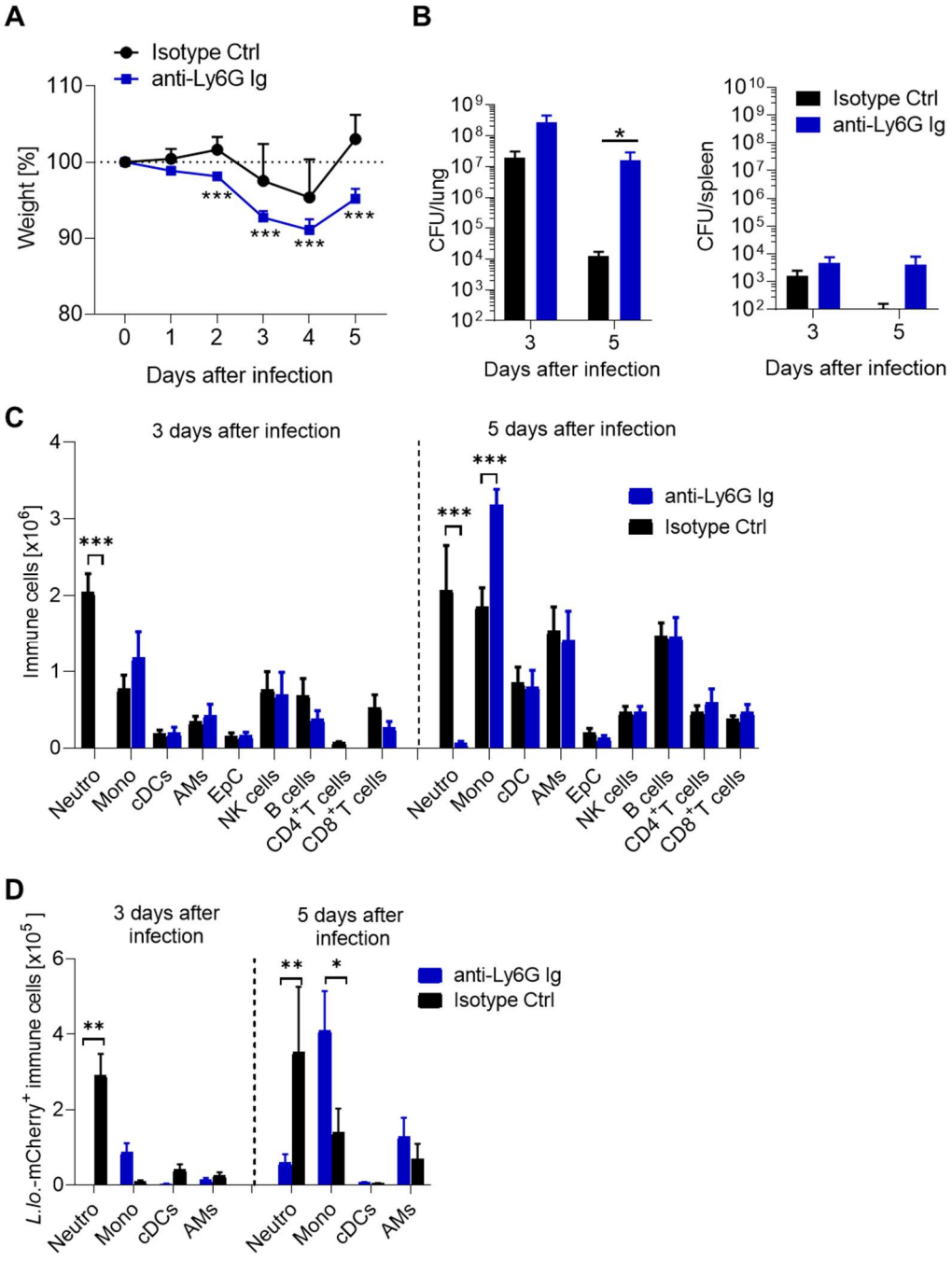

Figure 11: Neutrophils promote clearance of *L. longbeachae* from the lungs. **(A)** Weight of infected mice from as a percentage of weight on day of infection (day 0). **(B)** CFU in the lungs (left panel) or spleen (right panel) at the indicated time points**. (C)** Cell numbers at the indicated times after infection. **(D)** *L. longbeachae*-mCherry positive immune cells 3 and 5 days after infection. Immune cells were identified as illustrated in Fig. 4 and Fig. 5. Data shown represent the mean ± SEM of 2 pooled experiments (n = 5 mice per group and experiment). **P* < 0.05; ***P* < 0.01; ****P* < 0.001 (Two-way ANOVA). *L. lo., L. longbeachae*; Ctrl, control; Ig, Immunoglobulin; CFU, colony-forming unit.

3.2.6.2. The role of monocytes in *L. longbeachae* clearance

As an increased number of monocytes infiltrated the *L. longbeachae*-infected lungs during neutrophil depletion, we investigated the role of monocytes in the clearance of the bacteria. For this *Ccr2*$^{-/-}$ mice were infected with 2.5 x 10^5 CFU *L. longbeachae,* in which monocytes lack the ability to exit the bone marrow and infiltrate tissues, and WT mice served as a control. Although there was no difference in body weight between both groups (Fig. 12C), bacterial burden in the lungs of *Ccr2*$^{-/-}$ mice was over 10-fold higher 5 days after infection compared to control mice (Fig. 12D), demonstrating that monocytes were required for optimal defense of *L. longbeachae*.

Three days after infection, immune cell infiltration and bacterial internalization was comparable between *Ccr2*$^{-/-}$ and WT mice (Fig. 12E, F). However, 5 days after infection an about 10-fold increase in neutrophils could be observed in *Ccr2*$^{-/-}$ mice (Fig. 12E, F), demonstrating that a significant decrease of inflammatory monocytes affects immune cell recruitment.

Overall these results demonstrate that monocytes, like neutrophils (Fig. 11B), promote the defense against *L. longbeachae* during acute infection of the lungs.

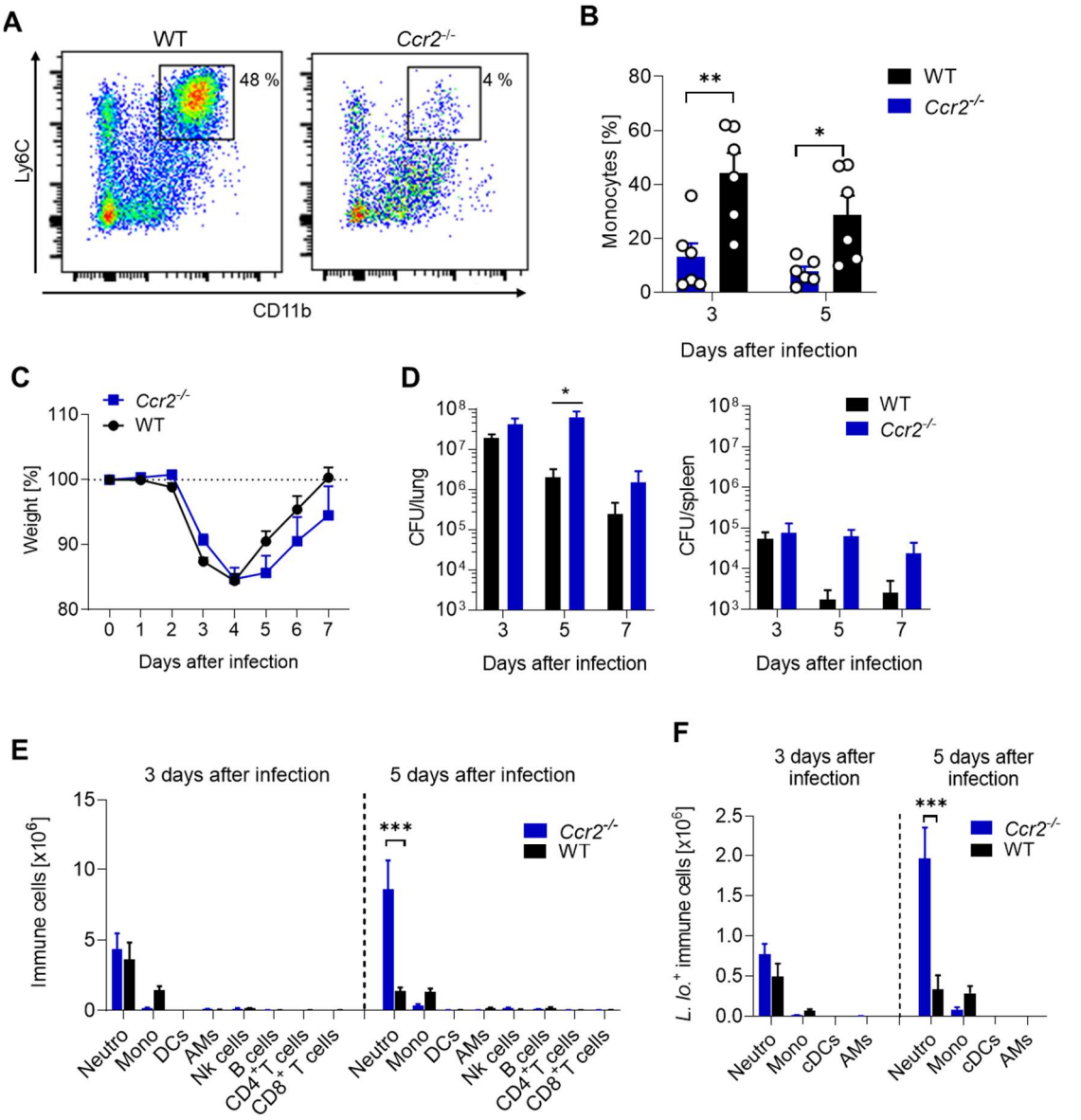

Figure 12: Monocytes promote the clearance of *L. longbeachae* from the lungs. (A) Representative dot plots of single viable CD45$^+$Ly6G$^-$ cells from the lungs of infected WT or *Ccr2*$^{-/-}$ mice from. Gated on Ly6C$^+$ CD11b$^+$ monocytes **(B)** Number of monocytes from (A). (**C)** Weight loss kinetics of *Ccr2*$^{-/-}$ mice and WT mice from (A). **(D)** CFU in the lungs (left panel) or spleen (right panel) at the indicated time points**. (E)** Cell numbers at the indicated times after infection, detected using an anti-*L. longbeachae* antibody staining **(F)** *L. longbeachae*-containing immune cells 3 and 5 days after infection. Immune cells were identified as illustrated in Fig. 4 and Fig. 5. Data shown in (B-F) represent the mean ± SEM of 2 pooled experiments (n = 3 mice per group and experiment). **P* < 0.05; ***P* < 0.01 ****P* < 0.001 (Two-way ANOVA). *L.lo., L. longbeachae*; CFU, colony-forming units.

3.3. Discussion

The overall goal of this study was to characterize the pulmonary infection of BL6 mice with *L. longbeachae*. Specifically, we aimed to quantify the kinetics of infection, identify the cell populations that internalize bacteria, and pinpoint immune cells essential for the host defense. Our results demonstrate that *L. longbeachae* was able to establish a productive pulmonary infection in mice, as recently described by other groups (Gobin *et al.*, 2009; Massis *et al.*, 2017). Three days after infection, the bacterial burden in the lungs had increased about 100-fold over the infectious dose, demonstrating a productive infection. Past that time point, the bacterial CFUs in the lung decreased progressively and mice recovered weight. Compared to *L. pneumophila*, infection with *L. longbeachae* resulted in an increased bacterial burden in the lungs and loss of body weight, suggesting a more virulent course of infection, confirming a recent study (Massis *et al.*, 2017). Several distinguishing features between the two species may explain the increased virulence. First, recent studies have revealed that *L. longbeachae* replicates efficiently independently of the growth phase at the time of infection (Newton *et al.*, 2010a), which may result in increased overall replication and pulmonary bacterial burden. Second, *L. longbeachae* can form an outer capsule, which might promote survival of the bacteria through inhibiting recognition of bacterial components by immune cells (Newton *et al.*, 2010a). Finally, Naip5/NLRC4 is fundamental in the protection against *L. pneumophila*, but not against *L. longbeachae* due to lack of flagellin in the latter (Cazalet *et al.*, 2010).

Pulmonary infection of mice with *L. longbeachae* resulted in a transient infiltration of immune cells into the lungs with a peak at day 5 after infection. Confocal microscopy imaging using our novel fluorescent *L. longbeachae* revealed the formation of infection foci in alveoli close to pulmonary bronchioles. These foci contained a large number of leukocyte clusters, suggesting early local defenses to prevent further bacterial spread. The large majority of infiltrating leukocytes were neutrophils followed by monocytes to a much lesser extent. Neutrophils are rapidly recruited to infected tissues by chemokines such as ligands for CCR1 (e.g. CCL5) and CXCR2 (e.g. CXCL5) upon infection (Amulic

et al., 2012; Arango Duque and Descoteaux, 2014). However, the precise mechanisms driving neutrophil accumulation into *L. longbeachae*-infected lungs remains to be elucidated. $CD4^+$ and $CD8^+$ T cell infiltration became apparent on day 7 after infection, possibly reflecting an ongoing adaptive immune response. The strong infiltration we observed during *L. longbeachae* infection is in apparent conflict with the recent claim that *L. longbeachae* is immunologically silent as argued by low concentrations of several cytokines in the lungs (Massis *et al.*, 2017). We could not detect cytokines in the lung due to technical problems, but the fact that neutrophils and other immune cells strongly infiltrate into the infected lung argue against an immunologically silent infection.

Consistent with a decrease in the pulmonary bacterial burden over time, the overall number of immune cells containing *L. longbeachae* decreased within 7 days of infection. Therefore, loss of mCherry signal may derive from degradation of the bacteria by those cells. Only myeloid cells had the capacity to take up *L. longbeachae* as demonstrated by *L. longbeachae*-mCherry infection studies. Those comprised mostly neutrophils, followed by monocytes and DCs to a much lesser extent. Neutrophils and monocytes exhibit potent microbiocidal mechanisms such as ROS, RNS, acidification of endolysosomes, proteases and antimicrobial peptides (Segal, 2005). In line with this, they were required for early *L. longbeachae* clearance, as demonstrated in cell-specific depletion experiments. Furthermore, depletion of neutrophils resulted in an increased infiltration of monocytes, whereas an impaired monocyte recruitment led to a higher recruitment of neutrophils. This may suggest a compensatory mechanism during infection. On the other hand, the observed higher bacterial burden could also stimulate stronger recruitment of neutrophils during infection.

At later stages of infection (day 7), however, the very few immune cells still containing *L. longbeachae* were basically DCs, which may provide *in situ* restimulation to T cells, thereby contributing to the increased infiltration of T cells into the lungs at that time point. T cells are not able to directly kill pathogens, but indirectly help to achieve sterilizing immunity by many different mechanisms. For instance, $CD4^+$ T cells produce IFNγ that activates myeloid cells to upregulate microbiocidal mechanisms so that vacuolar bacteria may be readily killed,

whereas $CD8^+$ T cell have the ability to efficiently kill cells harboring pathogens in their cytosol, thus making them available to effectors such as protective antibodies (Halle, 2017). However, $CD4^+$ and $CD8^+$ T cells do not apparently play major roles in *L. longbeachae* clearance as will be discussed in Chapter 4.

It is known that AMs are the primary host for *L. pneumophila*, serving as a niche for survival and replication (Robinson and Roy, 2006). Whether this also applies to infections with *L. longbeachae* is currently not known. Our results revealed a very low frequency of mCherry containing AMs (0.5 - 0.7 %) in the lungs. Alveolar macrophages are highly auto-fluorescent cells and this attribute may mask the positive mCherry signal. Therefore, an alternative option to detect bacteria inside of the cells would be a staining with anti-*L. longbeachae* antibodies in further experiments. However, in the few mCherry-containing alveolar macrophages we detected, the MFI of mCherry was highest, indicating more internalized bacteria. To clarify whether *L. longbeachae* is potentially able to establish an LCV similar to the one of *L. pneumophila* in immune cells, we analyzed the translocation of effector molecules into the host cell. We found that the bacteria were able to translocate effector molecules into all myeloid cells, indicating that the bacteria may be able to form this specialized vacuole. However, further studies are required to fully elucidate this question.

Altogether, these results highlight the important role of neutrophils in the early defense against *L. longbeachae* during pulmonary infection mice.

Chapter 4: The role of IL18 in the defense against *L. longbeachae*

4.1. Introduction

Cytokines are major coordinators of the immune response against microorganisms (Turner et al., 2014). For instance, IFNγ plays a crucial role by enhancing the microbiocidal function of macrophages (Schroder et al., 2004). IL18, a member of the IL1 family of cytokines, promotes IFNγ production by T cells and NK cells in synergy with IL12 and, thus, it is an important cytokine for the defense against invading bacteria (Dinarello et al., 2013).

IL18 is expressed as an inactive form, called proIL18, in the cytosol of myeloid cells and epithelial cells (Nowarski et al., 2015). Cleavage of proIL18 is required to generate functionally active IL18. Although inflammasome-dependent processing of proIL18 yields functional IL18 (Netea et al., 2000), it is unclear whether other inflammasome-independent proteases are also competent in this process, as it has been demonstrated for IL1β (Netea et al., 2000). Once activated in the cytosol, IL18 is released into the extracellular milieu by a so far undefined mechanism. However, it is unclear whether inflammasome-activation of gasdermin B, which induces pyroptosis and release of activated IL1β (Liu et al., 2016), is also important for the release of active IL18.

Extracellular IL18 binds to its heterodimeric receptor, which consists of a ligand-binding IL18R1 chain and an IL18RAP coreceptor (Dinarello, 2018; Boraschi et al., 2018). IL18R activation initiates NFκB- and STAT3-dependent intracellular signaling leading to expression of proinflammatory cytokines, such as IL-2 (Dinarello et al., 2013). Cytokines expressed in higher concentrations during infection with *L. pneumophila* include IL12, IL1β, IL8, IL10 and IFNγ (Brown et al., 2016; Massis et al., 2017).

Although IL18 expression resulted in higher IFNγ production during pulmonary infection with *L. pneumophila*, it had surprisingly no effect on bacterial clearance (Brown *et al.*, 2016). In contrast, the role of IL18 during *L. longbeachae* infection is unknown. Therefore, the main aim of this chapter was to elucidate the

function of IL18 and its corresponding IL18R in the defense against *L. longbeachae* during pulmonary infection of mice.

4.2. Results

4.2.1. *L. longbeachae* induces IL18R-dependent IFNγ in the lungs

In order to identify, which cytokines are expressed during pulmonary infection of mice with *L. longbeachae*, WT or *Il18r1*$^{-/-}$ mice were infected with 10^4 CFU *L. longbeachae*-mCherry, BALF was collected 5 days after infection and a Luminex-based cytokine assay was performed to measure IFNγ and IL18 levels. IFNγ levels were very low in uninfected and infected mice (low pg/ml range). On average they were about 4-fold higher in infected WT mice compared to their uninfected counterparts. (Fig. 13A). Deficiency in the IL18R resulted in reduced levels of IFNγ, confirming the role of IL18 in IFNγ induction (Dinarello *et al.*, 2013). In contrast, *L. longbeachae* infection did not alter IL18 levels in the BALF, whereas a deficiency in the IL18R lead to a tendency of increased IL18 levels, although again, the concentration of IL18 was very low also in WT and in infected mice (Fig. 13B).

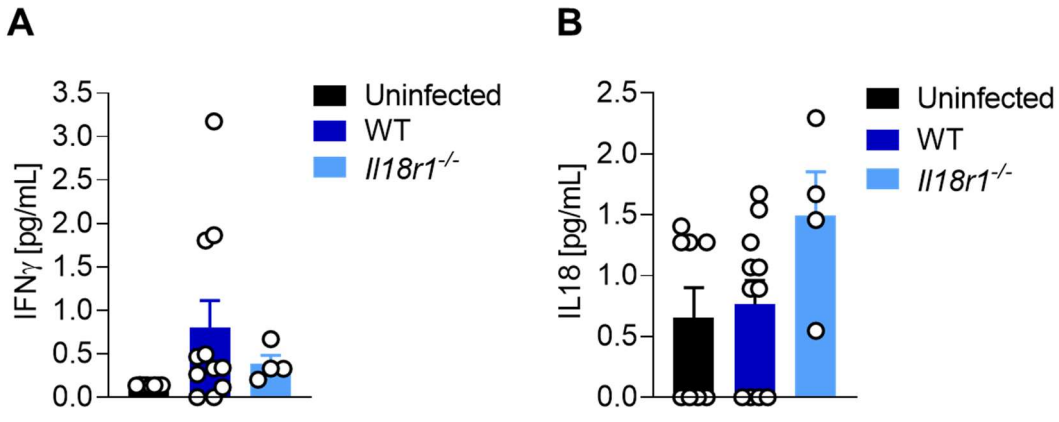

Figure 13: *L. longbeachae* infection induces production of IFNγ in the lungs. (A, B) IFNγ levels (A) or IL18 levels (B) in the BALF of WT and *Il18r*$^{-/-}$ mice 5 days after i.n. infection with 10^4 CFU *L. longbeachae*-mCherry. BALF from uninfected WT mice was used as control. Data are shown as mean ± SEM from 2 pooled experiments (n = 4-11 mice). WT, wild-type mice.

4.2.2. IL18 and its receptor promote clearance of *L. longbeachae*

We investigated the role of IL18 in the clearance of *L. longbeachae* from the mouse lungs by infecting WT, *Il18*$^{-/-}$ and *Il18r1*$^{-/-}$ mice. Infected mice lacking IL18 expression showed a more severe weight loss (Fig. 14A) and contained about 10-fold more bacteria in the lungs compared to WT mice 5 days after infection (Fig. 14B). Although IL18R-deficient mice did not show differences in weight loss (Fig. 14C), they contained more bacteria in the lungs (about 10-fold) than WT mice (Fig. 14D). These results demonstrate that IL18 and its receptor are key mediators in the reduction of *L. longbeachae* burden during the early stages of infection, which is in contrast to their irrelevance during *L. pneumophila* infection (Brown *et al.*, 2016).

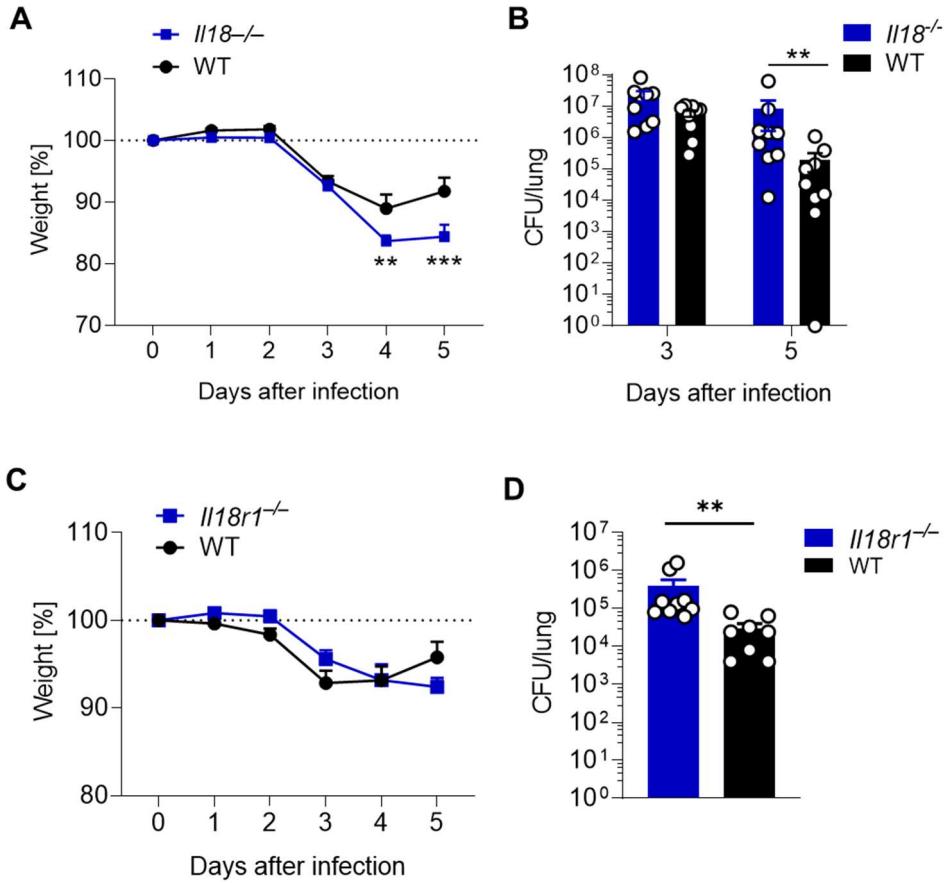

Figure 14: IL18 and its receptor promote the defense of *L. longbeachae* from infected lungs. WT, *Il18*$^{-/-}$ or *Il18r1*$^{-/-}$ mice were i.n. infected with 10^4 CFU *L. longbeachae*-mCherry and infection kinetics were compared between groups of WT and *Il18*$^{-/-}$ mice or WT and *il18r1*$^{-/-}$ mice. **(A, C)** Weight of (A) *Il18r*$^{-/-}$ or (C) *Il18r1*$^{-/-}$ mice as a percentage of weight on day of infection (day 0)). **(B, D)** *L. longbeachae* CFU in the lungs 3 and 5 days after infection of *Il18*$^{-/-}$ (B) or 5 days after infection *Il18r1*$^{-/-}$ (D) mice. Data shown represent the mean ± SEM of 2 pooled experiments (n = 5 or 4 mice per group and experiment). In (B-C) $^{**}P < 0.01$; $^{***}P < 0.001$ (Two-way ANOVA) and in (D) $^{**}P < 0.01$ (Student´s *t*-test). WT, wild-type mice; CFU, colony-forming unit.

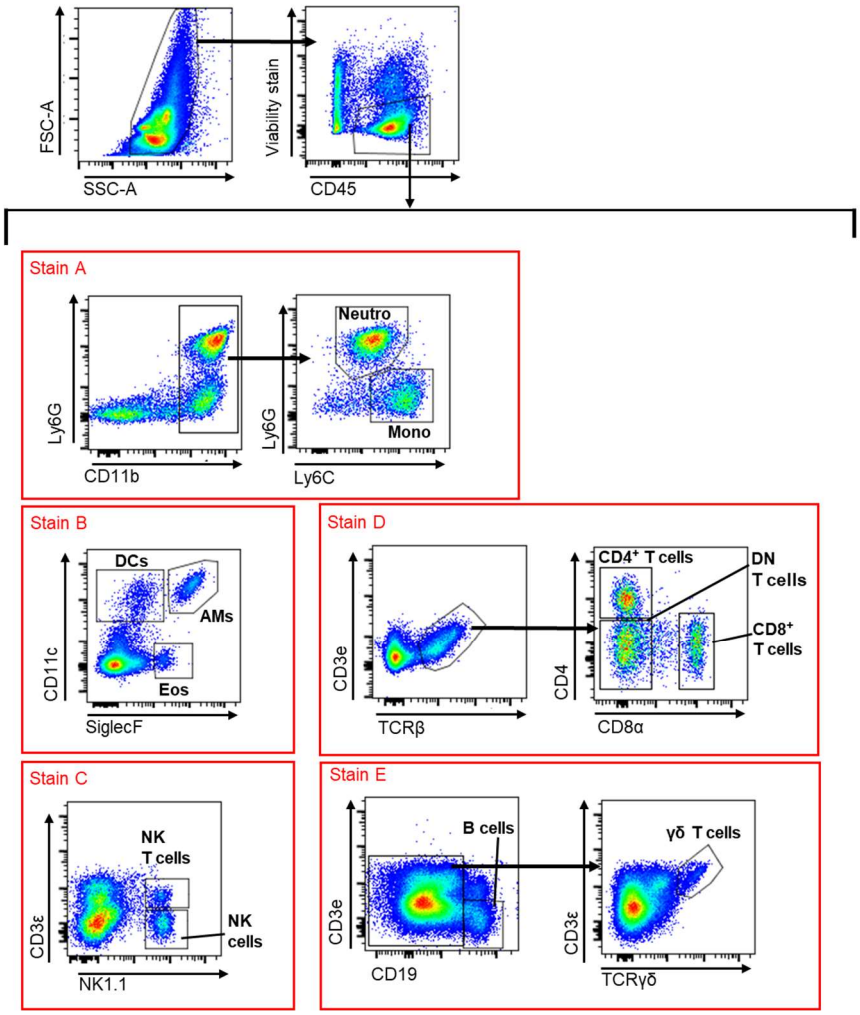

Figure 15: Gating strategy for identification of different cell types in the lungs. Single-cell suspensions of collagenase IV-digested lungs were stained and analyzed by flow cytometry. Cell types were identified as follows:
Alveolar macrophages (**AMs**) as Live CD45$^+$Siglec-F$^+$CD11c$^+$ cells.
Dendritic cells (**DCs**) as live CD45$^+$Siglec-F$^-$CD11c$^+$ events.
Neutrophils (**Neutro**) as live CD45$^+$CD11b$^+$Ly6G$^+$Ly6C$^{-/+}$ events.
Monocytes (**Mono**) as live CD45$^+$CD11b$^+$Ly-6G$^-$Ly-6C$^+$ events.
B cells as live CD45$^+$CD3ε$^-$CD19$^+$ events.
NK cells as live CD45$^+$CD3ε$^-$NK1.1^{+-}events.
NK T cells as live CD45$^+$CD3ε$^{-/+}$NK1.1^{+-} events.
CD4$^+$ T cells as live CD45$^+$CD3ε$^+$TCRβ$^+$D4$^+$CD8α$^-$ events.
CD8$^+$ T cells as live CD45$^+$CD3ε$^+$TCRβ$^+$CD4$^-$CD8α$^+$ events.
DN T cells as live CD45$^+$CD3ε$^+$TCRβ$^+$CD4$^-$CD8α$^-$ events.
γδ T cells as live CD45$^+$CD19$^-$CD3ε$^+$TCRγδ$^+$ events.
Only single cells were quantified by standard SSC-width versus SSC-area gating for each specific cell population (not shown for simplicity reasons).

After 5 days of infection with *L. longbeachae* immune cell infiltration was investigated using the gating strategy presented in Fig. 15. *Il-18r1*$^{-/-}$ mice showed a 1.7-fold higher number of neutrophils were present in the lungs compared to WT mice (Fig. 16A). In addition, more *L. longbeachae*-containing neutrophils were present in the lungs of *Il18r1*$^{-/-}$ mice (Fig. 16B). No differences were observed in other immune cell compartments (Fig. 16A, B). Altogether, these results demonstrate that IL18 and its receptor are contributing control of the bacterial burden of *L. longbeachae* early during infection.

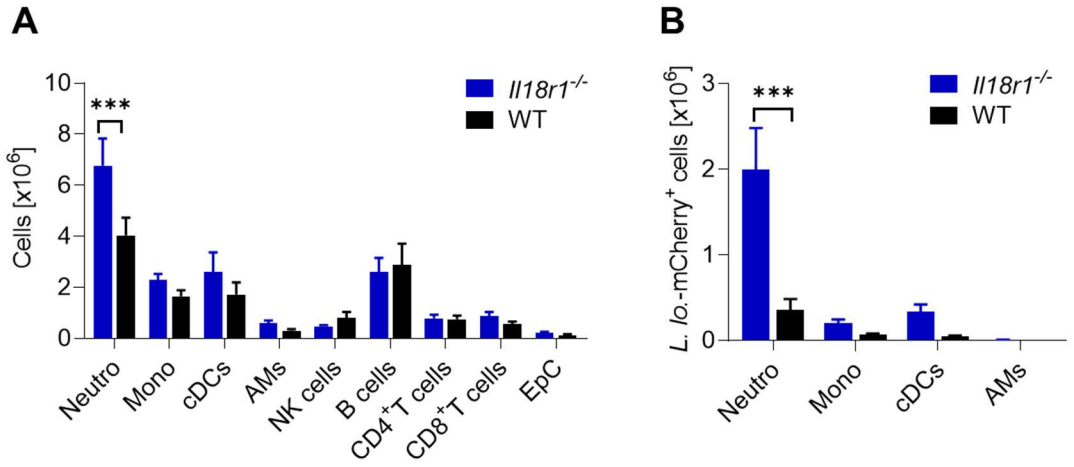

Figure 16: Increased infiltration of neutrophils in the lungs of *L. longbeachae*-infected *Il18r1*$^{-/-}$ mice. (A) Cell numbers in the lungs of *Il18r1*$^{-/-}$ mice 5 days after i.n. infection with 10^4 CFU *L. longbeachae*-mCherry. **(E)** *L. longbeachae*-mCherry positive immune cells 5 days after infection. Immune cells and epithelial cells were identified as illustrated in Fig. 15. Data shown represent the mean ± SEM of 2 pooled experiments (n = 5 or 4 mice per individual experiment). ***$P < 0.001$ (Student´s *t*-test). WT, wild-type mice.

4.2.3. Role of IL18R expression by immune cells in the defense against *L. longbeachae*

Having demonstrated that IL18 and its receptor are required for a reduction of the *L. longbeachae* burden from infected lungs, we aimed to identify cells that are expressing IL18R by flow cytometry and confocal microscopy. Anti-IL18R antibodies yield a very low signal in flow cytometry (Fig. 17A) and, thus, it was decided to generate knock-in reporter mice in cooperation with Prof. Kastenmüller, (University of Würzburg, Germany) termed IL18R1-tdTomato mice, in which tdTomato expression is under the control of the endogenous *Il18r1* gene (Fig 17B). Heterozygous IL18R1-tdTomato mice expressing tdTomato in one allele and *Il18r1* in the other allele were used for all experiments involving flow cytometry, whereas homozygous (and thus *Il18r1* knock-out) mice were used for confocal microscopy to increase sensitivity of detection.

As expected from a knock-in reporter mouse strain, cells expressing higher levels of IL18R1 on their cell surface also co-expressed high levels of tdTomato, (Fig. 17C). Because IL18R1-tdTomato reporter mice were heterozygous, surface IL18R1 expression was weaker compared to their WT counterparts, and thus IL18R1 surface staining with anti-IL18R1 antibodies could only be observed on those cells co-expressing high levels of tdTomato (Fig.17C). It is currently uncertain whether those cells that express lower levels of tdTomato and have no detectable IL18R1 surface signal still express functional IL18R1.

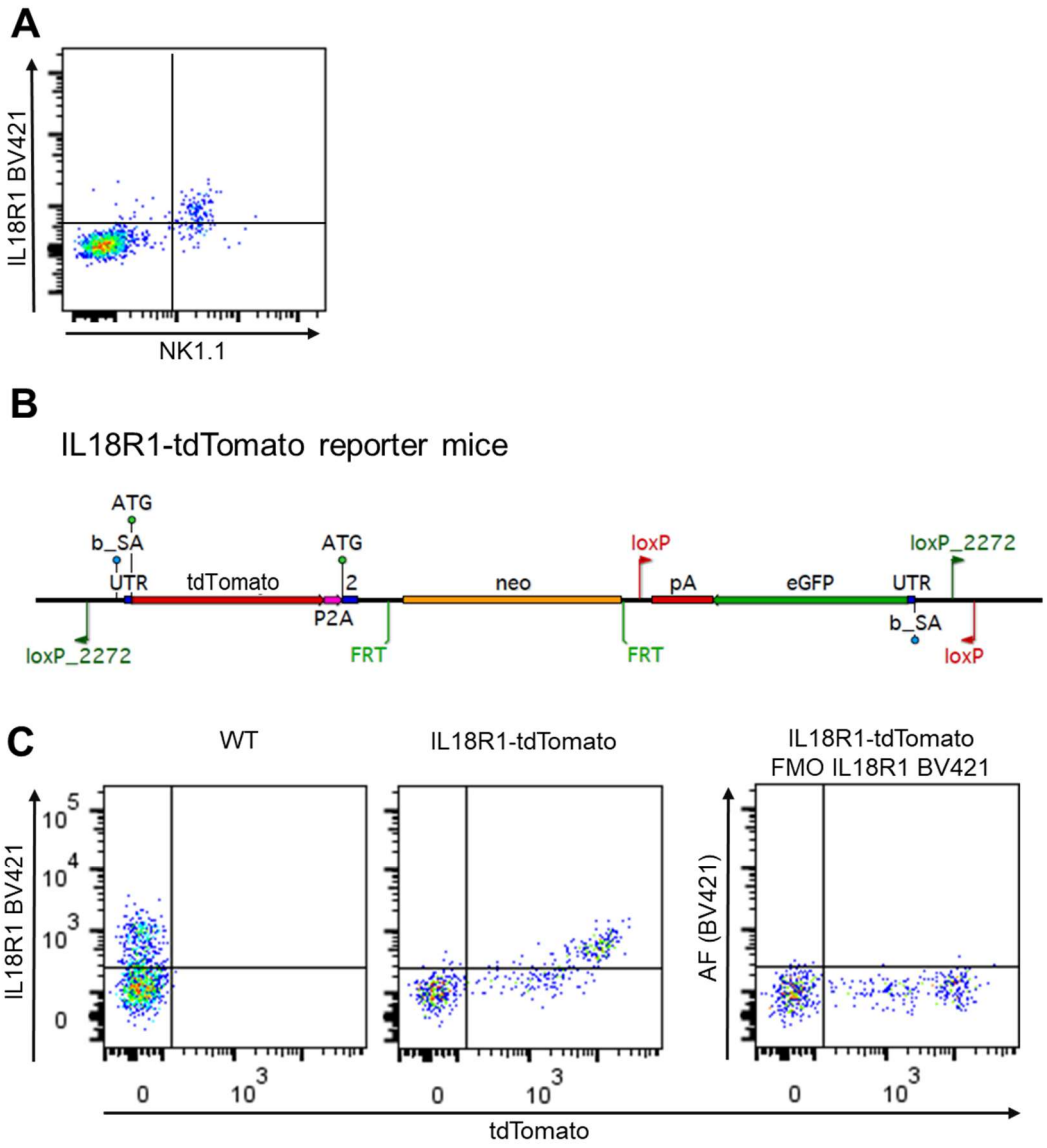

Figure 17: Detection of *Il18r1* expression using IL18R1-tdTomato reporter mice. (A) Representative flow cytometry dot plot showing IL18R1 surface staining on live, $CD45^{+}CD3\varepsilon^{-}TCR\beta^{-}$ NK cells. **(B)** Diagram illustrating the transgenic allele used to generate IL18R1-tdTomato knock-in reporter mice. As a result, the transgenic allele transcribes tdTomato but not *Il18r1*. Blue boxes: exons; B_SA: branch site and splice acceptor; neo: neomycin cassette for selection in embryonic stem cells; FRT: recognition sequence for flp recombinase-mediated neo removal; loxP, lox2272: recognition sequence for cre recombinase-mediated deletion. **(C)** Representative flow cytometry dot plots showing staining for surface IL18R1 and tdTomato expression in live $CD45^{+}$ cells from the lungs of WT and heterozygous IL18R1-tdTomato mice. In the right panel all antibodies minus IL18R1 BV421 (FMO control) were added. Data in (A) and (C) are representative of 5 independent experiments. WT, wild-type; FMO, fluorescence minus one; AF, autofluorescence

4.2.4. Analysis of IL18R expression by immune cells in the lung

We conducted a detailed analysis of IL18R1-tdTomato mice to identify immune cells with active *Il18r1* promoter transcription during steady state, as well as during *L. longbeachae* infection. We focused only on immune cells that had infiltrated the lungs, i.e. those that were located extravascular, because they are likely the main cells responding to local IL18 production in the lungs. Extravascular immune cells were readily identified by performing an *in vivo* intravascular leukocyte staining with AlexaFluor 488-labeled antibodies directed against CD45.2 (CD45.2-AF488) (Fig. 18A). Basically, all leukocytes in the blood were stained, demonstrating that CD45.2-AF488 administration i.v. reached all circulating leukocytes (Fig. 18A). In uninfected mice only about 5 % of all immune cells in the lungs were located extravascular and, therefore, did not stain with anti-CD45.2 antibody. Three days after infection with *L. longbeachae* ~50 % of cells did not stain with the anti-CD45 antibody and were thus located extravascular and lodged in the lung parenchymal tissue (Fig. 18A). The proportions and numbers of extravascular cells are shown in Fig. 18B and 18C and demonstrate a predominance of neutrophils and monocytes. These results were consistent with those obtained by analyzing unfractionated immune cells in the lung (Fig. 6C, D).

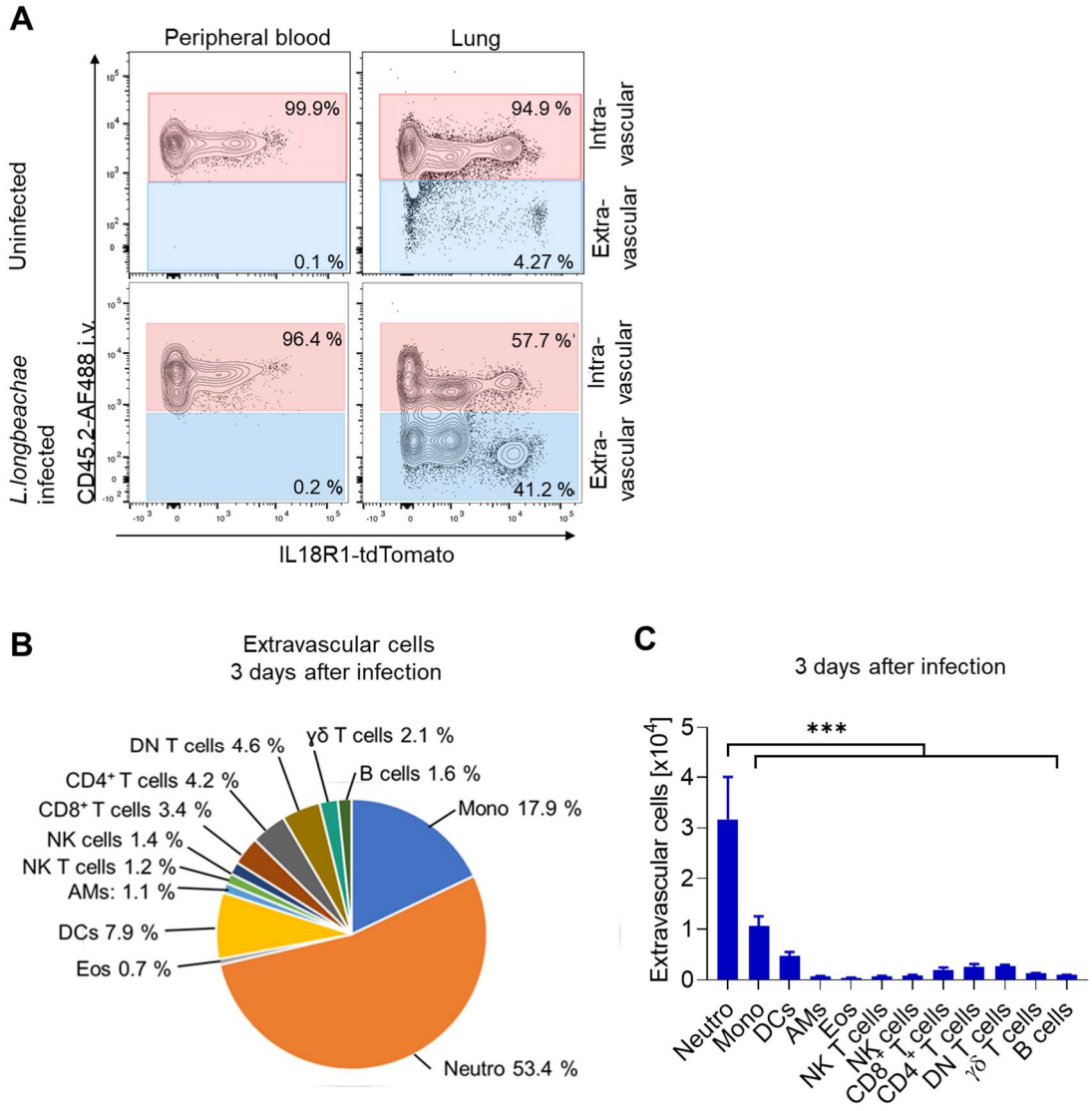

Figure 18*: In vivo* intravascular leukocyte staining to quantify immune cells subpopulations in the lung tissue during *L. longbeachae* infection. WT and IL18R1-tdTomato reporter mice were infected i.n. with 10^4 CFU *L. longbeachae* where indicated. Three days after infection an *in vivo* intravascular leukocyte staining was performed by i.v. injection of anti-CD45.2-AF488 antibodies 5 min before isolation of the lungs. **(A)** Representative flow cytometric dot plots of live leukocytes in blood (left panels) or lung (right panels) isolated from IL18R1-tdTomato mice that were uninfected (top panels) or infected 3 days earlier (bottom panels). Intravascular leukocytes are defined as CD45.2-AF488$^+$ cells (red gates); infiltrating, extravascular leukocytes are defined as CD45.2-AF488$^-$ cells (blue gates). **(B, C)** Proportion (B) and numbers (C) of the indicated immune cell types infiltrating the infected lungs. Identification of different immune cell populations and abbreviations as indicated in Fig. 15 with an additional gate to identify extravascular CD45.2-AF488$^-$ cells. Data are shown as mean percentage (B) or mean ± SEM (C) from 2 pooled experiments (n = 3 mice per group and experiment). In (C) *** $P < 0.001$ (One-way ANOVA).

We could distinguish two different tdTomato expression levels during steady state and infection: low and high (Fig. 19A). During infection, most cells (95.5 %) expressing high levels of IL18R1-tdTomato were lymphocytes, including $CD8^+$ αβ T cells (27.3 %), $CD4^+$ αβ T cells (28.9 %), NK cells (17.4 %), γδ T cells (16.3 %), $CD8^-CD4^-$ DN T cells (5.6 %) and NK T cells (3.3 %) (Fig. 19A, B), confirming previous studies showing IL18R expression by lymphoid cells and its role in promoting IFNγ production by those cells (Dinarello *et al.*, 2013). In contrast, most cells expressing low levels of IL18R1-tdTomato were neutrophils, comprising about 85 % of the total fraction (Fig. 19A, B).

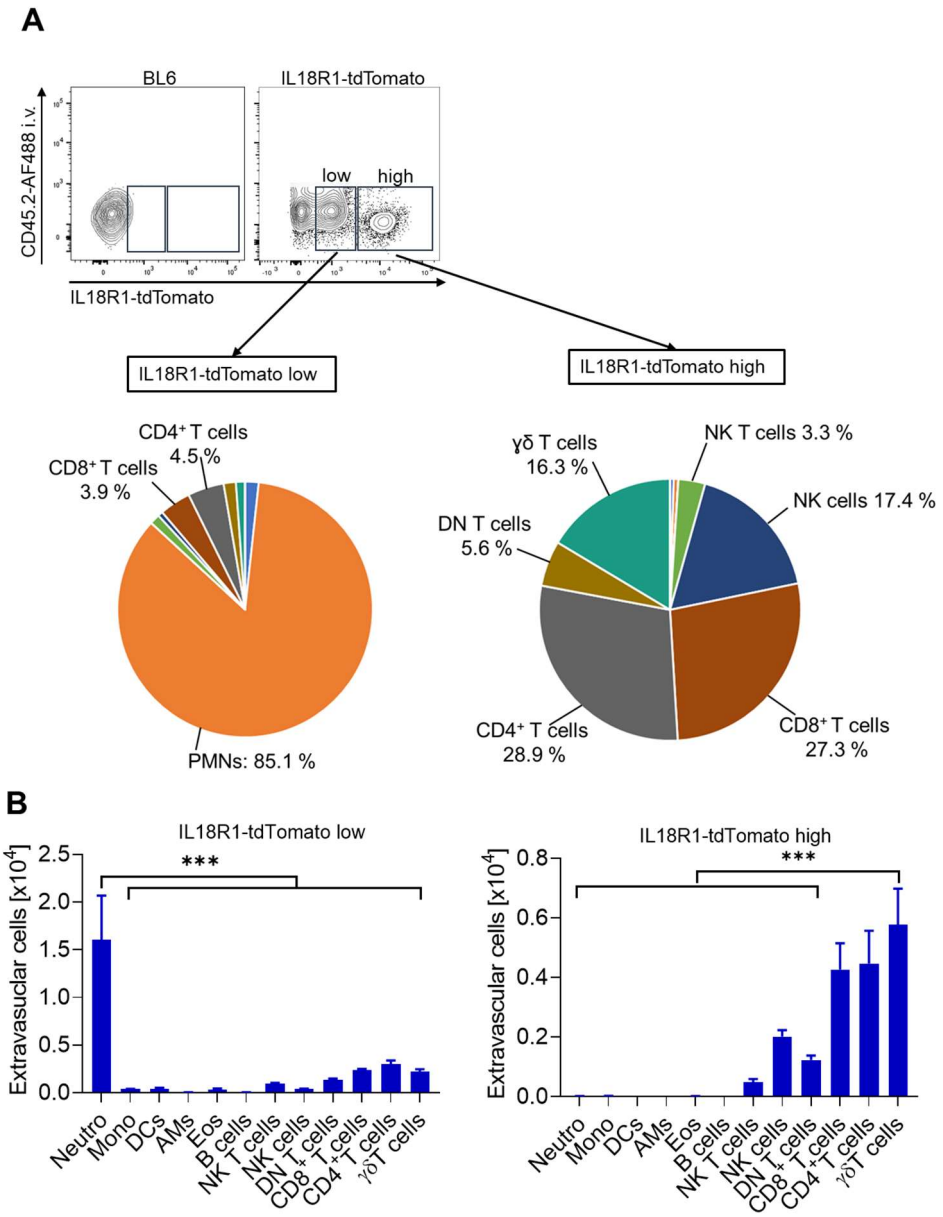

Figure 19: IL18R is highly expressed by lymphocytes. WT and IL18R1-tdTomato reporter mice were infected i.n. with 10^4 CFU *L. longbeachae*. Three days after infection an *in vivo* intravascular leukocyte staining was performed by i.v. injection of anti-CD45.2-AF488 antibodies 5 min before isolation of the lungs. **(A)** Representative flow cytometric dot plots showing different IL18R1-tdTomato expression levels. Pie charts show the average proportion of extravascular immune cells with the indicated expression level of IL18R1-tdTomato. **(B)** Number of immune cell subpopulations with low (left) or high (right) IL18R1-tdTomato expression. Identification of different immune cell populations and abbreviations as indicated in Fig. 15 with an additional gate to identify extravascular CD45.2-AF488$^-$ cells. Data are shown as mean percentage (A) or mean ± SEM (B) of 2 pooled experiments (n = 3 mice per group and experiment). In (B) *** $P < 0.001$ (One-way ANOVA).

Having identified cells that express the IL18R1, we assessed whether pulmonary infection with *L. longbeachae* modulated its expression level. We focused our analysis on T cells because they expressed high levels of IL18R and were detected extravascularly in the lung in steady state, as well as during infection. While infection did not affect IL18R1 expression by lung-infiltrating γδ T cells, it modulated expression of the receptor in αβ T cells (Fig. 20). A higher proportion of $CD4^+$ T cells and $CD8^+$ T cells expressed high IL18R1-tdTomato levels (Fig. 20). In contrast to this, infection induced an about 2-fold increase in the proportion of IL18R1-tdTomato negative DN T cells (Fig. 20).

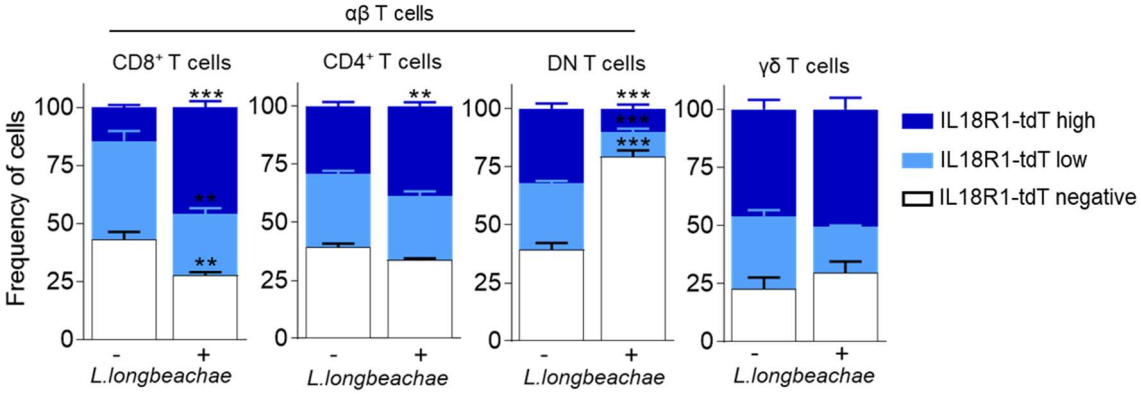

Figure 20: *L. longbeachae* infection modulates the fraction of IL18R1-expressing in αβ T cells in the lung. IL18R1-tdTomato reporter mice were infected i.n. with 10^4 CFU *L. longbeachae* or left uninfected. Three days after infection, an *in vivo* intravascular leukocyte staining was performed as detailed in legend for Figure 18. Cells were identified as indicated in Fig. 15 with an additional gate to identify extravascular $CD45.2\text{-}AF488^-$ cells. Data is shown as mean ± SEM of extravascular cells expressing different levels of IL18R1-tdT within the indicated T cell compartments from 2 pooled experiments (n = 3 mice per group and experiment). $^{**}P < 0.01$; $^{***}P < 0.001$ (Two-way ANOVA).

4.2.5. Role of IL18R expression by non-immune cells in the defense against *L. longbeachae*

4.2.5.1. IL18R expression by non-immune cells is required and sufficient for the defense against *L. longbeachae*

Next we investigated whether IL18R expression by non-immune cells is required for defense against *L. longbeachae*. For this, bone marrow chimeras (BMx) were generated in which the IL18R was expressed normally (WT BM into WT recipient, WT→WT), only by immune cells (WT BM into KO recipient, WT→*Il18r1*$^{-/-}$), only by non-immune cells (KO BM into WT recipient, *Il18r1*$^{-/-}$→WT) or not at all (KO BM into KO recipient, *Il18r1*$^{-/-}$→*Il18r1*$^{-/-}$) (Fig. 21A). After 12 weeks of reconstitution, the percentage of cells with the donor CD45 genotype was identified. αβ T cell chimerism was about 70 - 80 %, γδ T cell chimerism about 60 - 70 %, and neutrophil chimerism was at least 97 % 5 days after *L. longbeachae* infection (Fig. 21B). Any mice with a chimerism below 70 % for αβ T cells or below 50 % for γδ T cells were excluded from the experiment. Chimerism in neutrophils was higher than 95 % in all BMx mice.

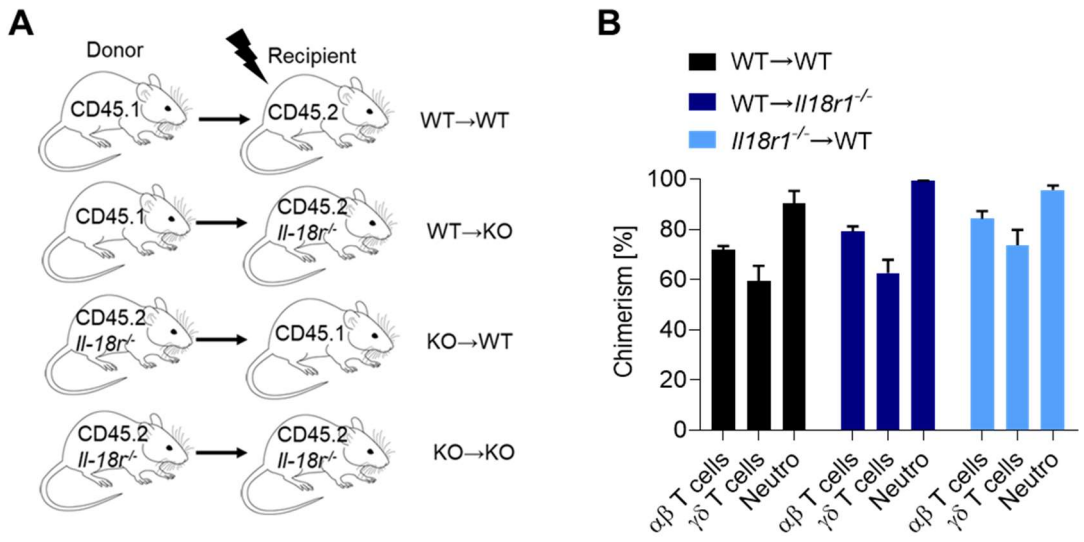

Figure 21: Generation of IL-18R1 bone marrow chimeras. (A) Bone marrow chimeras were generated by 9Gy irradiation of recipient mice and i.v. injection of $2x10^6$ donor bone marrow cells one day later. Reconstitution was allowed to proceed for 12 weeks. CD45 congenics were used to differentiate between donor and recipient cells. **(B)** Percentage of reconstitution (chimerism) for the indicated immune cell populations in the different bone marrow chimeras 5 days after i.n. infection with 10^4 CFU *L. longbeachae*-mCherry. Data shown as mean ± SEM of 2 pooled experiments (n = 3 mice per group and experiment). WT, wild-type; KO, *Il18r1*$^{-/-}$; CFU, colony-forming unit.

BMx mice were then infected with 10^4 CFU *L. longbeachae*-mCherry to quantify bacterial burden in the lungs 5 days after infection. Although all infected BMx mice showed a similar loss in body weight (Fig. 22A), there were differences in the bacterial load (Fig. 22B). Similar to our previous results using *Il18r1*$^{-/-}$ mice, *Il18r1*$^{-/-}$→*Il18r1*$^{-/-}$ BMx mice contained an about 100-fold higher bacterial burden in the lungs compared to their WT→WT counterparts (Fig. 22B), validating the use of BMx mice. Surprisingly, narrowing IL18R expression to the immune compartment (WT→*Il18r1*$^{-/-}$) did not rescue the bacterial burden (Fig. 22B). Instead, the *Il18r1*$^{-/-}$→WT mice in which IL18R expression was limited to the non-immune compartment showed a bacterial load similar to WT mice (Fig. 22B). These results indicate that IL18R expression by non-immune cells, but not by immune cells, is required and sufficient for the normal defense of *L. longbeachae* 5 days after infection.

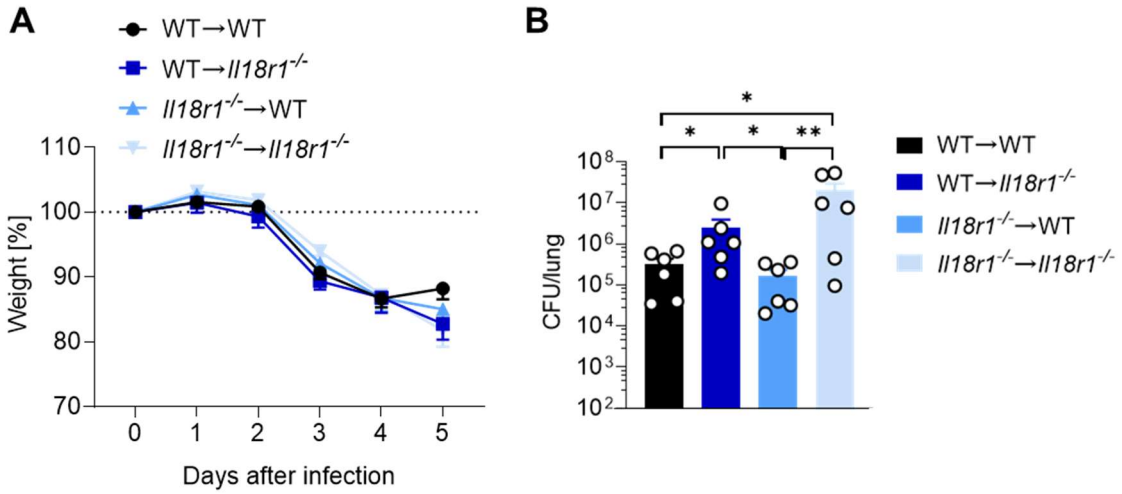

Figure 22: L18R expression by non-immune cells is required and sufficient for the defense of *L. longbeachae*. BMx mice as indicated in Fig. 21A were infected i.n. with 10^4 CFU *L. longbeachae*-mCherry. 5 days after infection lungs were dissected and analyzed. **(A)** Weight loss of the indicated BMx mice following infection. **(B)** CFU in the lungs of the indicated BMx mice 5 days after infection. Data shown as mean ± SEM from 2 pooled experiments (n = 3 mice per group and experiment). **P* < 0.05; ***P* < 0.01 (One-way ANOVA). CFU, colony-forming unit; WT, wild-type.

To confirm our results, we used a cre recombinase/*loxP* system to examine the role of $CD4^+$ T cells and $CD8^+$ T cells in *L longbeachae* infection. By generating heterozygous mice expressing cre recombinase under the *cd4* promoter crossed to a floxed *Il18r1* ($IL18R1^{flx/flx}$) mice, IL18R1 expression in αβ T cells ($CD4^+$ T cells, $CD8^+$ T cells, and DN T cells) was reduced to less than 1 % of the respective population in the lung 5 days after *L. longbeachae* infection (Fig. 23A), demonstrating efficient recombination. As expected, we did not observe recombination in the γδ T cell compartment, confirming that most of those cells do not have a history of CD4 expression (Pinheiro *et al.*, 2012). Mice in which αβ T cells lacked IL18R expression showed similar pulmonary bacterial burden as their control mice 5 days after infection with 10^4 CFU *L. longbeachae* (Fig. 23B), suggesting that IL18R expression by $CD4^+$- $CD8^+$- or DN αβ T cells was not required for the early defense of *L. longbeachae*.

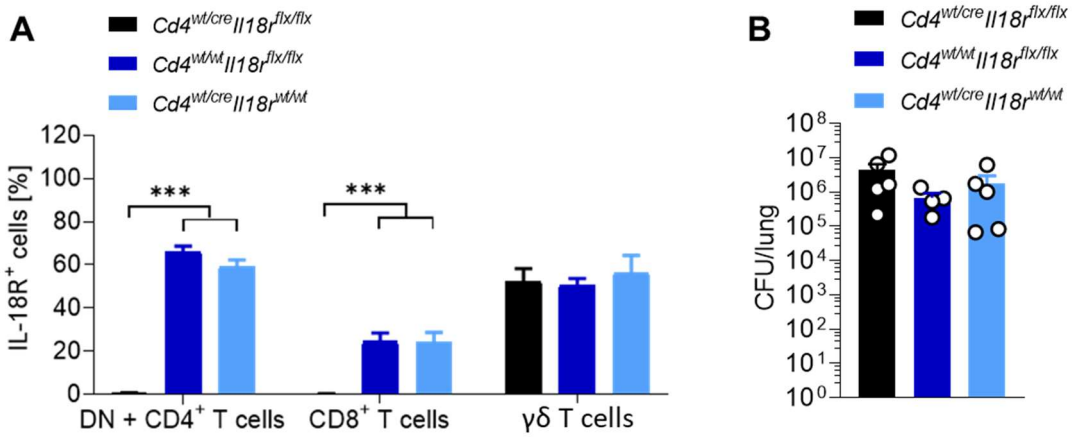

Figure 23: IL18R1 expression by CD4⁺ or CD8⁺ T cells does not contribute to the defense of *L. longbeachae* in the early phase of infection (A) Frequency of IL18R1⁺ T cells from the indicated mice 5 days after i.n. infection with 10^4 CFU *L. longbeachae*-mCherry. **(B)** CFU in the lungs of mice from (A). Data shown as mean ± SEM of 1 experiment (n = 4-5 mice per group). ***$P < 0.001$ (One-way ANOVA). Ig, Immunoglobulin; Ctrl, control; DN, double-negative; CFU, colony-forming unit.

To examine the role of NK cells in *L. longbeachae* control of bacterial burden, mice were treated with anti-NK1.1 antibody. NK cells were efficiently depleted from the lungs 5 days after infection with *L. longbeachae* (Fig. 24B). Depletion had no effect on the weight of infected mice (Fig. 24C) or bacterial burden in the *L. longbeachae* infected lungs, suggesting that NK cells and NK T cells play no protective role at the investigated time point (Fig. 24D).

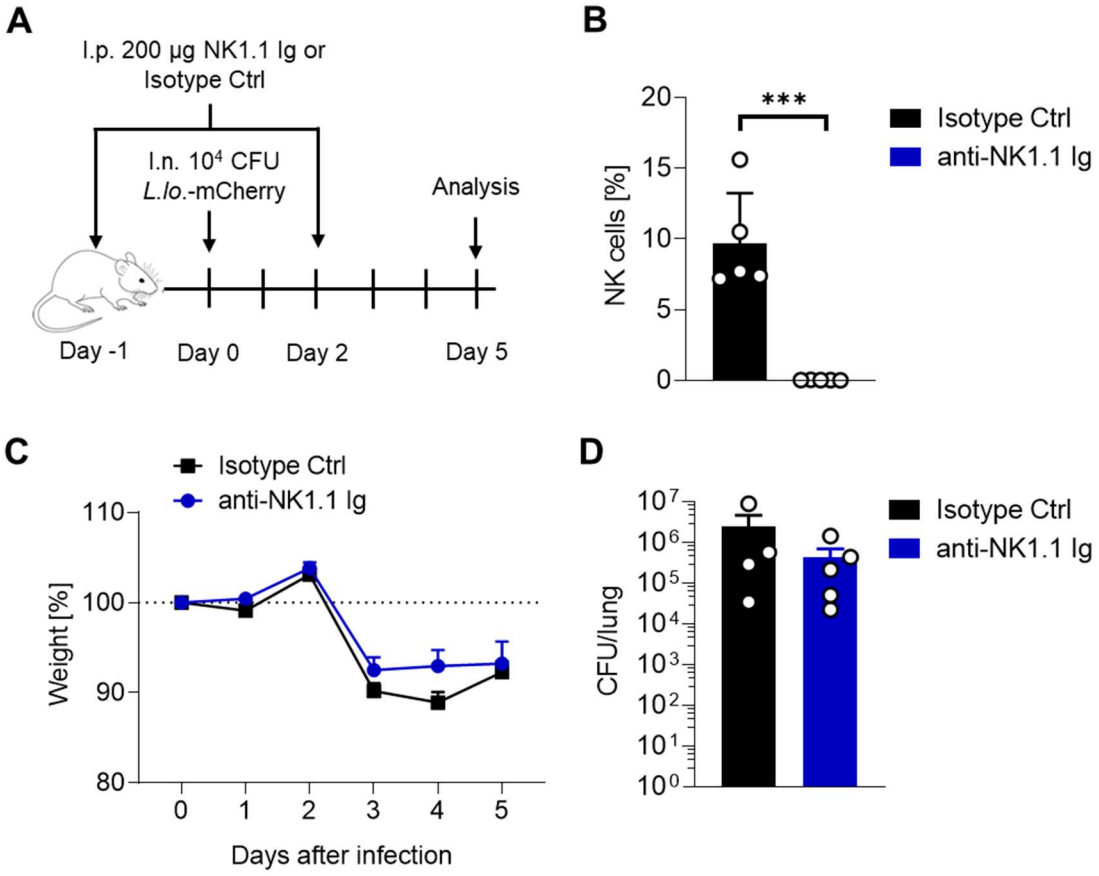

Figure 24: Depletion of NK1.1⁺ cells does not impair the bacterial burden of *L. longbeachae* in the acute phase of infection. **(A)** Diagram illustrating the experimental plan. **(B)** Number of NK cells 5 days after i.n. infection with 10^4 CFU *L. longbeachae*. Mice were depleted of NK1.1⁺ NK and NK T cells one day before infection. **(C, D)** Weight loss (C) and bacterial burden in the lungs (D) of mice treated as shown in (A). Data shown as mean ± SEM of 1 experiment (n = 4-5 mice per group). ***$P < 0.001$ (Student's *t*-test). *L. lo., L. longbeachae*; CFU, colony-forming unit; Ig, immunoglobulin; Ctrl, control.

4.2.5.2. Bronchiolar ciliated epithelial cells express IL18 receptor

As IL18R expression by non-immune cells appeared to be required for pulmonary defense of *L. longbeachae,* we aimed to identify those cells by flow cytometry and confocal microscopy using IL18R1-tdTomato reporter mice. Due to differences in sensitivity, all flow cytometric experiments were performed using heterozygous IL18R1-tdTomato mice, whereas all those involving confocal microscopy were performed on homozygous IL18R1-tdTomato mice.

Within non-immune cells, IL18R1-tdTomato was mainly expressed by pulmonary epithelial cells (EpC), as identified through surface staining with anti-EpCAM antibodies by flow cytometry (Fig. 25A, B). About 90 % of the $EpCAM^+$ epithelial cells expressed IL18R1-tdTomato (Fig. 25C). Since bronchiolar EpC, but not alveolar EpC, express high EpCAM levels, these results suggest that $IL18R1^+$ EpC are located in bronchioles. In contrast, a very low proportion of endothelial cells and other stromal cells showed tdTomato, and most of those that expressed it did so at lower levels than EpC (Fig. 25B). IL-18R1-tdTomato expression by stromal cells was not modulated during infection with *L. longbeachae* (Fig. 25B). These results identify EpC as the main expressors of IL18R1 within the non-immune compartment.

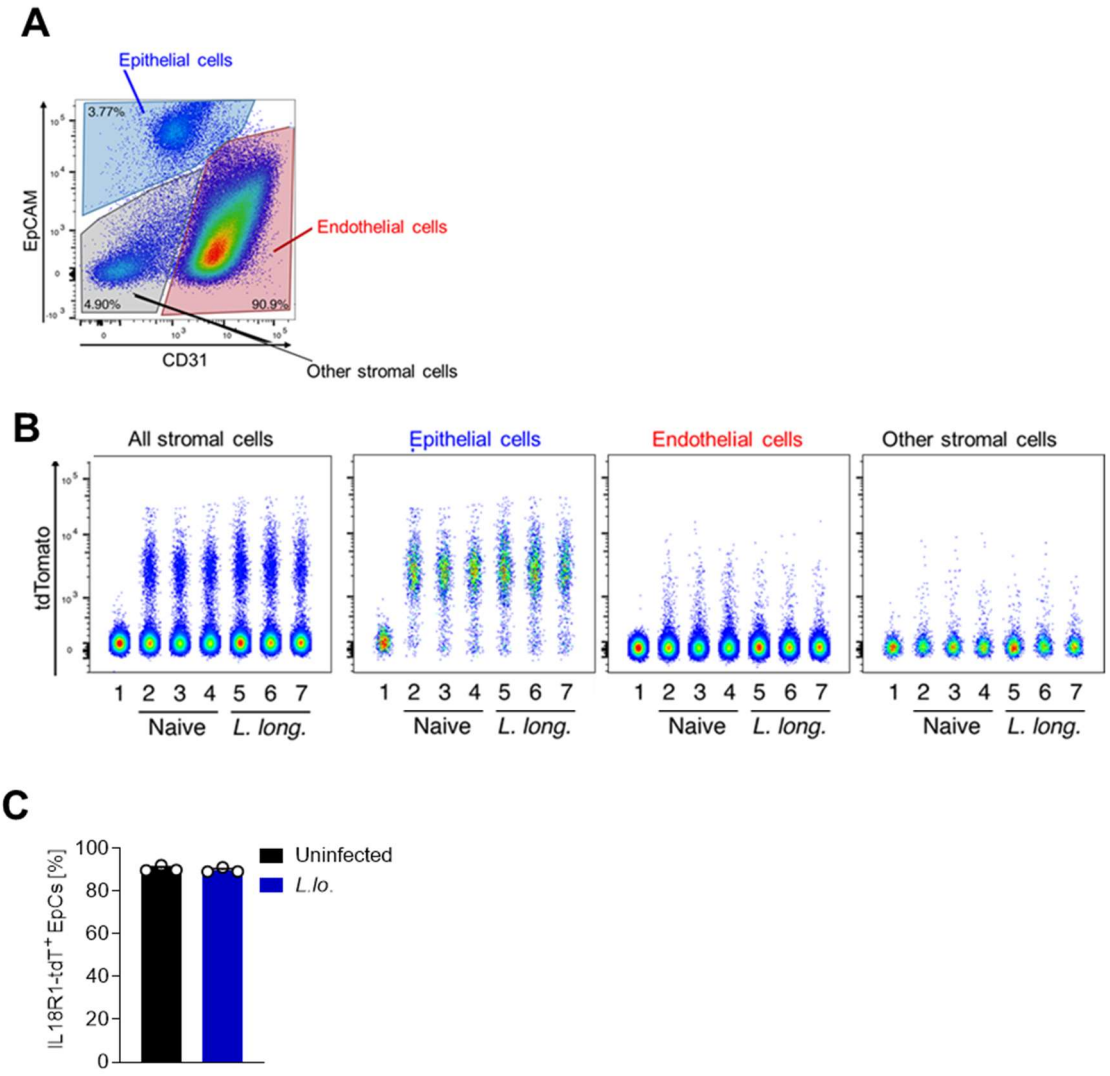

Figure 25: Pulmonary epithelial cells express the IL18R. (A) Representative flow cytometry gates on CD45^{-}Ter119^{-} pulmonary stromal cells to identify epithelial cells (EpCAM^{+}CD31^{-}), endothelial cells (EpCAM^{-}CD31^{+}) and other stromal cells (EpCAM^{-}CD31^{-}). **(B)** Flow cytometry dot plots showing IL18R1-tdTomato expression by different stromal cell populations identified as in (A) from naive mice or 3 days after i.n. infection with 10^4 CFU *L. longbeachae*. Numbers on the x-axis indicate different mice (1, naive WT mice). **(C)** Proportion of IL-18R1-tdTomato^{+} cells within the EpC compartment as gated in (A). Data shown as mean ± SEM from a representative (n = 3 mice per group) of 5 independent experiments. *L.long. or L.lo., L. longbeachae*.

To identify the precise location of IL18R1^{+} EpC in the lungs, confocal microscopy was performed on lung vibratome sections from IL18R1-tdT mice. Confirming our flow cytometric data, most tdTomato expression by non-immune cells was restricted to epithelial cells of conducting bronchioles, with very few single tdTomato^{+} CD45^{-} non-immune cells scattered in the alveolar region (Fig. 26).

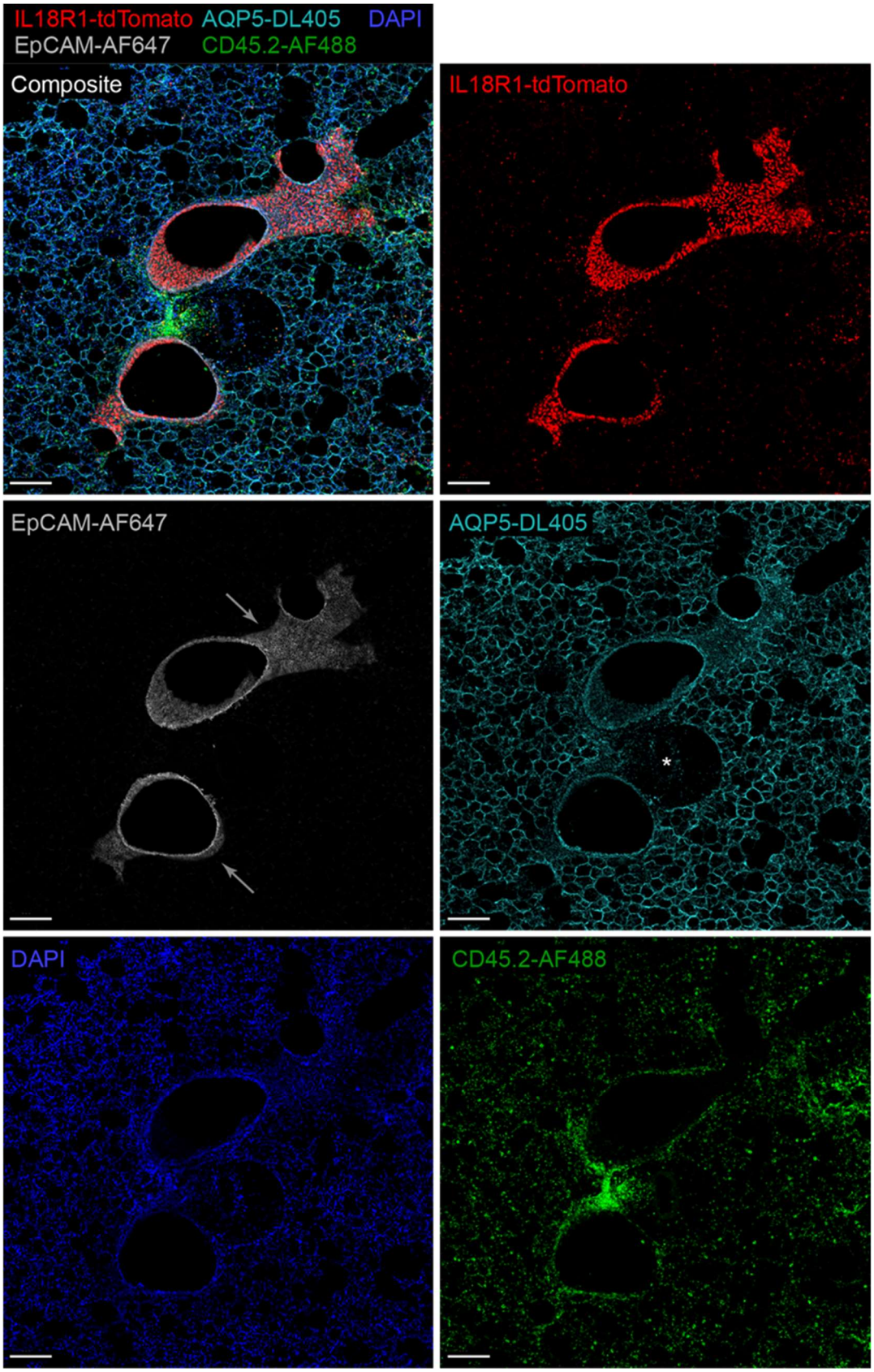

Figure 26: (legend on next page)

Epithelial cells in the mouse bronchioles are mainly ciliated EpC and secretory club cells, with a minor contribution of mucus-producing goblet cells (Murray, 2010). To further identify which type of bronchiolar EpC expresses IL18R1, super-resolution confocal microscopy was performed. Cilia in epithelial cells were identified by staining for EpCAM and acetylated tubulin (Ott and Lippincott-Schwartz, 2012), whereas club cells were identified by staining for uteroglobin (Rokicki *et al.*, 2016b). All IL18R1-tdT$^+$ EpC in the bronchiolar wall were ciliated (Fig. 27 and Fig. 28). We did not detect IL18R1-tdT$^+$ club cells (Fig. 27 and 28). Only occasionally, we observed epithelial cells in the bronchiolar wall that were neither club cells (negative for uteroglobin) nor ciliated cells (negative for acetylated tubulin). These cells were presumably rare goblet cells, which did not express IL18R1-tdT (Fig. 28).

Figure 26: Bronchial epithelial cells express IL18R1. Confocal microscopy image of vibratome lung section from a homozygous IL18R1-tdT mouse. Five fluorochrome differentiation as well as autofluorescence removal were performed by spectral unmixing. Bronchiolar epithelial cells are EpCAM$^+$; alveolar EpC are aquaporin 5 (AQP5)$^+$; leukocytes are CD45.2$^+$. Nuclei are DAPI$^+$. Arrows indicate bronchioli; *, blood vessel lumen. Similar results were obtained in 5 independent experiments. AF, AlexaFluor; DL, Dylight. Bar, 200µm.

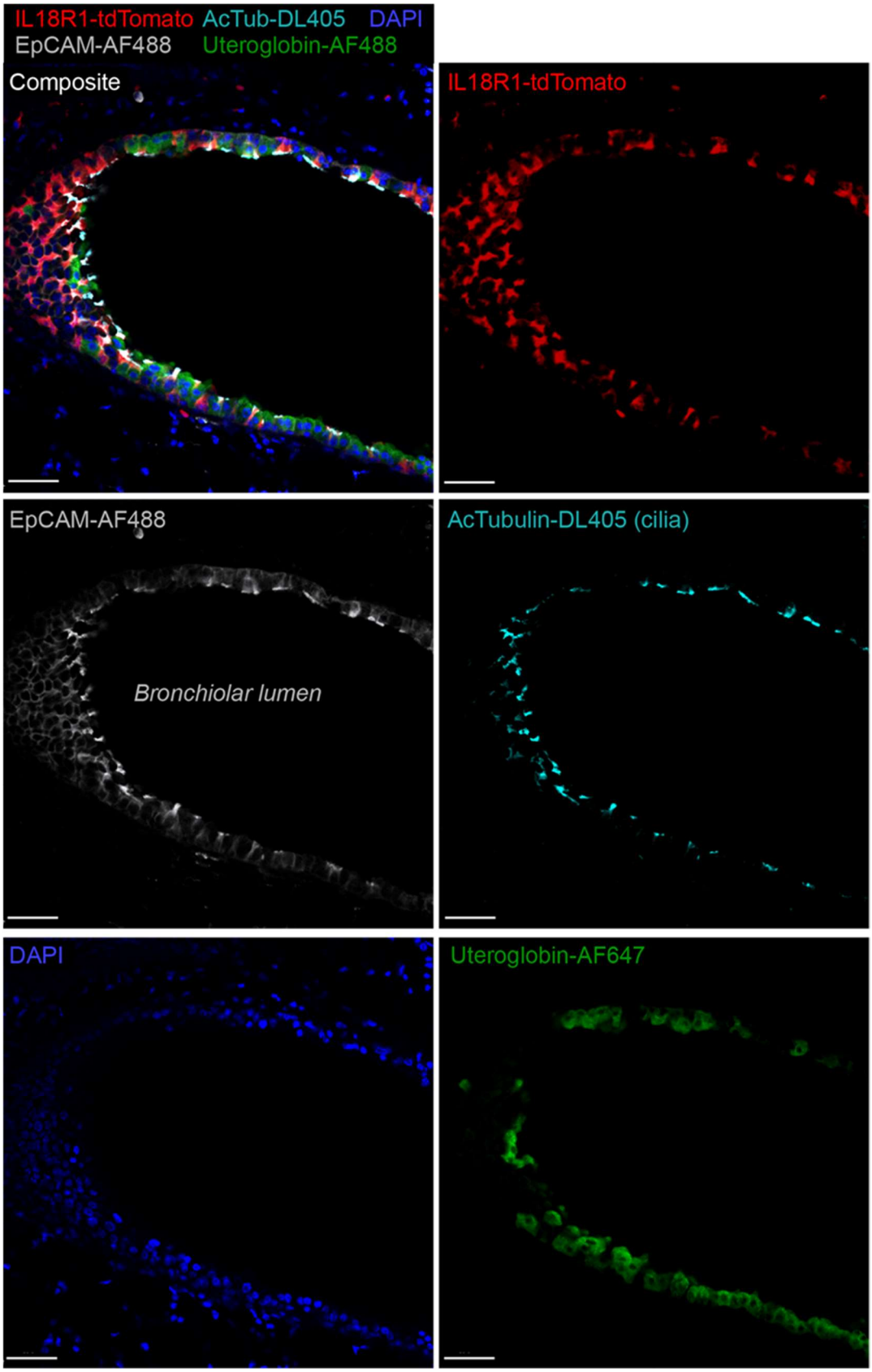

Figure 27: (legend on the second next page)

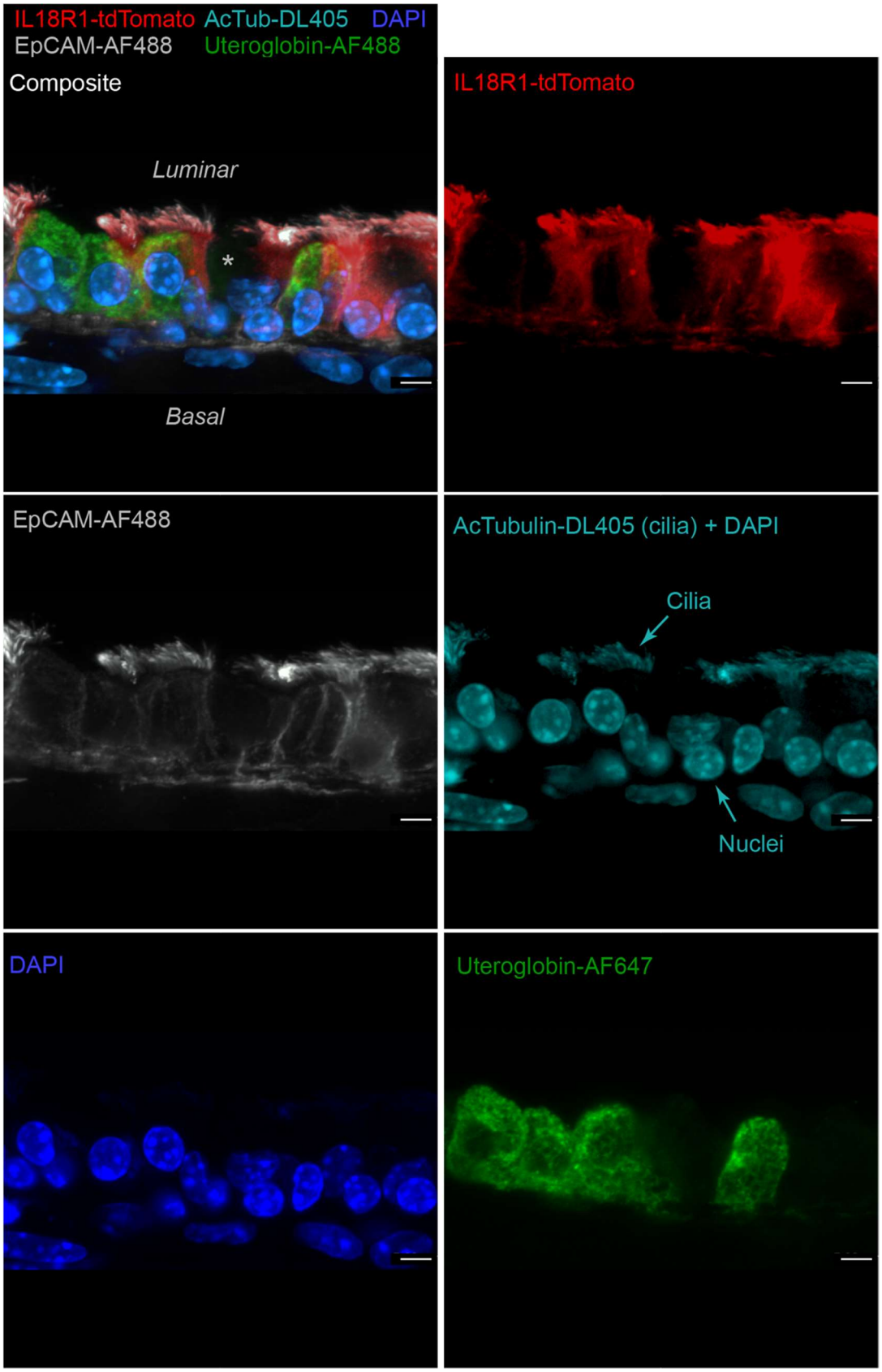

Figure 28: (figure legend on next page)

Figure 27: Bronchial ciliated epithelial cells express IL18R1. Confocal microscopy image of vibratome lung section from a homozygous IL18R1-tdT mouse. Shown is a detail from the bronchiolar wall. Five fluorochrome differentiation as well as autofluorescence removal were performed by spectral unmixing. Bronchiolar epithelial cells are EpCAM$^+$; ciliated EpC are positive for acetylated tubulin (AcTub); Club cells are uteroglobin$^+$; Nuclei are DAPI$^+$. Similar results were obtained in 5 independent experiments. AF, AlexaFluor; DL, Dylight. Bar, 50µm.

Figure 28: Bronchial ciliated epithelial cells express IL18R1. High magnification AiryScan confocal microscopy image of vibratome lung section from a homozygous IL18R1-tdT mouse. Shown is a detail from the bronchiolar wall. Five fluorochrome differentiation as well as autofluorescence removal were performed by spectral unmixing. However, due to the set-up of the AiryScan microscope, spectral detection for DL405 also detected DAPI signal. Bronchiolar epithelial cells are EpCAM$^+$; ciliated EpC are positive for acetylated tubulin (AcTub); Club cells are uteroglobin$^+$; Nuclei are DAPI$^+$. Similar results were obtained in 5 independent experiments. *, presumably a rare globet cell negative for acetylated tubulin, uteroglobin and tdTomato. AF, AlexaFluor; DL, Dylight. Bar, 5µm.

4.2.5.3. Role of the IL18/IL18R axis on ciliary beating frequency and mucus production by pulmonary epithelial cells

We investigated whether IL18 modulated EpC-autonomous antibacterial defenses in bronchioles. Cilia beating by ciliated EpC and mucus production by adjacent secretory EpC are amongst the main EpC-autonomous defense mechanisms in the bronchiolar wall (Whitsett and Alenghat, 2015). Thus, we quantified the effect of IL18 or its receptor on mucus production by goblet cells.

Mucus in the lung is mainly produced by goblet cells, which are specialized EpC situated in the bronchiolar wall adjacent to IL18R1$^+$ ciliated EpC. Mucin (MUC) 5A, B and C are the main mucus components, with MUC5B being required for airway defense against bacterial infection (Roy *et al.*, 2014). Consistent with their inducible nature, we observed an increase of lung MUC5AC and MUC5B upon infection with *L. longbeachae* (Fig. 29A, B). However, this increase was independent of IL18 or IL18R1 expression (Fig. 29A, B), suggesting that these molecules did not modulate mucus production.

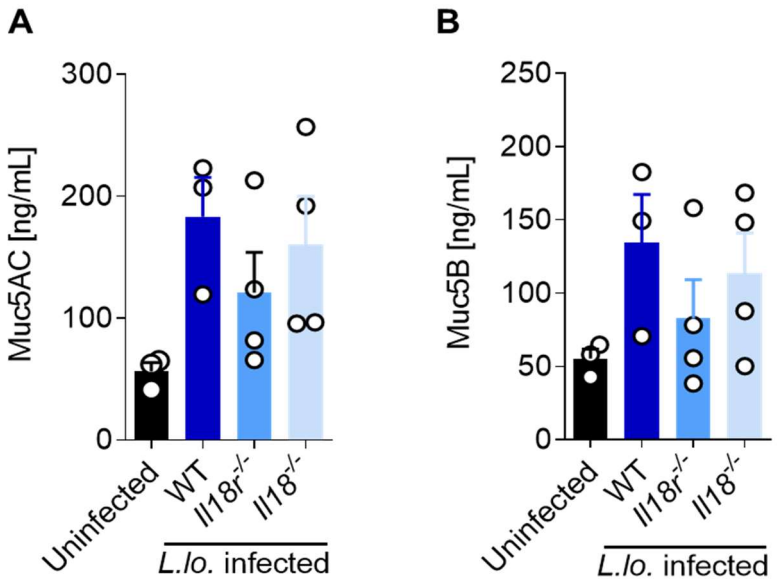

Figure 29: Role of IL18 on mucus production by pulmonary epithelial cells. (A, B) MUC5AC and MUC5B concentration in the lungs of the indicated mice. Mice were i.n. infected with 10^4 CFU *L. longbeachae* 5 days before analysis. Data shown as mean ± SEM of 1 experiment (n = 3-4 mice per group) *L.lo., L. longbeachae.*

4.2.5.4. IL18R expression by non-immune cells promotes *L. longbeachae* killing by pulmonary neutrophils

We investigated whether signaling via the IL18R on pulmonary epithelial cells contributes to a reduction of *L. longbeachae* CFUs by enhancing the bactericidal capacity of neutrophils during infection. For this, we generated BMx in which the IL18R1 was not expressed in any cells (*Il18r1*$^{-/-}$→*Il18r1*$^{-/-}$) or only in non-immune cells (*Il18r1*$^{-/-}$→WT). BMx mice were allowed to reconstitute for 12 weeks. The level of reconstitution was similar to that in previous experiments (Fig. 21B): about 98 % for the neutrophil compartment and about 70 - 80% for the T cell compartment (Fig. 30B). All mice had at least 70 % reconstitution in the T cell compartment.

BMx mice were infected i.n. with 10^4 CFU *L. longbeachae*-mcherry, and 3 days later, pulmonary neutrophils containing similar levels of *L. longbeachae* (similar mCherry expression levels) were FACS sorted (Fig. 30A). Sorted *L. longbeachae*-containing neutrophils were split into two equal aliquots to monitor their ability to kill *L. longbeachae ex vivo*. The first aliquot was lysed and plated out on BCYE agar plates, whereas the second aliquot was incubated at 37 °C for further 30 min before being lysed and plated on BCYE agar plates (Fig. 30C). Neutrophils from BMx mice expressing the IL18R only in non-immune cells eliminated about 40 % more bacteria over the period of 30 min as their counterparts deficient in IL18R expression (*Il18r1*$^{-/-}$→ *Il18r1*$^{-/-}$) (Fig. 30C). These results suggest that IL-18R expression by stromal cells enhanced *L. longbeachae* killing by pulmonary neutrophils.

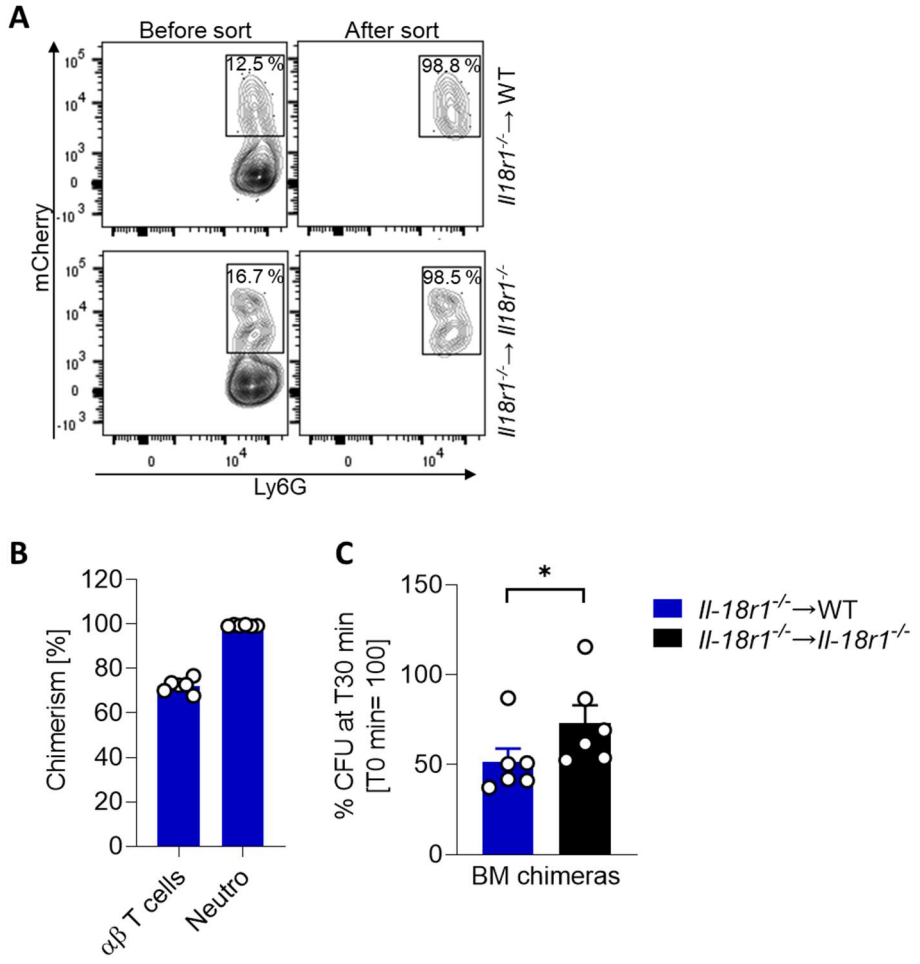

Figure 30: IL18R expression by non-immune cells promotes *L. longbeachae* killing by pulmonary neutrophils. (A) Representative flow cytometry gates on viable $CD45^+CD11b^+Ly6C^-$ cells before (left) and after (right) sorting of $mCherry^+$ neutrophils from *Il18r*$^{-/-}$→*Il18r*$^{-/-}$ and *Il18r*$^{-/-}$→WT BMx chimeras **(B)** Percentage of reconstitution (chimerism) for the indicated immune cell populations in the different bone marrow chimeras 3 days after infection i.n. with 10^4 CFU *L. longbeachae*-mCherry. **(C)** Percentage of *L. longbeachae* CFUs in neutrophils of mice without IL18R expression by immune cells or non-immune cells (*Il18r*$^{-/-}$→Il18r$^{-/-}$) or of mice with expression of the IL18R only by non-immune cells (*Il18r*$^{-/-}$→WT) after 30 min normalized to T0 = 100 %. Data shown in (B, C) represents the mean ± SEM of 2 pooled experiments (n = 3 mice per group and experiment). In (C) **P* < 0.05 (Student's *t*-test). WT, wild-type; CFU, colony-forming unit.

4.3. Discussion

The main aim of this chapter was to elucidate the function of IL18 and its corresponding IL18R in the defense against *L. longbeachae* during pulmonary infection in mice.

Our results showed that IL18 and its receptor contribute to efficient clearance of *L. longbeachae* from the lungs. This stands in contrast to infections with *L. pneumophila*, where IL18 has no effect on the bacterial burden, indicating different mechanisms in protection against the two bacteria (Brown *et al.*, 2016). During infection with *L. longbeachae* we observed increased levels of IFNγ, of which about 45 % was dependent on IL18R signaling, while about 55 % was produced in an IL18R-independent manner. The role of IFNγ in the defense of *L. longbeachae* is unknown yet. However, a recent study revealed that mucosa associated invariant T (MAIT) cells are activated by *L. longbeachae* and promote an IFNγ-dependent clearance of the bacteria in the late phase of infection (10 days after infection) (Wang *et al.*, 2018).

IL18 is secreted by macrophages and dendritic cells upon stimulation and induces IFNγ production by mostly lymphocytes through binding to its corresponding IL18R (Nakahira *et al.*, 2002). Using IL18R1-tdTomato reporter mice, we found high IL18R1 expression by αβ T cells, DN T cells, γδ T cells, NK cells, and NK T cells, as well as low expression of the receptor by neutrophils. This is in line with *Il18r1* mRNASeq data (IMMGEN) and supports the reliability of the IL18R1-tdTomato reporter. This reporter mouse line is advantageous over antibody staining in mice because of the weak signal of the latter.

The source for IL18R-independent IFNγ during *L. longbeachae* infection may be NK cells, unconventional T cells or, at later stages of infection, by antigen-specific T cells. NK cells possess activating receptors (e.g. IL12R) which may be upregulated during infection and result in IFNγ production after stimulation (Mah and Cooper, 2016). Likewise, unconventional T cells, such as NK T cells, γδ T cells or MAIT cells may be activated by recognizing specific bacterial components via their TCR that induce IFNγ production (Balato *et al.*, 2009; Provine *et al.*, 2018).

Surprisingly, IL18R expression by non-immune cells, but apparently not by immune cells, was required and sufficient for the defense against *L. longbeachae* during pulmonary infection, as indicated using BMx mice. This was further supported by the finding that mice in which $CD4^+$ T cells and $CD8^+$ T cells lacked IL18R1 expression did not have an altered bacterial burden. Likewise, depletion of NK/ NK T cells did not lead to a higher bacterial burden in the *L. longbeachae* infected lungs, indicating that those cells are not required for early control of the bacteria. However, we detected an increasing infiltration of $CD4^+$ and $CD8^+$ T lymphocytes starting from day 7 after *L. longbeachae* infection. Therefore, it is likely that those T cells contribute to the late defense against the bacteria, reflecting an ongoing adaptive immune response.

Further microscopy imaging revealed that the pulmonary IL18R1 expressing non-immune were ciliated epithelial cells in the bronchiolar wall of the lungs. This was confirmed by flow cytometry analysis, although mild collagenase IV digestion resulted in the loss of many epithelial cells, giving the false impression that all pulmonary epithelial cells express IL18R1-tdTomato, when in fact secretory bronchiolar club cells and goblet cells did not express the receptor as demonstrated by confocal microscopy. IL18R expression has been described for epithelial cell lines or intestinal epithelial cells, where signaling via this receptor is involved in negative regulation of goblet cell maturation and has to be strictly maintained in equilibrium to prevent tissue damage during colitis (Nowarski *et al.*, 2015). In the lungs, goblet cells promote the defense of pathogens by producing mucus, which contains mainly mucin glycoproteins, including MUC5AC and MUC5B (Ma *et al.*, 2018). Although overall mucus production was enhanced in infected mice, IL18R signaling in pulmonary ciliated epithelial cells did not affect the expression of MUC5AC or MUC5B by goblet cells, suggesting that other defense mechanisms play a role in reducing *L. longbeachae* burden in the lungs. In this regard, it has been described that *L. pneumophila* increases expression of MUC5AC via ERK-JNK and NFκB pathways after effector proteins are translocated (Morinaga *et al.*, 2012). A similar mechanism may also induce mucus production by goblet cells during infection with *L. longbeachae*, although this remains to be elucidated. At the level of protection through the pulmonary

epithelial barrier, IL18R signaling in ciliated epithelial cells may be able to enhance ciliary beating frequency, thereby promoting bacterial clearance. This possibility could be tested by quantifying the ciliary beating frequency in infected WT and *Il18r1*$^{-/-}$ mice using high-speed video microscopy in further experiments.

Using BMx mice which express the IL18R only in the non-immune compartment we further investigated whether signaling via this receptor promote bacterial killing by other immune cells. IL18R signaling in pulmonary ciliated epithelial cells enhanced the *L. longbeachae* killing by neutrophils. The mechanism behind this finding is currently under investigation. A possibility is that IL18 induces production of pro-inflammatory cytokines in ciliated epithelial cells, which may activate neutrophils and thereby promote the clearance of *L. longbeachae*. For instance, a study with epithelial cell lines has shown that IL18R signaling induces IL8 secretion, which may have an impact on neutrophil recruitment (Krásná *et al.*, 2005; Kolinska *et al.*, 2008). However, it is unlikely that this is the responsible mechanism because BMx mice lacking IL18R1 expression in non-immune cells had increased neutrophil recruitment upon infection. Other proinflammatory cytokines produced by epithelial cells such as TNFα, IL1ß or GM-CSF can, in principle, amplify antimicrobicidal functions in neutrophils, including production of ROS (Lee *et al.*, 2004; Kato and Kitagawa, 2006). Therefore, to further investigate the mechanism behind our finding, the production of ROS and RNS by neutrophils could be analyzed by culturing infected neutrophils with supernatant from epithelial cells derived from BMx mice in which the IL18R is only expressed on non-immune cells.

This chapter highlights a protective pathway of IL18R signaling in epithelial cells that promotes the microbicidal activity of neutrophils and thereby clearance of *L. longbeachae* from the lungs.

Chapter 5: General discussion

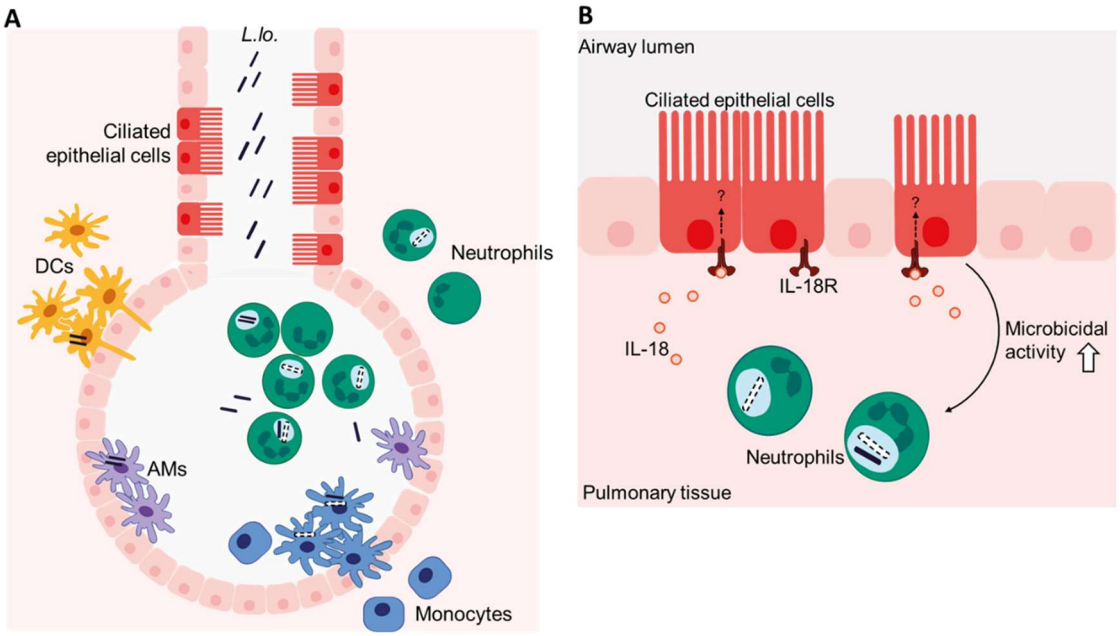

Figure 31: Immune response to *L. longbeachae* pulmonary infection. (A) During infection, *L. longbeachae* reaches the alveoli of the lungs, where it encounters different non-immune cells and immune cells. Mainly neutrophils, but also other myeloid cells, take up the bacteria and eliminate them. **(B)** Pulmonary ciliated epithelial cells express IL18R. Binding of IL18 to this receptor induces intracellular signaling. While this has no effect on mucus production, IL18R signaling in pulmonary ciliated epithelial cells enhances the microbicidal activity of neutrophils via a still unknown mechanism.

This work has focused on the cellular mechanisms and the role of IL18 and its corresponding receptor in the defense against *L. longbeachae*.

Early during infection, we observed infiltration of immune cells into the lungs, with neutrophils being the dominant cell population, followed by monocytes and dendritic cells, confirming a recent study (Gobin *et al.*, 2009). Recruitment of those cells during infections is usually mediated by chemokines initially produced by pulmonary epithelial cells or tissue-resident cells (Sokol and Luster, 2015). However, the mechanism for recruitment of immune cells during infection with *L. longbeachae* still remains to be elucidated. After reaching the infected tissue, myeloid cells internalized *L. longbeachae*. Confocal microscopy imaging revealed the formation of infection foci in the alveoli close to pulmonary bronchioles, which has been previously observed (Gobin *et al.*, 2009). Those

contained a large number of leukocytes and bacteria, suggesting a local defense to possibly prevent further spread of the bacteria. In the acute phase of infection mainly neutrophils and monocytes contributed to the clearance of *L. longbeachae* from the lungs. Most likely pulmonary defense by neutrophils is mediated through their potent microbiocidal mechanisms. Those include ROS, RNS, acidification of endolysosomes, proteases and antimicrobial peptides (Segal, 2005). Monocytes, on the other hand, can mature to monocyte-derived cells with functions similar to DCs and tissue-resident macrophages (Brown *et al.*, 2017). During later time points lymphocytes increasingly infiltrate the lungs and may promote the late defense against *L. longbeachae*, as it has been shown for MAIT cells (Wang et al. 2018).

During infection with *L. longbeachae* we observed increased levels of IFNγ production. IL18 is known to be a potent inducer of IFNγ in T cells and NK cells, thereby promoting microbial clearance (Dinarello *et al.*, 2013). High IL-18R expression was identified by αβ T cells, DN T cells, γδ T cells, NK cells and pulmonary ciliated epithelial cells using IL18R1-tdTomato reporter mice. Surprisingly, IL18R expression by immune cells was apparently irrelevant for the defense against L. lo. Rather, expression by non-immune cells was required and sufficient to reduce the burden of *L. longbeachae* from the lungs. Confocal microscopy and flow cytometry analysis revealed that pulmonary ciliated epithelial cells were the IL18R expressing cells. Signaling via this receptor on pulmonary ciliated epithelial cells did not influence mucus production by bystander goblet cells. However, IL18R signaling in ciliated epithelial cells enhanced the microbicidal activity of neutrophils via a still unknown mechanism and thereby promotes clearance of *L. longbeachae* from the lungs (Fig.19B).

Overall, this work highlights the role of neutrophils and pulmonary ciliated epithelial cells in the defense of *L. longbeachae* and demonstrated a pathway of IL18R signaling for efficient clearance of the bacteria.

References

Abdelrazik Othman, A. and Salah Abdelazim, M. (2017) ‘Ventilator-Associated Pneumonia in Adult Intensive Care Unit Prevalence and Complications’. *The Egyptian Journal of Critical Care Medicine*, 5(2), pp. 61–63

Abe, T., Marutani, Y. and Shoji, I. (2019) ‘Cytosolic DNA-Sensing Immune Response and Viral Infection’. *Microbiology and Immunology*, 63(2), pp. 51–64

Actor, J.K. (2012) 'Elsevier´s Integrated Review Immunology and Microbiology'. Phiadelphia; *Elsevier Sanders*, pp. 1-192

Alli, O.A.T., Gao, L.-Y., Pedersen, L.L., Zink, S., Radulic, M., Doric, M. and Abu Kwaik, Y. (2000) ‘Temporal Pore Formation-Mediated Egress from Macrophages and Alveolar Epithelial Cells by Legionella Pneumophila’. *Infection and Immunity*, 68(11), pp. 6431–6440

Amalia Alcón, Fabregas, Torres. and Fabregas (2005) ‘Pathophysiology of Pneumonia’. *Clinics in Chest Medicine*, 26(1), pp. 39–46.

Amulic, B., Cazalet, C., Hayes, G.L., Metzler, K.D. and Zychlinsky, A. (2012) ‘Neutrophil Function: From Mechanisms to Disease’. *Annual Review of Immunology*, 30(1), pp. 459–489

Ang, D.K.Y., Ong, S.Y., Brown, A.S., Hartland, E.L. and van Driel, I.R. (2012) ‘A Method for Quantifying Pulmonary Legionella Pneumophila Infection in Mouse Lungs by Flow Cytometry’. *BMC Research Notes*, 5, p. 448

Antunes, M.A., Morales, M.M., Pelosi, P. and Macêdo Rocco, P.R. (2013) ‘Lung Resident Stem Cells’. In *Resident Stem Cells and Regenerative Therapy*. Elsevier, pp. 105–122

Appelt, S. and Heuner, K. (2017) ‘The Flagellar Regulon of Legionella−A Review’. *Frontiers in Cellular and Infection Microbiology*, 7, p. 454

Arango Duque, G. and Descoteaux, A. (2014) ‘Macrophage Cytokines: Involvement in Immunity and Infectious Diseases’. *Frontiers in Immunology*, 5, p. 491

Asare, R. (2006) 'Molecular Pathogenesis of Legionella Longbeachae'. *Electronic Theses and Dissertations*, paper 51

Asare, R. and Abu Kwaik, Y. (2007) ‘Early Trafficking and Intracellular Replication of *Legionella Longbeachaea* within an ER-Derived Late Endosome-like Phagosome’. *Cellular Microbiology*, 9(6), pp. 1571–1587

Asare, R., Santic, M., Gobin, I., Doric, M., Suttles, J., Graham, J.E., Price, C.D. and Abu Kwaik, Y. (2007) ‘Genetic Susceptibility and Caspase Activation in

Mouse and Human Macrophages Are Distinct for *Legionella Longbeachae* and *L. Pneumophila*'. *Infection and Immunity*, 75(4), pp. 1933–1945

Atkinson, S., Valadas, E., Smith, S.M., Lukey, P.T. and Dockrell, H.M. (2000) 'Monocyte-Derived Macrophage Cytokine Responses Induced by M. Bovis BCG'. *Tubercle and Lung Disease*, 80(4), pp. 197–207

Bacigalupe, R., Lindsay, D., Edwards, G. and Fitzgerald, J.R. (2017) 'Population Genomics of *Legionella Longbeachae* and Hidden Complexities of Infection Source Attribution'. *Emerging Infectious Diseases*, 23(5), pp. 750–757

Balato, A., Unutmaz, D. and Gaspari, A.A. (2009) 'Natural Killer T Cells: An Unconventional T-Cell Subset with Diverse Effector and Regulatory Functions'. *Journal of Investigative Dermatology*, 129(7), pp. 1628–1642

Bals, R. and Hiemstra, P.S. (2004) 'Innate Immunity in the Lung: How Epithelial Cells Fight against Respiratory Pathogens'. *European Respiratory Journal*, 23(2), pp. 327–333

Baskerville, A., Dowsett, A.B., Fitzgeorge, R.B., Hambleton, P. and Broster, M. (1983) 'Ultrastructure of Pulmonary Alveoli and Macrophages in Experimental Legionnaires' Disease'. *The Journal of Pathology*, 140(2), pp. 77–90

Beauté, J., Robesyn, E. and de Jong, B. (2013) 'Legionnaires' Disease in Europe: All Quiet on the Eastern Front?' *European Respiratory Journal*, 42(6), pp. 1454–1458

Betts, J.G., Desaix, P., Johnson, E., Johnson, J.E., Korol, O., Kruse, D., Poe, B., Wise, J.A., Womble, M. and Young, K.A. (2013) 'Anatomy & Physiology'. p. 1420

Bevan, M.J. (2004) 'Helping the $CD8^+$ T-Cell Response'. *Nature Reviews Immunology*, 4(8), pp. 595–602

Bhan, U., Trujillo, G., Lyn-Kew, K., Newstead, M.W., Zeng, X., Hogaboam, C.M., Krieg, A.M. and Standiford, T.J. (2008) 'Toll-Like Receptor 9 Regulates the Lung Macrophage Phenotype and Host Immunity in Murine Pneumonia Caused by Legionella Pneumophila'. *Infection and Immunity*, 76(7), pp. 2895–2904

Bhat, P., Leggatt, G., Waterhouse, N. and Frazer, I.H. (2017) 'Interferon-γ Derived from Cytotoxic Lymphocytes Directly Enhances Their Motility and Cytotoxicity'. *Cell Death & Disease*, 8(6), p. e2836

Biet, F., Locht, C. and Kremer, L. (2002) 'Immunoregulatory Functions of Interleukin 18 and Its Role in Defense against Bacterial Pathogens'. *Journal of Molecular Medicine*, 80(3), pp. 147–162

Boraschi, D., Italiani, P., Weil, S. and Martin, M.U. (2018) 'The Family of the Interleukin-1 Receptors'. *Immunological Reviews*, 281(1), pp. 197–232

Boring, L., Gosling, J., Chensue, S.W., Kunkel, S.L., Farese, R.V., Broxmeyer, H.E. and Charo, I.F. (1997) 'Impaired Monocyte Migration and Reduced Type 1 (Th1) Cytokine Responses in C-C Chemokine Receptor 2 Knockout Mice.' *Journal of Clinical Investigation*, 100(10), pp. 2552–2561

Borregaard, N. (2010) 'Neutrophils, from Marrow to Microbes'. *Immunity*, 33(5), pp. 657–670

Boyton, R.J. and Openshaw, P.J. (2002) 'Pulmonary Defences to Acute Respiratory Infection'. *British Medical Bulletin*, 61(1), pp. 1–12

Brembilla, N.C., Senra, L. and Boehncke, W.-H. (2018) 'The IL-17 Family of Cytokines in Psoriasis: IL-17A and Beyond'. *Frontiers in Immunology*, 9

Brieland, J., Freeman, P., Chrisp, C. and Hurley, M. (1994) 'Replicative Legionella Pneumophila Lung Infection in Intratracheally Inoculated A/J Mice'. 145(6), p. 10

Brieland, Jackson, C., Hurst, S., Loebenberg, D., Muchamuel, T., Debets, R., Kastelein, R., Churakova, T., Abrams, J., Hare, R. and O'Garra, A. (2000) 'Immunomodulatory Role of Endogenous Interleukin-18 in Gamma Interferon-Mediated Resolution of Replicative Legionella Pneumophila Lung Infection'. *Infection and Immunity*, 68(12), pp. 6567–6573

Brown (2013) 'Mouse Models of Legionnaires' Disease'. In Hilbi, H. (ed.) *Molecular Mechanisms in Legionella Pathogenesis*. Berlin, Heidelberg: Springer Berlin Heidelberg, pp. 271–291

Brown., Yang, C., Fung, K.Y., Bachem, A., Bourges, D., Bedoui, S., Hartland, E.L. and van Driel, I.R. (2016) 'Cooperation between Monocyte-Derived Cells and Lymphoid Cells in the Acute Response to a Bacterial Lung Pathogen'. *PLoS Pathogens*, 12(6), p. e1005691

Brown., Yang, C., Hartland, E.L. and van Driel, I.R. (2017) 'The Regulation of Acute Immune Responses to the Bacterial Lung Pathogen *Legionella Pneumophila*'. *Journal of Leukocyte Biology*, 101(4), pp. 875–886

Buchrieser, C. (2011) 'Legionella: From Protozoa to Humans'. *Front Microbiol,* p. 3

Burstein, D., Amaro, F., Zusman, T., Lifshitz, Z., Cohen, O., Gilbert, J.A., Pupko, T., Shuman, H.A. and Segal, G. (2016) 'Genomic Analysis of 38 Legionella Species Identifies Large and Diverse Effector Repertoires'. *Nature Genetics*, 48(2), pp. 167–175

Button, B., Cai, L.-H., Ehre, C., Kesimer, M., Hill, D.B., Sheehan, J.K., Boucher, R.C. and Rubinstein, M. (2012) 'A Periciliary Brush Promotes the Lung Health by Separating the Mucus Layer from Airway Epithelia'. *Science*, 337(6097), pp. 937–941

Cabello, F.C. and Pruzzo, C. (eds.) (1988) *Bacteria, Complement and the Phagocytic Cell*. Berlin, Heidelberg: Springer Berlin Heidelberg, pp.349-356

Cai, S., Batra, S., Langohr, I., Iwakura, Y. and Jeyaseelan, S. (2016) 'IFN-γ Induction by Neutrophil-Derived IL-17A Homodimer Augments Pulmonary Antibacterial Defense'. *Mucosal Immunology*, 9(3), pp. 718–729

Carroll, R.G. (2007) 'Elsevier's Integrated Physiology'. Philadelphia, PA: Mosby Elsevier, pp. 1-256

Cazalet, C., Gomez-Valero, L., Rusniok, C., Lomma, M., Dervins-Ravault, D., Newton, H.J., Sansom, F.M., Jarraud, S., Zidane, N., Ma, L., Bouchier, C., Etienne, J., Hartland, E.L. and Buchrieser, C. (2010) 'Analysis of the Legionella Longbeachae Genome and Transcriptome Uncovers Unique Strategies to Cause Legionnaires' Disease'. *PLoS Genetics*, 6(2), p. e1000851

Charles A Janeway, J., Travers, P., Walport, M. and Shlomchik, M.J. (2001) 'T Cell-Mediated Cytotoxicity'. *Immunobiology: The Immune System in Health and Disease. 5th Edition*. Available at: https://www.ncbi.nlm.nih.gov/books/NBK27101/ (Accessed: 3 July 2019).

Chen, D.J., Procop, G.W., Vogel, S., Yen-Lieberman, B. and Richter, S.S. (2015) 'Utility of PCR, Culture, and Antigen Detection Methods for Diagnosis of Legionellosis' Onderdonk, A.B. (ed.). *Journal of Clinical Microbiology*, 53(11), pp. 3474–3477

Chen, K. and Kolls, J.K. (2013) 'T Cell–Mediated Host Immune Defenses in the Lung'. *Annual Review of Immunology*, 31(1), pp. 605–633

Cilloniz, C., Ewig, S., Polverino, E., Marcos, M.A., Esquinas, C., Gabarrus, A., Mensa, J. and Torres, A. (2011) 'Microbial Aetiology of Community-Acquired Pneumonia and Its Relation to Severity'. *Thorax*, 66(4), pp. 340–346

Clarke, S.W. and Pavia, D. (1980) 'Lung mucus production and mucociliary clearance: Methods of assessment'. *B JClin Pharmacol,* 9(6), p. 537-546

Copenhaver, A.M., Casson, C.N., Nguyen, H.T., Fung, T.C., Duda, M.M., Roy, C.R. and Shin, S. (2014) 'Alveolar Macrophages and Neutrophils Are the Primary Reservoirs for Legionella Pneumophila and Mediate Cytosolic Surveillance of Type IV Secretion' Flynn, J.L. (ed.). *Infection and Immunity*, 82(10), pp. 4325–4336

Corridoni, D., Arseneau, K.O., Cifone, M.G. and Cominelli, F. (2014) 'The Dual Role of Nod-Like Receptors in Mucosal Innate Immunity and Chronic Intestinal Inflammation'. *Frontiers in Immunology*, 5

Corthay, A. (2006) 'A Three-Cell Model for Activation of Naïve T Helper Cells'. *Scandinavian Journal of Immunology*, 64(2), pp. 93–96

Cunha, B.A., Burillo, A. and Bouza, E. (2016) ‘Legionnaires’ Disease’. *The Lancet*, 387(10016), pp. 376–385

Daley, J.M., Thomay, A.A., Connolly, M.D., Reichner, J.S. and Albina, J.E. (2008) ‘Use of Ly6G-Specific Monoclonal Antibody to Deplete Neutrophils in Mice’. *Journal of Leukocyte Biology*, 83(1), pp. 64–70

Davis, G.S., Winn, W.C., Gump, D.W. and Beaty, H.N. (1983) ‘The Kinetics of Early Inflammatory Events During Experimental Pneumonia Due to Legionella Pneumophila in Guinea Pigs’. *Journal of Infectious Diseases*, 148(5), pp. 823–835

De Filippo, K., Dudeck, A., Hasenberg, M., Nye, E., van Rooijen, N., Hartmann, K., Gunzer, M., Roers, A. and Hogg, N. (2013) ‘Mast Cell and Macrophage Chemokines CXCL1/CXCL2 Control the Early Stage of Neutrophil Recruitment during Tissue Inflammation’. *Blood*, 121(24), pp. 4930–4937

Delves, P.J. and Roitt, I.M. (eds.) (1998) '*Encyclopedia of Immunology*.' 2nd ed. San Diego: Academic Press, pp.3072

Dinarello, C.A. (1999) ‘IL-18: A TH1-Inducing, Proinflammatory Cytokine and New Member of the IL-1 Family’. *The Journal of Allergy and Clinical Immunology*, 103(1 Pt 1), pp. 11–24

Dinarello, C.A. (2018) ‘Overview of the IL-1 Family in Innate Inflammation and Acquired Immunity’. *Immunological Reviews*, 281(1), pp. 8–27

Dinarello., Novick, D., Kim, S. and Kaplanski, G. (2013) ‘Interleukin-18 and IL-18 Binding Protein’. *Frontiers in Immunology*, 4

Doherty, P. ‘MHC Restriction of T Cell Responses’. p. 30.

Dolinsky, S., Haneburger, I., Cichy, A., Hannemann, M., Itzen, A. and Hilbi, H. (2014) ‘The Legionella Longbeachae Icm/Dot Substrate SidC Selectively Binds Phosphatidylinositol 4-Phosphate with Nanomolar Affinity and Promotes Pathogen Vacuole-Endoplasmic Reticulum Interactions’. *Infection and Immunity*, 82(10), pp. 4021–4033

Duncan F Rogers. (2007) ‘Physiology of Airway Mucus Secretion and Pathophysiology of Hypersecretion’. *RESPIRATORY CARE*, 52(9), p. 16.

Eisele, N.A. and Anderson, D.M. (2011) ‘Host Defense and the Airway Epithelium: Frontline Responses That Protect against Bacterial Invasion and Pneumonia’. *Journal of Pathogens*, 2011, pp. 1–16

Ensminger, A.W. and Isberg, R.R. (2009) ‘Legionella Pneumophila Dot/Icm Translocated Substrates: A Sum of Parts’. *Current Opinion in Microbiology*, 12(1), pp. 67–73

Erle, D.J. and Pabst, R. (2000) ‘Intraepithelial Lymphocytes in the Lung: A Neglected Lymphocyte Population’. *American Journal of Respiratory Cell and Molecular Biology*, 22(4), pp. 398–400

Ersching, J., Efeyan, A., Mesin, L., Jacobsen, J.T., Pasqual, G., Grabiner, B.C., Dominguez-Sola, D., Sabatini, D.M. and Victora, G.D. (2017) ‘Germinal Center Selection and Affinity Maturation Require Dynamic Regulation of MTORC1 Kinase’. *Immunity*, 46(6), pp. 1045-1058.e6

Fahy, J.V. and Dickey, B.F. (2010) ‘Airway Mucus Function and Dysfunction’. *New England Journal of Medicine*, 363(23), pp. 2233–2247

Fan, X. and Rudensky, A.Y. (2016) ‘Hallmarks of Tissue-Resident Lymphocytes’. *Cell*, 164(6), pp. 1198–1211

Fitzgeorge, R.B., Baskerville, A., Broster, M., Hambleton, P. and Dennis, P.J. (1983) ‘Aerosol Infection of Animals with Strains of *Legionella Pneumophila* of Different Virulence: Comparison with Intraperitoneal and Intranasal Routes of Infection’. *Journal of Hygiene*, 90(1), pp. 81–89

Forman, H.J. and Torres, M. (2002) ‘Reactive Oxygen Species and Cell Signaling’. *American Journal of Respiratory and Critical Care Medicine*, 166(supplement_1), pp. S4–S8

Fraser, D.W., Tsai, T.R., Orenstein, W., Parkin, W.E., Beecham, H.J., Sharrar, R.G., Harris, J., Mallison, G.F., Martin, S.M., McDade, J.E., Shepard, C.C., Brachman, P.S. and the Field Investigation Team* (1977) ‘Legionnaires’ Disease: Description of an Epidemic of Pneumonia’. *New England Journal of Medicine*, 297(22), pp. 1189–1197

French, C.A. (2009) ‘Respiratory Tract’. In *Cytology*. Elsevier, pp. 65–103

Garbi, N. and Lambrecht, B.N. (2017) ‘Location, Function, and Ontogeny of Pulmonary Macrophages during the Steady State’. *Pflügers Archiv - European Journal of Physiology*, 469(3–4), pp. 561–572

Garc, J.E.L., Mart, M.R., Losada, J.P. and Arellano, J.L.P. (1999) ‘Evaluation of Inflammatory Cytokine Secretion by Human Alveolar Macrophages’. p. 9

Gereige, R.S. and Laufer, P.M. (2013) ‘Pneumonia’. *Pediatrics in Review*, 34(10), p. 438

Gewirtz, A.T., Navas, T.A., Lyons, S., Godowski, P.J. and Madara, J.L. (2001) ‘Cutting Edge: Bacterial Flagellin Activates Basolaterally Expressed TLR5 to Induce Epithelial Proinflammatory Gene Expression’. *The Journal of Immunology*, 167(4), pp. 1882–1885

Ginhoux, F. and Jung, S. (2014) ‘Monocytes and Macrophages: Developmental Pathways and Tissue Homeostasis’. *Nature Reviews Immunology*, 14(6), pp. 392–404

Gobin, I., Susa, M., Begic, G., Hartland, E.L. and Doric, M. (2009) ‘Experimental Legionella Longbeachae Infection in Intratracheally Inoculated Mice’. *Journal of Medical Microbiology*, 58(Pt 6), pp. 723–730

Goral, S. (2011) ‘The Three-Signal Hypothesis of Lymphocyte Activation/Targets for Immunosuppression’. *Dialysis & Transplantation*, 40(1), pp. 14–16

Grabiec, A.M. and Hussell, T. (2016) ‘The Role of Airway Macrophages in Apoptotic Cell Clearance Following Acute and Chronic Lung Inflammation’. *Seminars in Immunopathology*, 38(4), pp. 409–423

Grewal, I.S. and Flavell, R.A. (1996) ‘The Role of CD40 Ligand in Costimulation and T-Cell Activation’. *Immunological Reviews*, 153, pp. 85–106

Greyer, M., Whitney, P.G., Stock, A.T., Davey, G.M., Tebartz, C., Bachem, A., Mintern, J.D., Strugnell, R.A., Turner, S.J., Gebhardt, T., O’Keeffe, M., Heath, W.R. and Bedoui, S. (2016) ‘T Cell Help Amplifies Innate Signals in CD8 + DCs for Optimal CD8 + T Cell Priming’. *Cell Reports*, 14(3), pp. 586–597

Guermonprez, P., Valladeau, J., Zitvogel, L., Théry, C. and Amigorena, S. (2002) ‘A NTIGEN P RESENTATION AND T C ELL S TIMULATION BY D ENDRITIC C ELLS’. *Annual Review of Immunology*, 20(1), pp. 621–667

Halle, S. (2017) ‘Mechanisms and Dynamics of T Cell-Mediated Cytotoxicity In Vivo’. *Trends in Immunology*, 38(6), pp. 432–443

Hallstrand, T.S., Hackett, T.L., Altemeier, W.A., Matute-Bello, G., Hansbro, P.M. and Knight, D.A. (2014) ‘Airway Epithelial Regulation of Pulmonary Immune Homeostasis and Inflammation’. *Clinical Immunology*, 151(1), pp. 1–15

Harty, J.T., Tvinnereim, A.R. and White, D.W. (2000) ‘CD8+ T Cell Effector Mechanisms in Resistance to Infection’. *Annual Review of Immunology*, 18(1), pp. 275–308

Hawn, T.R., Smith, K.D., Aderem, A. and Skerrett, S.J. (2006) ‘Myeloid Differentiation Primary Response Gene (88)– and Toll-Like Receptor 2–Deficient Mice Are Susceptible to Infection with Aerosolized *Legionella Pneumophila*’. *The Journal of Infectious Diseases*, 193(12), pp. 1693–1702

Hayashida, S., Harrod, K.S. and Whitsett, J.A. (2000) ‘Regulation and Function of CCSP during Pulmonary *Pseudomonas Aeruginosa* Infection in Vivo’. *American Journal of Physiology-Lung Cellular and Molecular Physiology*, 279(3), pp. L452–L459

He, W., Wan, H., Hu, L., Chen, P., Wang, X., Huang, Z., Yang, Z.-H., Zhong, C.-Q. and Han, J. (2015) 'Gasdermin D Is an Executor of Pyroptosis and Required for Interleukin-1β Secretion'. *Cell Research*, 25(12), pp. 1285–1298

Hernández-Santos, N., Wiesner, D.L., Fites, J.S., McDermott, A.J., Warner, T., Wüthrich, M. and Klein, B.S. (2018) 'Lung Epithelial Cells Coordinate Innate Lymphocytes and Immunity against Pulmonary Fungal Infection'. *Cell Host & Microbe*, 23(4), pp. 511-522.e5

Herold, S., Mayer, K. and Lohmeyer, J. (2011) 'Acute Lung Injury: How Macrophages Orchestrate Resolution of Inflammation and Tissue Repair'. *Frontiers in Immunology*, 2

Heuner, K. and Steinert, M. (2003) 'The Flagellum of Legionella Pneumophila and Its Link to the Expression of the Virulent Phenotype'. *International Journal of Medical Microbiology*, 293(2–3), pp. 133–143

Hochweller, K., Miloud, T., Striegler, J., Naik, S., Hämmerling, G.J. and Garbi, N. (2009) 'Homeostasis of Dendritic Cells in Lymphoid Organs Is Controlled by Regulation of Their Precursors via a Feedback Loop'. *Blood*, 114(20), pp. 4411–4421

Holland, T., Wohlleber, D., Marx, S., Kreutzberg, T., Vento-Asturias, S., Schmitt-Mbamunyo, C., Welz, M., Janas, M., Komander, K., Eickhoff, S., Brewitz, A., Hasenberg, M., Männ, L., Gunzer, M., Wilhelm, C., Kastenmüller, W., Knolle, P., Abdullah, Z., Kurts, C. and Garbi, N. (2018) 'Rescue of T-Cell Function during Persistent Pulmonary Adenoviral Infection by Toll-like Receptor 9 Activation'. *Journal of Allergy and Clinical Immunology*, 141(1), pp. 416-419.e10

Hoshino, K., Tsutsui, H., Kawai, T., Takeda, K., Nakanishi, K., Takeda, Y. and Akira, S. (1999) 'Cutting Edge: Generation of IL-18 Receptor-Deficient Mice: Evidence for IL-1 Receptor-Related Protein as an Essential IL-18 Binding Receptor'. *The Journal of Immunology*, 162(9), pp. 5041–5044

Howrylak, J.A. and Nakahira, K. (2017a) 'Inflammasomes: Key Mediators of Lung Immunity'. *Annual Review of Physiology*, 79(1), pp. 471–494

Howrylak, J.A. and Nakahira, K. (2017b) 'Inflammasomes: Key Mediators of Lung Immunity'. *Annual Review of Physiology*, 79(1), pp. 471–494

Hubber, A. and Roy, C.R. (2010) 'Modulation of Host Cell Function by *Legionella Pneumophila* Type IV Effectors'. *Annual Review of Cell and Developmental Biology*, 26(1), pp. 261–283

Ishikawa, Y., Yoshimoto, T. and Nakanishi, K. (2006) 'Contribution of IL-18-Induced Innate T Cell Activation to Airway Inflammation with Mucus Hypersecretion and Airway Hyperresponsiveness'. *International Immunology*, 18(6), pp. 847–855

Islam, M.A., Pröll, M., Hölker, M., Tholen, E., Tesfaye, D., Looft, C., Schellander, K. and Cinar, M.U. (2013) 'Alveolar Macrophage Phagocytic Activity Is Enhanced with LPS Priming, and Combined Stimulation of LPS and Lipoteichoic Acid Synergistically Induce pro-Inflammatory Cytokines in Pigs'. *Innate Immunity*, 19(6), pp. 631–643

Joannides, M. (1931) 'THE MECHANISM OF PNEUMONIA'. *Archives of Internal Medicine*, 47(1), p. 24

Jones, D. and Padilla-Parra, S. (2016) 'The β-Lactamase Assay: Harnessing a FRET Biosensor to Analyse Viral Fusion Mechanisms'. *Sensors*, 16(7), p. 950.

Juncadella, I.J., Kadl, A., Sharma, A.K., Shim, Y.M., Hochreiter-Hufford, A., Borish, L. and Ravichandran, K.S. (2013) 'Apoptotic Cell Clearance by Bronchial Epithelial Cells Critically Influences Airway Inflammation'. *Nature*, 493(7433), pp. 547–551

Kaplanski, G. (2018) 'Interleukin-18: Biological Properties and Role in Disease Pathogenesis'. *Immunological Reviews*, 281(1), pp. 138–153

Kato, A., Hulse, K.E., Tan, B.K. and Schleimer, R.P. (2013) 'B-Lymphocyte Lineage Cells and the Respiratory System'. *Journal of Allergy and Clinical Immunology*, 131(4), pp. 933–957

Kato, T. and Kitagawa, S. (2006) 'Regulation of Neutrophil Functions by Proinflammatory Cytokines'. *International Journal of Hematology*, 84(3), pp. 205–209

Kepler, T.B. and Perelson, A.S. (1993) 'Cyclic Re-Entry of Germinal Center B Cells and the Efficiency of Affinity Maturation'. *Immunology Today*, 14(8), pp. 412–415

van Kessel, K.P.M., Bestebroer, J. and van Strijp, J.A.G. (2014) 'Neutrophil-Mediated Phagocytosis of Staphylococcus Aureus'. *Frontiers in Immunology*, 5

Kolinska, J., Lisa, V., Clark, J.A., Kozakova, H., Zakostelecka, M., Khailova, L., Sinkora, M., Kitanovicova, A. and Dvorak, B. (2008) 'Constitutive Expression of IL-18 and IL-18R in Differentiated IEC-6 Cells: Effect of TNF- *α* and IFN- *γ* Treatment'. *Journal of Interferon & Cytokine Research*, 28(5), pp. 287–296

Kopf, M., Schneider, C. and Nobs, S.P. (2015) 'The Development and Function of Lung-Resident Macrophages and Dendritic Cells'. *Nature Immunology*, 16(1), pp. 36–44

Krásná, E., Kolesár, L., Slavcev, A., Valhová, S., Kronosová, B., Jaresová, M. and Stríz, I. (2005) 'IL-18 Receptor Expression on Epithelial Cells Is Upregulated by TNF Alpha'. *Inflammation*, 29(1), pp. 33–37

Lambert, L. and Culley, F.J. (2017) ‘Innate Immunity to Respiratory Infection in Early Life’. *Frontiers in Immunology*, 8

Lambrecht, B.N. (2006) ‘Alveolar Macrophage in the Driver’s Seat’. *Immunity*, 24(4), pp. 366–368

Le Bourhis, L., Guerri, L., Dusseaux, M., Martin, E., Soudais, C. and Lantz, O. (2011) ‘Mucosal-Associated Invariant T Cells: Unconventional Development and Function’. *Trends in Immunology*, 32(5), pp. 212–218

Lee, J.-K., Kim, S.-H., Lewis, E.C., Azam, T., Reznikov, L.L. and Dinarello, C.A. (2004) ‘Differences in Signaling Pathways by IL-1β and IL-18’. *Proceedings of the National Academy of Sciences of the United States of America*, 101(23), pp. 8815–8820

LeibundGut-Landmann, S., Weidner, K., Hilbi, H. and Oxenius, A. (2011) ‘Nonhematopoietic Cells Are Key Players in Innate Control of Bacterial Airway Infection’. *The Journal of Immunology*, 186(5), pp. 3130–3137

Leiva-Juárez, M.M., Kolls, J.K. and Evans, S.E. (2018) ‘Lung Epithelial Cells: Therapeutically Inducible Effectors of Antimicrobial Defense’. *Mucosal Immunology*, 11(1), pp. 21–34

Leung, B.P., Culshaw, S., Gracie, J.A., Hunter, D., Canetti, C.A., Campbell, C., Cunha, F., Liew, F.Y. and McInnes, I.B. (2001) ‘A Role for IL-18 in Neutrophil Activation’. *The Journal of Immunology*, 167(5), pp. 2879–2886

Levinson, W. (2016) ‘Humoral Immunity’. In *Review of Medical Microbiology and Immunology*. New York, NY: McGraw-Hill Education. Available at: accessmedicine.mhmedical.com/content.aspx?aid=1132263498 (Accessed: 20 August 2019).

Linsley, P.S., Clark, E.A. and Ledbetter, J.A. (1990) ‘T-Cell Antigen CD28 Mediates Adhesion with B Cells by Interacting with Activation Antigen B7/BB-1.’ *Proceedings of the National Academy of Sciences*, 87(13), pp. 5031–5035

Liu, X., Zhang, Z., Ruan, J., Pan, Y., Magupalli, V.G., Wu, H. and Lieberman, J. (2016) ‘Inflammasome-Activated Gasdermin D Causes Pyroptosis by Forming Membrane Pores’. *Nature*, 535(7610), pp. 153–158

Lively, M.W. (2012) ‘Early Onset Pneumonia Following Pulmonary Contusion: The Case of Stonewall Jackson’. *Military Medicine*, 177(3), pp. 315–317

Lloyd, C.M. and Marsland, B.J. (2017) ‘Lung Homeostasis: Influence of Age, Microbes, and the Immune System’. *Immunity*, 46(4), pp. 549–561

Loo, Y.-M. and Gale, M. (2011) ‘Immune Signaling by RIG-I-like Receptors’. *Immunity*, 34(5), pp. 680–692

Lorey, S.L., Huang, Y.C. and Sharma, V. (2004) 'Constitutive Expression of Interleukin-18 and Interleukin-18 Receptor MRNA in Tumour Derived Human B-Cell Lines'. *Clinical and Experimental Immunology*, 136(3), pp. 456–462

Lynch, J.P. and Zhanel, G.G. (2010) 'Streptococcus Pneumoniae: Epidemiology and Risk Factors, Evolution of Antimicrobial Resistance, and Impact of Vaccines': *Current Opinion in Pulmonary Medicine*, p. 1

Ma, J., Rubin, B.K. and Voynow, J.A. (2018) 'Mucins, Mucus, and Goblet Cells'. *Chest*, 154(1), pp. 169–176

Maddaly, R., Pai, G., Balaji, S., Sivaramakrishnan, P., Srinivasan, L., Sunder, S.S. and Paul, S.F.D. (2010) 'Receptors and Signaling Mechanisms for B-Lymphocyte Activation, Proliferation and Differentiation – Insights from Both in Vivo and in Vitro Approaches'. *FEBS Letters*, 584(24), pp. 4883–4894

Madhi, S. (2008) 'Vaccines to Prevent Pneumonia and Improve Child Survival'. *Bulletin of the World Health Organization*, 86(5), pp. 365–372

Maelfait, J., Roose, K., Vereecke, L., Mc Guire, C., Sze, M., Schuijs, M.J., Willart, M., Itati Ibañez, L., Hammad, H., Lambrecht, B.N., Beyaert, R., Saelens, X. and van Loo, G. (2016) 'A20 Deficiency in Lung Epithelial Cells Protects against Influenza A Virus Infection' tenOever, B.R. (ed.). *PLOS Pathogens*, 12(1), p. e1005410

Mah, A.Y. and Cooper, M.A. (2016) 'Metabolic Regulation of Natural Killer Cell IFN-γ Production'. *Critical Reviews in Immunology*, 36(2), pp. 131–147

Man, S.M., Karki, R. and Kanneganti, T.-D. (2017) 'Molecular Mechanisms and Functions of Pyroptosis, Inflammatory Caspases and Inflammasomes in Infectious Diseases'. *Immunological Reviews*, 277(1), pp. 61–75

Mandell, L.A. (2015) 'Community-Acquired Pneumonia: An Overview'. *Postgraduate Medicine*, 127(6), pp. 607–615.

Mardiney, M. and Malech, H.L. (1996) 'Enhanced Engraftment of Hematopoietic Progenitor Cells in Mice Treated With Granulocyte Colony-Stimulating Factor Before Low-Dose Irradiation: Implications for Gene Therapy'. p. 9

Mascarenhas, D.P.A. and Zamboni, D.S. (2017a) 'Inflammasome Biology Taught by *Legionella Pneumophila*'. *Journal of Leukocyte Biology*, 101(4), pp. 841–849

Mascarenhas, D.P.A. and Zamboni, D.S. (2017b) 'Inflammasome Biology Taught by *Legionella Pneumophila*'. *Journal of Leukocyte Biology*, 101(4), pp. 841–849

Massis, L.M., Assis-Marques, M.A., Castanheira, F.V.S., Capobianco, Y.J., Balestra, A.C., Escoll, P., Wood, R.E., Manin, G.Z., Correa, V.M.A., Alves-Filho, J.C., Cunha, F.Q., Buchrieser, C., Borges, M.C., Newton, H.J. and Zamboni, D.S.

(2017) ‘Legionella Longbeachae Is Immunologically Silent and Highly Virulent In Vivo’. *The Journal of Infectious Diseases*, 215(3), pp. 440–451

Medzhitov, R. (2017) ‘Ruslan Medzhitov’. *Current Biology*, 27(12), pp. R577–R578

Melchers, F. and Andersson, J. (1984) ‘B Cell Activation: Three Steps and Their Variations’. *Cell*, 37(3), pp. 715–720

Mody, C.H., Paine, R., Shahrabadi, M.S., Simon, R.H., Pearlman, E., Eisenstein, B.I. and Toews, G.B. (1993) ‘Legionella Pneumophila Replicates within Rat Alveolar Epithelial Cells’. *Journal of Infectious Diseases*, 167(5), pp. 1138–1145

Molmeret, M. and Abu Kwaik, Y. (2002) ‘How Does Legionella Pneumophila Exit the Host Cell?’ *Trends in Microbiology*, 10(6), pp. 258–260

Molmeret, M., Bitar, D.M., Han, L. and Kwaik, Y.A. (2004) ‘Disruption of the Phagosomal Membrane and Egress of Legionella Pneumophila into the Cytoplasm during the Last Stages of Intracellular Infection of Macrophages and Acanthamoeba Polyphaga’. *Infection and Immunity*, 72(7), pp. 4040–4051

Montanaro-Punzengruber, J.C., Hicks, L., Meyer, W. and Gilbert, G.L. (1999) ‘Australian Isolates of Legionella Longbeachae Are Not a Clonal Population’. *J. CLIN. MICROBIOL.*, 37, p. 6.

Morinaga, Y., Yanagihara, K., Araki, N., Migiyama, Y., Nagaoka, K., Harada, Y., Yamada, K., Hasegawa, H., Nishino, T., Izumikawa, K., Kakeya, H., Yamamoto, Y., Kohno, S. and Kamihira, S. (2012) ‘Live *Legionella Pneumophila* Induces MUC5AC Production by Airway Epithelial Cells Independently of Intracellular Invasion’. *Canadian Journal of Microbiology*, 58(2), pp. 151–157

Mukhopadhyay, S., Hoidal, J.R. and Mukherjee, T.K. (2006) ‘Role of TNFα in Pulmonary Pathophysiology’. *Respiratory Research*, 7(1), p. 125

Murray, J.F. (2010) ‘The Structure and Function of the Lung’. *Int J Tuberc Lung Dis*, 14(4), pp. 391-396

Naeem, A., Rai, S.N. and Pierre, L. (2019) ‘Histology, Alveolar Macrophages’. In *StatPearls*. Treasure Island (FL): StatPearls Publishing. Available at: http://www.ncbi.nlm.nih.gov/books/NBK513313/ (Accessed: 20 August 2019)

Nagai, H. (2002) ‘A Bacterial Guanine Nucleotide Exchange Factor Activates ARF on Legionella Phagosomes’. *Science*, 295(5555), pp. 679–682

Nakahira, M., Ahn, H.-J., Park, W.-R., Gao, P., Tomura, M., Park, C.-S., Hamaoka, T., Ohta, T., Kurimoto, M. and Fujiwara, H. (2002) ‘Synergy of IL-12 and IL-18 for IFN-γ Gene Expression: IL-12-Induced STAT4 Contributes to IFN-γ Promoter Activation by Up-Regulating the Binding Activity of IL-18-Induced Activator Protein 1’. *The Journal of Immunology*, 168(3), pp. 1146–1153

Nakamura, K., Okamura, H., Wada, M., Nagata, K. and Tamura, T. (1989) 'Endotoxin-Induced Serum Factor That Stimulates Gamma Interferon Production'. *Infection and Immunity*, 57(2), pp. 590–595

Nakanishi, K., Yoshimoto, T., Tsutsui, H. and Okamura, H. (2001) 'Interleukin-18 regulates both Th1 and Th2 responses'. *Annual Review of Immunology*, 19(1), pp. 423–474

Netea, M.G., Kullberg, B.J., Verschueren, I. and Van Der Meer, J.W. (2000) 'Interleukin-18 Induces Production of Proinflammatory Cytokines in Mice: No Intermediate Role for the Cytokines of the Tumor Necrosis Factor Family and Interleukin-1beta'. *European Journal of Immunology*, 30(10), pp. 3057–3060

Newton, H.J., Ang, D.K.Y., van Driel, I.R. and Hartland, E.L. (2010a) 'Molecular Pathogenesis of Infections Caused by Legionella Pneumophila'. *Clinical Microbiology Reviews*, 23(2), pp. 274–298

Newton, H.J., Ang, D.K.Y., van Driel, I.R. and Hartland, E.L. (2010b) 'Molecular Pathogenesis of Infections Caused by Legionella Pneumophila'. *Clinical Microbiology Reviews*, 23(2), pp. 274–298

Nicod, L.P. (2005) 'Lung Defences: An Overview'. *European Respiratory Review*, 14(95), pp. 45–50

Novick, D., Kim, S., Kaplanski, G. and Dinarello, C.A. (2013) 'Interleukin-18, More than a Th1 Cytokine'. *Seminars in Immunology*, 25(6), pp. 439–448

Nowarski, R., Jackson, R., Gagliani, N., de Zoete, M.R., Palm, N.W., Bailis, W., Low, J.S., Harman, C.C.D., Graham, M., Elinav, E. and Flavell, R.A. (2015) 'Epithelial IL-18 Equilibrium Controls Barrier Function in Colitis'. *Cell*, 163(6), pp. 1444–1456

Ogura, T., Ueda, H., Hosohara, K., Tsuji, R., Nagata, Y., Kashiwamura, S. and Okamura, H. (2001) 'Interleukin-18 Stimulates Hematopoietic Cytokine and Growth Factor Formation and Augments Circulating Granulocytes in Mice'. *Blood*, 98(7), pp. 2101–2107

Oliva, G., Sahr, T. and Buchrieser, C. (2018) 'The Life Cycle of L. Pneumophila: Cellular Differentiation Is Linked to Virulence and Metabolism'. *Frontiers in Cellular and Infection Microbiology*, 8, p. 3

O'Neill, L.A.J., Golenbock, D. and Bowie, A.G. (2013) 'The History of Toll-like Receptors — Redefining Innate Immunity'. *Nature Reviews Immunology*, 13(6), pp. 453–460

Opitz, B., van Laak, V., Eitel, J. and Suttorp, N. (2010) 'Innate Immune Recognition in Infectious and Noninfectious Diseases of the Lung'. *American Journal of Respiratory and Critical Care Medicine*, 181(12), pp. 1294–1309

Ott, C. and Lippincott-Schwartz, J. (2012) ‘Visualization of Live Primary Cilia Dynamics Using Fluorescence Microscopy’. *Current Protocols in Cell Biology*, 04, p. 1-24

Øvrevik, J., Låg, M., Holme, J.A., Schwarze, P.E. and Refsnes, M. (2009) ‘Cytokine and Chemokine Expression Patterns in Lung Epithelial Cells Exposed to Components Characteristic of Particulate Air Pollution’. *Toxicology*, 259(1–2), pp. 46–53

Paardekooper, L.M., Dingjan, I., Linders, P.T.A., Staal, A.H.J., Cristescu, S.M., Verberk, W.C.E.P. and van den Bogaart, G. (2019) ‘Human Monocyte-Derived Dendritic Cells Produce Millimolar Concentrations of ROS in Phagosomes Per Second’. *Frontiers in Immunology*, 10, p. 1216

Pabst, R. and Tschernig, T. (1995) ‘Lymphocytes in the Lung: An Often Neglected Cell: Numbers, Characterization and Compartmentalization’. *Anatomy and Embryology*, 192(4), pp. 293–299

Payne. (1987) ‘Phagocytosis of Legionella Pneumophila Is Mediated by Human Monocyte Complement Receptors’. *The Journal of Experimental Medicine*, 166(5), pp. 1377–1389.

Peake, H.L., Currie, A.J., Stewart, G.A. and McWilliam, A.S. (2003) ‘Nitric Oxide Production by Alveolar Macrophages in Response to House Dust Mite Fecal Pellets and the Mite Allergens, Der p 1 and Der p 2’. *The Journal of Allergy and Clinical Immunology*, 112(3), pp. 531–537

Percival, S.L. and Williams, D.W. (2014) ‘Legionella’. In *Microbiology of Waterborne Diseases*. Elsevier, pp. 155–175

Pereira, M.S.F., Marques, G.G., DelLama, J.E. and Zamboni, D.S. (2011) ‘The Nlrc4 Inflammasome Contributes to Restriction of Pulmonary Infection by Flagellated Legionella Spp. That Trigger Pyroptosis’. *Frontiers in Microbiology*, 2

Peteranderl, C., Sznajder, J.I., Herold, S. and Lecuona, E. (2017) ‘Inflammatory Responses Regulating Alveolar Ion Transport during Pulmonary Infections’. *Frontiers in Immunology*, 18(8), p. 446

Pinheiro, M.B., Antonelli, L.R., Sathler-Avelar, R., Vitelli-Avelar, D.M., Spindola-de-Miranda, S., Guimarães, T.M.P.D., Teixeira-Carvalho, A., Martins-Filho, O.A. and Toledo, V.P.C.P. (2012) ‘CD4-CD8-Aβ and Γδ T Cells Display Inflammatory and Regulatory Potentials during Human Tuberculosis’. *PLOS ONE*, 7(12), p. e50923

Pinkerton, J.W., Kim, R.Y., Robertson, A.A.B., Hirota, J.A., Wood, L.G., Knight, D.A., Cooper, M.A., O’Neill, L.A.J., Horvat, J.C. and Hansbro, P.M. (2017) ‘Inflammasomes in the Lung’. *Molecular Immunology*, 86, pp. 44–55

Porra, L. (2006) ‘Lung Structure and Function Studied by Synchrotron Radiation’. *Helsinki University Central Hospital*, p. 1-81

Provine, N.M., Binder, B., FitzPatrick, M.E.B., Schuch, A., Garner, L.C., Williamson, K.D., van Wilgenburg, B., Thimme, R., Klenerman, P. and Hofmann, M. (2018) ‘Unique and Common Features of Innate-Like Human Vδ2+ γδT Cells and Mucosal-Associated Invariant T Cells’. *Frontiers in Immunology*, 9, p. 756

Puligandla, P.S. and Laberge, J.-M. (2008) ‘Respiratory Infections: Pneumonia, Lung Abscess, and Empyema’. *Seminars in Pediatric Surgery*, 17(1), pp. 42–52

Punt, J. (2013) ‘Adaptive Immunity’. In *Cancer Immunotherapy*. Elsevier, pp. 41–53

Rackley, C.R. and Stripp, B.R. (2012) ‘Building and Maintaining the Epithelium of the Lung’. *The Journal of Clinical Investigation*, 122(8), pp. 2724–2730

Rhoades, R. and Bell, D.R. (2009) 'Medical Physiology: Principles for Clinical Medicine'. Lippincott Williams & Wilkins, p. 1-727

Robinson, C.G. and Roy, C.R. (2006) ‘Attachment and Fusion of Endoplasmic Reticulum with Vacuoles Containing Legionella Pneumophila’. *Cellular Microbiology*, 8(5), pp. 793–805

de la Roche, M., Asano, Y. and Griffiths, G.M. (2016) ‘Origins of the Cytolytic Synapse’. *Nature Reviews Immunology*, 16(7), pp. 421–432

Rohmann, K., Tschernig, T., Pabst, R., Goldmann, T. and Drömann, D. (2011) ‘Innate Immunity in the Human Lung: Pathogen Recognition and Lung Disease’. *Cell and Tissue Research*, 343(1), pp. 167–174

Rokicki, W., Rokicki, M., Wojtacha, J. and Dżeljijli, A. (2016a) ‘The Role and Importance of Club Cells (Clara Cells) in the Pathogenesis of Some Respiratory Diseases’. *Kardiochirurgia i Torakochirurgia Polska = Polish Journal of Cardio-Thoracic Surgery*, 13(1), pp. 26–30

Rokicki, W., Rokicki, M., Wojtacha, J. and Dżeljijli, A. (2016b) ‘The Role and Importance of Club Cells (Clara Cells) in the Pathogenesis of Some Respiratory Diseases’. *Polish Journal of Cardio-Thoracic Surgery*, 13(1), pp. 26–30

Roy, C.R. (2002) ‘Exploitation of the Endoplasmic Reticulum by Bacterial Pathogens’. *Trends in Microbiology*, 10(9), pp. 418–424

Roy, M.G., Livraghi-Butrico, A., Fletcher, A.A., McElwee, M.M., Evans, S.E., Boerner, R.M., Alexander, S.N., Bellinghausen, L.K., Song, A.S., Petrova, Y.M., Tuvim, M.J., Adachi, R., Romo, I., Bordt, A.S., Bowden, M.G., Sisson, J.H., Woodruff, P.G., Thornton, D.J., Rousseau, K., De la Garza, M.M., Moghaddam, S.J., Karmouty-Quintana, H., Blackburn, M.R., Drouin, S.M., Davis, C.W., Terrell,

K.A., Grubb, B.R., O'Neal, W.K., Flores, S.C., Cota-Gomez, A., Lozupone, C.A., Donnelly, J.M., Watson, A.M., Hennessy, C.E., Keith, R.C., Yang, I.V., Barthel, L., Henson, P.M., Janssen, W.J., Schwartz, D.A., Boucher, R.C., Dickey, B.F. and Evans, C.M. (2014) 'Muc5b Is Required for Airway Defence'. *Nature*, 505(7483), pp. 412–416

Rubins, J.B. (2003) 'Alveolar Macrophages'. *American Journal of Respiratory and Critical Care Medicine*, 167(2), pp. 103–104

Sattar, S.B.A. and Sharma, S. (2019) *Bacterial Pneumonia*. StatPearls Publishing Available at: https://www.ncbi.nlm.nih.gov/books/NBK513321/ (Accessed: 10 April 2019).

Sawada, S., Scarborough, J.D., Killeen, N. and Littman, D.R. (1994) 'A Lineage-Specific Transcriptional Silencer Regulates CD4 Gene Expression during T Lymphocyte Development'. *Cell*, 77(6), pp. 917–929

Schenck, L.P., Surette, M.G. and Bowdish, D.M.E. (2016) 'Composition and Immunological Significance of the Upper Respiratory Tract Microbiota'. *FEBS Letters*, 590(21), pp. 3705–3720

Schmeck, B., N'Guessan, P.D., Ollomang, M., Lorenz, J., Zahlten, J., Opitz, B., Flieger, A., Suttorp, N. and Hippenstiel, S. (2006) 'Legionella Pneumophila-Induced NF- B- and MAPK-Dependent Cytokine Release by Lung Epithelial Cells'. *European Respiratory Journal*, 29(1), pp. 25–33

Schmidt-Ioanas, M. and Lode, H. (2006) 'Treatment of Pneumonia in Elderly Patients'. *Expert Opinion on Pharmacotherapy*, 7(5), pp. 499–507

Schnoor, M. (2015) 'Endothelial Actin-Binding Proteins and Actin Dynamics in Leukocyte Transendothelial Migration'. *The Journal of Immunology*, 194(8), pp. 3535–3541

Schroder, K., Hertzog, P.J., Ravasi, T. and Hume, D.A. (2004) 'Interferon-γ: An Overview of Signals, Mechanisms and Functions'. *Journal of Leukocyte Biology*, 75(2), pp. 163–189

Schroder, K. and Tschopp, J. (2010) 'The Inflammasomes'. *Cell*, 140(6), pp. 821–832

Schuelein, R., Ang, D.K.Y., van Driel, I.R. and Hartland, E.L. (2011) 'Immune Control of Legionella Infection: An in Vivo Perspective'. *Frontiers in Microbiology*, 2, p. 126

Segal. A.W. (2005) 'How neutrophils kill microbes'. *Annual Review of Immunology*, 23(1), pp. 197–223

Segal, G., Feldman, M. and Zusman, T. (2005) 'The Icm/Dot Type-IV Secretion Systems of *Legionella Pneumophila* and *Coxiella Burnetii*'. *FEMS Microbiology Reviews*, 29(1), pp. 65–81

Sellge, G. and Kufer, T.A. (2015) 'PRR-Signaling Pathways: Learning from Microbial Tactics'. *Seminars in Immunology*, 27(2), pp. 75–84

Shi, J., Zhao, Y., Wang, K., Shi, X., Wang, Y., Huang, H., Zhuang, Y., Cai, T., Wang, F. and Shao, F. (2015) 'Cleavage of GSDMD by Inflammatory Caspases Determines Pyroptotic Cell Death'. *Nature*, 526(7575), pp. 660–665

Singh, Y.D. (2012) 'Pathophysiology of Community Acquired Pneumonia'. *J Assoc Physicians India*, 60, p. 3.

Smeltz, R.B., Chen, J., Hu-Li, J. and Shevach, E.M. (2001) 'Regulation of Interleukin (Il)-18 Receptor α Chain Expression on $Cd4^+$ T Cells during T Helper (Th)1/Th2 Differentiation'. *The Journal of Experimental Medicine*, 194(2), pp. 143–154

Smith-Garvin, J.E., Koretzky, G.A. and Jordan, M.S. (2009) 'T Cell Activation'. *Annual Review of Immunology*, 27(1), pp. 591–619

Soda, E.A., Barskey, A.E., Shah, P.P., Schrag, S., Whitney, C.G., Arduino, M.J., Reddy, S.C., Kunz, J.M., Hunter, C.M., Raphael, B.H. and Cooley, L.A. (2017) 'Vital Signs: Health Care–Associated Legionnaires' Disease Surveillance Data from 20 States and a Large Metropolitan Area — United States, 2015'. *MWR Morb Mortal Weekly Rep.*, 66(22), p. 6

Soini, Y. (2011) 'Claudins in Lung Diseases'. *Respiratory Research*, 12(1), p. 70

Sokol, C.L. and Luster, A.D. (2015) 'The Chemokine System in Innate Immunity'. *Cold Spring Harbor Perspectives in Biology*, 7(5), p. a016303

Steinman, R.M. and Hemmi, H. (2006) 'Dendritic Cells: Translating Innate to Adaptive Immunity'. In Pulendran, B. and Ahmed, R. 'From Innate Immunity to Immunological Memory'. *Springer Berlin Heidelberg*, pp. 17–58

Stone, B.J. and Kwaik, Y.A. (1998) 'Expression of Multiple Pili by Legionella Pneumophila: Identification and Characterization of a Type IV Pilin Gene and Its Role in Adherence to Mammalian and Protozoan Cells'. *INFECT. IMMUN.*, 66, pp. 1768-1775

Stumbles, P.A., Upham, J.W. and Holt, P.G. (2003) 'Airway Dendritic Cells: Co-Ordinators of Immunological Homeostasis and Immunity in the Respiratory Tract'. *APMIS*, 111(7–8), pp. 741–755

Sugawara, S., Uehara, A., Nochi, T., Yamaguchi, T., Ueda, H., Sugiyama, A., Hanzawa, K., Kumagai, K., Okamura, H. and Takada, H. (2001) 'Neutrophil

Proteinase 3-Mediated Induction of Bioactive IL-18 Secretion by Human Oral Epithelial Cells'. *The Journal of Immunology*, 167(11), pp. 6568–6575

Sun, H., Sun, C., Xiao, W. and Sun, R. (2019) 'Tissue-Resident Lymphocytes: From Adaptive to Innate Immunity'. *Cellular & Molecular Immunology*, 16(3), pp. 205–215

Susa, M., Ticac, B., Rukavina, T., Doric, M. and Marre, R. (1998) 'Legionella Pneumophila Infection in Intratracheally Inoculated T Cell-Depleted or -Nondepleted A/J Mice'. *The Journal of Immunology*, p. 7

Symmes, B.A., Stefanski, A.L., Magin, C.M. and Evans, C.M. (2018) 'Role of Mucins in Lung Homeostasis: Regulated Expression and Biosynthesis in Health and Disease'. *Biochemical Society Transactions*, 46(3), pp. 707–719

Takeda, K., Tsutsui, H., Yoshimoto, T., Adachi, O., Yoshida, N., Kishimoto, T., Okamura, H., Nakanishi, K. and Akira, S. (1998) 'Defective NK Cell Activity and Th1 Response in IL-18–Deficient Mice'. *Immunity*, 8(3), pp. 383–390

Takeuchi, O. and Akira, S. (2010) 'Pattern Recognition Receptors and Inflammation'. *Cell*, 140(6), pp. 805–820

Tan, H.-L. and Rosenthal, M. (2013) 'IL-17 in Lung Disease: Friend or Foe?' *Thorax*, 68(8), pp. 788–790

Tapia, V.S., Daniels, M.J.D., Palazón-Riquelme, P., Dewhurst, M., Luheshi, N.M., Rivers-Auty, J., Green, J., Redondo-Castro, E., Kaldis, P., Lopez-Castejon, G. and Brough, D. (2019) 'The Three Cytokines IL-1β, IL-18, and IL-1α Share Related but Distinct Secretory Routes'. *Journal of Biological Chemistry*, 294(21), pp. 8325–8335

Tenthorey, J.L., Haloupek, N., López-Blanco, J.R., Grob, P., Adamson, E., Hartenian, E., Lind, N.A., Bourgeois, N.M., Chacón, P., Nogales, E. and Vance, R.E. (2017) 'The Structural Basis of Flagellin Detection by NAIP5: A Strategy to Limit Pathogen Immune Evasion'. *Science*, 358(6365), pp. 888–893

Tessmer, A., Welte, T., Schmidt-Ott, R., Eberle, S., Barten, G., Suttorp, N. and Schaberg, T. (2011) 'Influenza Vaccination Is Associated with Reduced Severity of Community-Acquired Pneumonia'. *European Respiratory Journal*, 38(1), pp. 147–153

Théry, C. and Amigorena, S. (2001) 'The Cell Biology of Antigen Presentation in Dendritic Cells'. *Current Opinion in Immunology*, 13(1), pp. 45–51

Thoma-Uszynski, S. (2001) 'Induction of Direct Antimicrobial Activity Through Mammalian Toll-Like Receptors'. *Science*, 291(5508), pp. 1544–1547

Thompson, M.R., Kaminski, J.J., Kurt-Jones, E.A. and Fitzgerald, K.A. (2011) 'Pattern Recognition Receptors and the Innate Immune Response to Viral Infection'. *Viruses*, 3(6), pp. 920–940

Tilley, A.E., Walters, M.S., Shaykhiev, R. and Crystal, R.G. (2015) 'Cilia Dysfunction in Lung Disease'. *Annual Review of Physiology*, 77(1), pp. 379–406

Tong, N. (2004) 'Background Paper 6.22 Pneumonia'. *Background Paper*, p. 55.

Torres, A. and Cillóniz, C. (2015) 'Clinical Management of Bacterial Pneumonia'. *Springer International Publishing*, pp.1-98

Torres, A., Peetermans, W.E., Viegi, G. and Blasi, F. (2013) 'Risk Factors for Community-Acquired Pneumonia in Adults in Europe: A Literature Review'. *Thorax*, 68(11), pp. 1057–1065

Tsutsumi, N., Kimura, T., Arita, K., Ariyoshi, M., Ohnishi, H., Yamamoto, T., Zuo, X., Maenaka, K., Park, E.Y., Kondo, N., Shirakawa, M., Tochio, H. and Kato, Z. (2014) 'The Structural Basis for Receptor Recognition of Human Interleukin-18'. *Nature Communications*, 5(1), p. 5340

Turner, M.D., Nedjai, B., Hurst, T. and Pennington, D.J. (2014) 'Cytokines and Chemokines: At the Crossroads of Cell Signalling and Inflammatory Disease'. *Biochimica et Biophysica Acta (BBA) - Molecular Cell Research*, 1843(11), pp. 2563–2582

Vance, R.E. (2016) 'Cytosolic DNA Sensing: The Field Narrows'. *Immunity*, 45(2), pp. 227–228

Ventola, C.L. (2015) 'The Antibiotic Resistance Crisis'. *Pharmacy and Therapeutics*, 40(4), pp. 277–283.

Vieira, O.V., Botelho, R.J. and Grinstein, S. (2002) 'Phagosome Maturation: Aging Gracefully'. *Biochemical Journal*, 366(3), pp. 689–704

Wang, H., D'Souza, C., Lim, X.Y., Kostenko, L., Pediongco, T.J., Eckle, S.B.G., Meehan, B.S., Shi, M., Wang, N., Li, S., Liu, L., Mak, J.Y.W., Fairlie, D.P., Iwakura, Y., Gunnersen, J.M., Stent, A.W., Godfrey, D.I., Rossjohn, J., Westall, G.P., Kjer-Nielsen, L., Strugnell, R.A., McCluskey, J., Corbett, A.J., Hinks, T.S.C. and Chen, Z. (2018) 'MAIT Cells Protect against Pulmonary Legionella Longbeachae Infection'. *Nature Communications*, 9(1), p. 3350

Wang, J. (2018) 'Neutrophils in Tissue Injury and Repair'. *Cell and Tissue Research*, 371(3), pp. 531–539

Whiley, H. and Bentham, R. (2011) '*Legionella Longbeachae* and Legionellosis'. *Emerging Infectious Diseases*, 17(4), pp. 579–583

Whitsett, J.A. and Alenghat, T. (2015) 'Respiratory Epithelial Cells Orchestrate Pulmonary Innate Immunity'. *Nature Immunology*, 16(1), pp. 27–35

WHO. (2019) *Pneumonia*. Available at: https://www.who.int/news-room/fact-sheets/detail/pneumonia (Accessed: 6 August 2019).

WHO. (2018) *The Top 10 Causes of Death*. Available at: https://www.who.int/news-room/fact-sheets/detail/the-top-10-causes-of-death (Accessed: 2 July 2019).

Wissinger, E., Goulding, J. and Hussell, T. (2009) 'Immune Homeostasis in the Respiratory Tract and Its Impact on Heterologous Infection'. *Seminars in Immunology*, 21(3), pp. 147–155

Wood, R.E., Newton, P., Latomanski, E.A. and Newton, H.J. (2015) 'Dot/Icm Effector Translocation by Legionella Longbeachae Creates a Replicative Vacuole Similar to That of Legionella Pneumophila despite Translocation of Distinct Effector Repertoires'. *Infection and Immunity*, 83(10), pp. 4081–4092

Wright, E.K., Goodart, S.A., Growney, J.D., Hadinoto, V., Endrizzi, M.G., Long, E.M., Sadigh, K., Abney, A.L., Bernstein-Hanley, I. and Dietrich, W.F. (2003) 'Naip5 Affects Host Susceptibility to the Intracellular Pathogen Legionella Pneumophila'. *Current Biology*, 13(1), pp. 27–36

Wright, J.R. (2003) 'Pulmonary Surfactant: A Front Line of Lung Host Defense'. *Journal of Clinical Investigation*, 111(10), pp. 1453–1455

Xu, Z., Zan, H., Pone, E.J., Mai, T. and Casali, P. (2012) 'Immunoglobulin Class-Switch DNA Recombination: Induction, Targeting and Beyond'. *Nature Reviews Immunology*, 12(7), pp. 517–531

Yanagi, S., Tsubouchi, H., Miura, A., Matsumoto, N. and Nakazato, M. (2015) 'Breakdown of Epithelial Barrier Integrity and Overdrive Activation of Alveolar Epithelial Cells in the Pathogenesis of Acute Respiratory Distress Syndrome and Lung Fibrosis'. *BioMed Research International*, 2015, pp. 1–12

Yang, R., Yang, E., Shen, L., Modlin, R.L., Shen, H. and Chen, Z.W. (2018) 'IL-12+IL-18 Cosignaling in Human Macrophages and Lung Epithelial Cells Activates Cathelicidin and Autophagy, Inhibiting Intracellular Mycobacterial Growth'. *The Journal of Immunology*, 200(7), pp. 2405–2417

Yoshida, S.-I. and Mizuguchi, Y. (1986) 'Multiplication of *Legionella Pneumophila* Philadelphia-1 in Cultured Peritoneal Macrophages and Its Correlation to Susceptibility of Animals'. *Canadian Journal of Microbiology*, 32(5), pp. 438–442

Yoshimoto, T., Takeda, K., Tanaka, T., Ohkusu, K., Kashiwamura, S., Okamura, H., Akira, S. and Nakanishi, K. (1998) 'IL-12 Up-Regulates IL-18 Receptor Expression on T Cells, Th1 Cells, and B Cells: Synergism with IL-18 for IFN-γ Production'. *The Journal of Immunology*, 161(7), p. 9.

Zar, H.J., Madhi, S.A., Aston, S.J. and Gordon, S.B. (2013) 'Pneumonia in Low and Middle Income Countries: Progress and Challenges'. *Thorax*, 68(11), pp. 1052–1056

Zhan, X.-Y., Hu, C.-H. and Zhu, Q.-Y. (2015) 'Legionella Pathogenesis and Virulence Factors'. *Annals of Clinical and Laboratory Research*, 3(2), pp. 1-16

Zhang, J., Roberts, A.I., Liu, C., Ren, G., Xu, G., Zhang, L., Devadas, S. and Shi, Y. (2013) 'A Novel Subset of Helper T Cells Promotes Immune Responses by Secreting GM-CSF'. *Cell Death and Differentiation*, 20(12), pp. 1731–1741

Zhang, N. and Bevan, M.J. (2011) 'CD8+ T Cells: Foot Soldiers of the Immune System'. *Immunity*, 35(2), pp. 161–168

Ziltener, P., Reinheckel, T. and Oxenius, A. (2016) 'Neutrophil and Alveolar Macrophage-Mediated Innate Immune Control of Legionella Pneumophila Lung Infection via TNF and ROS'. *PLOS Pathogens*, 12(4), p. e1005591

Zinkernagel, M., R., Althage, A., Adler, B.., Blanden, R.V., Davidson, W. F., Kees, U., Dunlop, M.B.C. and Sheffler, D.C. (1977) 'H-2 restriction of cell-mediated immunity to an intracellular bacterium: effector T cells are specific for Listeria antigen in association with H-21 region-coded self-markers'. *Journal of Experimental Medicine,* 145(5): pp. 1353-67